

# ornl

OAK RIDGE  
NATIONAL  
LABORATORY

MARTIN MARIETTA

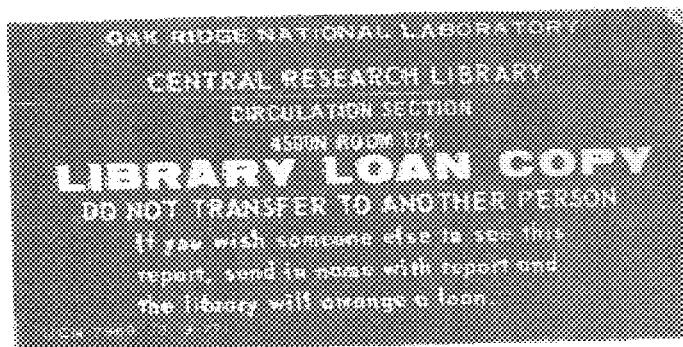
OPERATED BY  
MARTIN MARIETTA ENERGY SYSTEMS, INC.  
FOR THE UNITED STATES  
DEPARTMENT OF ENERGY



ORNL/TM-9229

## Site Characterization of the West Chestnut Ridge Site

R. H. Ketelle  
D. D. Huff



Printed in the United States of America. Available from  
National Technical Information Service  
U.S. Department of Commerce  
5285 Port Royal Road, Springfield, Virginia 22161  
NTIS price codes—Printed Copy: A08; Microfiche A01

This report was prepared as an account of work sponsored by an agency of the United States Government. Neither the United States Government nor any agency thereof, nor any of their employees, makes any warranty, express or implied, or assumes any legal liability or responsibility for the accuracy, completeness, or usefulness of any information, apparatus, product, or process disclosed, or represents that its use would not infringe privately owned rights. Reference herein to any specific commercial product, process, or service by trade name, trademark, manufacturer, or otherwise, does not necessarily constitute or imply its endorsement, recommendation, or favoring by the United States Government or any agency thereof. The views and opinions of authors expressed herein do not necessarily state or reflect those of the United States Government or any agency thereof.

ENERGY DIVISION  
SITE CHARACTERIZATION OF THE  
WEST CHESTNUT RIDGE SITE

R. H. Ketelle

D. D. Huff\*

\*ENVIRONMENTAL SCIENCES DIVISION

September 1984

Prepared by the  
OAK RIDGE NATIONAL LABORATORY  
Oak Ridge, Tennessee 37831  
operated by  
Martin Marietta Energy Systems, Inc.  
for the  
U.S. DEPARTMENT OF ENERGY  
under Contract No. DE-AC05-84OR21400



3 4456 0040860 9



# CONTENTS

	<u>Page</u>
LIST OF FIGURES . . . . .	v
LIST OF TABLES . . . . .	vii
ACKNOWLEDGMENTS . . . . .	ix
SUMMARY . . . . .	xi
ABSTRACT . . . . .	xv
1. INTRODUCTION . . . . .	1
2. TOPOGRAPHY, PHYSIOGRAPHY, AND GEOMORPHOLOGY OF THE SITE . . . . .	3
2.1 Site Topography . . . . .	3
2.2 Physiography and Geomorphology . . . . .	6
3. GEOLOGY . . . . .	13
3.1 Regional Geologic Setting . . . . .	13
3.2 Stratigraphy and Areal Geology . . . . .	13
3.3 Structural Geology . . . . .	17
3.4 Bedrock Characteristics . . . . .	23
4. SOILS . . . . .	29
4.1 Physical Properties of Site Soils . . . . .	29
4.1.1 Characteristics of Surficial Soils . . . . .	29
4.1.2 Characteristics of Subsurface Soils . . . . .	32
4.2 Geochemical Characteristics of Site Soils . . . . .	36
4.2.1 Physical Characteristics of Test Specimens . . . . .	38
4.2.2 Chemical Characteristics of Knox Residuum . . . . .	38
4.2.3 Chemical Characteristics of Soil Water and Surface Water . . . . .	38
4.3 Radionuclide Sorption and Desorption Characteristics of Knox Residuum . . . . .	43
4.4 Soil Mineralogy . . . . .	54
4.4.1 Surface Soil Horizons . . . . .	56
4.4.1.1 Gravel and Sand Morphology . . . . .	59
4.4.1.2 Clay and Silt Mineralogy . . . . .	59
4.4.2 Residual Soils . . . . .	62
4.4.2.1 Gravel and Sand Morphology . . . . .	64
4.4.2.2 Clay and Silt Mineralogy . . . . .	65
4.5 Soil Processes . . . . .	65
4.5.1 Carbonate Rock Weathering Rates . . . . .	65
4.5.2 Soil Erosion Rates . . . . .	68
4.5.3 Karst Processes . . . . .	72
5. SITE GEOHYDROLOGY . . . . .	75
5.1 Permeability of Soil and Rock . . . . .	75
5.1.1 Soil Permeability . . . . .	75

	<u>Page</u>
5.1.2 Permeability of Weathered Rock . . . . .	77
5.1.3 Permeability of Unweathered Rock . . . . .	78
5.2 Moisture-Suction and Permeability-Suction Characteristics of Residuum Samples . . . . .	78
5.2.1 Results of Moisture-Suction Tests . . . . .	79
5.2.2 Results of Permeability Tests Performed at <100% Saturation . . . . .	79
5.3 Groundwater Fluctuations and Flow Paths . . . . .	81
5.3.1 Groundwater Fluctuations . . . . .	81
5.3.2 Maximum Water Table Elevation . . . . .	83
5.3.3 Groundwater Flow Paths . . . . .	83
6. SURFACE WATER HYDROLOGY . . . . .	89
6.1 Precipitation . . . . .	89
6.2 Surface Water Flows . . . . .	92
6.3 Water Budget Estimates . . . . .	96
REFERENCES . . . . .	103
APPENDIX A: WELL HYDROGRAPHS . . . . .	107
APPENDIX B: GROUNDWATER TRACER TEST . . . . .	129

## LIST OF FIGURES

	<u>Page</u>
Fig. 2.1. Location of the West Chestnut Ridge Site . . . . .	4
Fig. 2.2. Topography of the West Chestnut Ridge Site . . . . .	5
Fig. 2.3. Topographic profile crossing the site from northwest to southeast . . . . .	7
Fig. 2.4. Physiographic map of Tennessee . . . . .	8
Fig. 2.5. Geomorphic features on the West Chestnut Ridge Site .	9
Fig. 2.6. Photolinear features identified on aerial photography from November 1939 and March 1977 . . . . .	12
Fig. 3.1. Geological map of the Oak Ridge Reservation . . . . .	14
Fig. 3.2. Geologic cross section through the Oak Ridge Reservation . . . . .	15
Fig. 3.3. Stratigraphic column of bedrock formations on the West Chestnut Ridge Site . . . . .	16
Fig. 3.4. Areal geologic map of the West Chestnut Ridge Site . .	18
Fig. 3.5. Comparison of (a) topographic linear features and (b) straight stream segment orientations . . . . .	22
Fig. 3.6. Approximate configuration of the top of the weathered bedrock zone . . . . .	25
Fig. 3.7. Approximate configuration of the top of continuous bedrock . . . . .	26
Fig. 3.8. Generalized geologic profile through the West Chestnut Ridge Site . . . . .	27
Fig. 4.1. Soil survey map of the West Chestnut Ridge Site . . .	30
Fig. 4.2. Percent saturation vs soil sample depth . . . . .	35
Fig. 4.3. Strength vs depth and liquidity index vs depth plots for Knox residuum on the West Chestnut Ridge Site . .	37
Fig. 4.4. Range of uranium (VI) $R_s$ values for six soil samples - ambient pH conditions . . . . .	45
Fig. 4.5. Range of strontium $R_s$ values for six soil samples - ambient pH conditions . . . . .	46

Fig. 4.6.	Range of cesium $R_S$ values for six soil samples - ambient pH conditions . . . . .	47
Fig. 4.7.	Range of cobalt $R_S$ values for six soil samples - ambient pH conditions . . . . .	48
Fig. 4.8.	Europium $R_S$ values for one soil sample - ambient pH conditions . . . . .	49
Fig. 4.9.	Thorium $R_S$ values for one soil sample - ambient pH conditions . . . . .	50
Fig. 4.10.	Technetium $R_S$ values for one soil sample - ambient pH conditions . . . . .	51
Fig. 4.11.	Range of iodine $R_S$ values for six soil samples - ambient pH conditions . . . . .	52
Fig. 4.12.	Distribution of KCL (1M) exchangeable Al, Mg, and Ca in the soil profiles . . . . .	60
Fig. 5.1.	Recommended moisture-suction curves . . . . .	80
Fig. 5.2.	Well elevation vs maximum water table elevations, soil wells . . . . .	84
Fig. 5.3.	Well elevation vs maximum water table elevations, bedrock wells . . . . .	85
Fig. 6.1.	Drainage area for Ish Creek (CWDF) and location map for seven temporary stream flow monitoring points . . . . .	90
Fig. 6.2.	Location map and drainage areas for continuous stream flow discharge measuring stations, recording rain gage, and selected groundwater monitoring wells . . . . .	91
Fig. 6.3.	Flood frequency curves for Walker Branch and Ish Creek, based upon the Gumbel extreme-value frequency distribution . . . . .	99
Fig. B.1.	Monitoring locations used in dye tracer tests . . . . .	132

LIST OF TABLES

	<u>Page</u>
Table 3.1. Comparison of bedrock joint and fracture orientations in two study areas on Chestnut Ridge . . . . .	20
Table 4.1. Classification of soils on the West Chestnut Ridge Site Disposal Area . . . . .	31
Table 4.2. Summary of index and physical properties for Shelby tube samples . . . . .	33
Table 4.3. Summary of index and physical properties from the engineering properties test series . . . . .	34
Table 4.4. Elemental analyses of Knox residuum from West Chestnut Ridge by ICP Spectrometry . . . . .	39
Table 4.5. Dissolved constituents in Knox residuum soil waters .	41
Table 4.6. Surface water physicochemical parameters . . . . .	42
Table 4.7. Summary of radionuclide sorption data . . . . .	44
Table 4.8. Preliminary mineralogical data . . . . .	55
Table 4.9. Physical and chemical properties of selected samples from surface soil profiles . . . . .	58
Table 4.10. Mineralogical composition of the clay fractions from selected horizons of surface soil profiles . . . . .	61
Table 4.11. Physical and chemical properties of selected samples from borehole residuum cores . . . . .	63
Table 4.12. Mineralogical composition of the clay fractions of selected samples from residuum cores . . . . .	66
Table 4.13. Cation exchange capacities of the clay fractions of residuum before and after citrate-bicarbonate-dithionite (CBD) treatments . . . . .	67
Table 4.14. Rates of chemical weathering of limestone in temperate climates . . . . .	69
Table 4.15. Estimated annual soil erosion potential of West Chestnut Ridge Site soils . . . . .	71
Table 5.1. Summary of field and laboratory soil permeability test results . . . . .	76

	<u>Page</u>
Table 5.2. Recommended range of values for curves of relative permeability versus soil suction . . . . .	82
Table 6.1. Comparisons of monthly precipitation at the West Chestnut Ridge Site (WCRS), Walker Branch Watershed (WBW), and Oak Ridge townsite (ORT) weather stations for calendar year 1983 . . . . .	93
Table 6.2. Rainfall vs frequency for areas up to 10 square miles in Anderson and Knox counties, Tennessee . . . .	94
Table 6.3. Summary of intermittent flow measurement data for July 15, 1982, to July 11, 1983 . . . . .	95
Table 6.4. Monthly flow data for monitoring stations on the West Chestnut Ridge Site . . . . .	97
Table 6.5. Estimated frequency of peak discharges on Ish Creek . . . . .	98
Table 6.6. Precipitation - Runoff comparison at West Chestnut Ridge flow measuring sites . . . . .	100
Table B.1. Comparison of flow rates at West Chestnut Ridge Site sites during the tracer experiment . . . . .	136

## ACKNOWLEDGMENTS

The authors wish to acknowledge all staff members who have contributed directly to performance of specific technical studies supporting this project. Our thanks go also to M. Goodson and S. Edwards for rapidly and efficiently word processing the manuscript.



## SUMMARY

Site characterization investigations performed to date on the West Chestnut Ridge Site have included a geomorphic analysis; geologic mapping; surficial soil mapping; subsurface sampling and testing; physical, chemical, and mineralogic characterization of site soils; field and laboratory geohydrologic testing; groundwater fluctuation monitoring; and surface water discharge and precipitation monitoring.

The West Chestnut Ridge Site is typical of Knox terrain throughout the Chestnut Ridge strike belt. Broad-crested ridges with steep northwest flanks and moderately sloping southeast flanks typify Knox terrain. The relief of ridge crests above valley floors is approximately 100 m. The drainage pattern on the site is weakly rectangular. Five karst zones have been identified on the site, where karst zone development is apparently stratigraphically controlled. Karst zones in other areas of Chestnut Ridge occur in similar stratigraphic intervals, suggesting that the karst zones are either discontinuous or are not expressed at the surface throughout their full extent.

Geologic mapping of the site is based largely on the identification of characteristic lithologies of sandstone and chert in residual soil, because the extensive weathering and residual soil formation have covered most bedrock on the site. One crosscutting structural feature has been identified by aerial photograph interpretation and surficial soil mapping. This feature trends near N10°W and passes through the headwater confluence area of Ish Creek. Local bedding strike and dip are quite similar to the regional structural trend. Because of the lack of joint and fracture orientation data about the bedrock, a terrain analysis approach to geologic structural analysis was used. This analysis concluded that there may be four prominent fracture or joint sets which have influenced groundwater flow and terrain evolution in the Chestnut Ridge strike belt.

Surficial soils on the site were mapped in support of the site characterization. Soil types on the site are predominantly Paleudults, though minor areas of Entisols and Inceptisols occur. Paleudults are soils which have developed over long periods of time. Colluvial and erosional processes are locally active.

Subsurface investigations performed on the site include seismic refraction surveys to profile the bedrock surface in selected areas, soil drilling and sampling, and rotary drilling in bedrock. Electromagnetic terrain conductivity has been used in selected areas of the site to identify groundwater flow pathways. Information obtained from the subsurface investigations has been used to evaluate soil and bedrock conditions on the site.

A conceptual model of subsurface conditions includes residual soils, weathering bedrock, and unweathered bedrock zones. The extensively leached residual soils overlie the zone of weathering carbonate bedrock. The weathering bedrock zone ranges from <1 to >30 m thick and is a zone of mixed weathering carbonate boulders and pinnacles, and of solution cavities variably filled with water, mud, and gravel. At depth, the southeast dipping bedrock is essentially unweathered except along bedding planes and open fractures. Based on information obtained to date, the Chapultepec Dolomite is associated with the deepest weathering zones in bedrock.

Residual soils on the West Chestnut Ridge Site are predominantly clays of low to high plasticity with varying amounts of silt, fine sand, and chert gravel present. Soil strength is inversely proportional to the liquidity index of the soils and typically decreases with depth as moisture content increases. Site soils have very strong moisture-retention characteristics, and even during late summer and autumn the saturation indices are generally >90% below depths of 3 m.

Residual soils on the site are slightly acid and very weakly buffered. Chemical analyses of natural and synthetic soil waters indicate that the soils have been extensively leached and that very few soluble ions remain. An interesting aspect of site soils is that they contain very little carbonate above the weathering bedrock zone. Surface waters which show the influence of the bedrock aquifer have a nearly neutral pH and contain more dissolved carbonate than soil water. Water in headwater reaches, which tend to be wetweather streams, are chemically similar to soil water. Favorable sorption ratios are obtained for cobalt, cesium, strontium, thorium, europium, and uranium. Sorption ratios <1 were obtained for iodine and technetium.

Mineralogically, the surface soils are more complex than the residuum obtained from depths >10 m. Surficial soils contain kaolinite, illite, vermiculite, an aluminum-hydroxy interlayered vermiculite, gibbsite, quartz, and iron oxides, including the magnetic species maghemite. By comparison, the samples obtained from depths >10 m contained kaolinite, illite, vermiculite, quartz, and amorphous iron and aluminum oxides. The presence of aluminum-hydroxy interlayered vermiculite in the surficial soils is attributed to prolonged weathering.

Active soil processes include colluvial and alluvial processes, surface erosion, continuing residuum formation by bedrock weathering, and karst-related soil movement. Estimates of erosion based on the universal soil loss equation are presented.

Field geohydrologic testing included performance of falling head permeability tests in soil, packer permeability tests in bedrock, and one aquifer pump test in the weathered bedrock zone. The range of permeability values obtained encompasses four orders of magnitude. The mean permeability of the soils is approximately  $10^{-6}$  cm/s. The bedrock and weathered bedrock zones with measurable permeabilities have mean permeabilities on the order of  $10^{-4}$  cm/s.

Groundwater fluctuations in observation wells in soil and bedrock were monitored beginning in October 1983. Responses to large storms occur within 1 to 5 days in most wells. Maximum well fluctuations varied from <1 m to as much as 15 m. Groundwater gradients indicate flow toward the nearest perennial surface water bodies. A dye tracer test was performed in one karst flow system on the site. The estimated flow rate in the system tested was 240 to 380 m/d and discharge was detected in a surface stream near the Clinch River. Subsurface flow paths directly to the Clinch River may exist.

Surface water flow monitoring suggests that significant subsurface flow occurs at some of the flow monitoring points. Low flow and peak flow measurements have been obtained and flow rating curves have been developed for each monitoring station. Precipitation data for the site are very similar to those obtained at the Walker Branch Watershed. A water budget estimate suggests that the Ish Creek downstream monitoring station does not lose significant flow to deep groundwater flow or to

interbasin flow. Substantial surface flow losses to the groundwater system appear to occur at surface water monitoring stations in two other smaller drainages.

## ABSTRACT

This report summarizes the results of investigations performed to date on the West Chestnut Ridge Site, on the Department of Energy (DOE) Oak Ridge Reservation. The investigations performed include geomorphic observations, areal geologic mapping, surficial soil mapping, subsurface investigations, soil geochemical and mineralogical analyses, geohydrologic testing, groundwater fluctuation monitoring, and surface water discharge and precipitation monitoring.



## 1. INTRODUCTION

This report presents results and an interpretation of extensive investigations that have been performed on the West Chestnut Ridge Site. The site is under study for development of a centralized low-level radioactive waste disposal site to accept wastes from the three Department of Energy (DOE) facilities located on the DOE Oak Ridge Reservation (ORR).

The purpose of this report is to summarize and integrate the results of a multifaceted site investigation which includes areal geology and geomorphology, soil and bedrock investigations, geochemical and mineralogical aspects of site soils, and surface water and groundwater flow studies. The objective of this report is to present a synthesis of the available information regarding the site to provide an understanding of the overall site geologic and geohydrologic systems. For this reason, the most significant aspects of the ongoing site investigations are highlighted in this document.

The site investigations were initiated in 1980 with selection of the site in a reservation wide site survey (Allen et al. 1980; Lee et al. 1983). In the 1980 survey, 10 exploratory borings were made and a 15-cm (6-in.) observation well was installed in each borehole. In 1982 additional preliminary geologic investigations, including areal geologic mapping of the site and a preliminary seismic refraction survey, were completed. Temporary surface water discharge monitoring stations were installed, and stream discharge measurement was initiated.

In 1983 additional site characterization investigations were performed, including

- o subsurface investigations, soil testing, field hydrologic testing, and observation well installation by Woodward-Clyde Consultants (1984);
- o seismic profiling of the bedrock surface by the Tennessee Valley Authority (Staub and Hopkins 1984);
- o geochemical studies of site soils to determine radionuclide adsorption properties (Seeley and Kelmers 1984); and
- o installation and calibration of permanent surface water discharge monitoring facilities.

In 1984 site characterization activities have continued, including

- o acquisition of surface water discharge data,
- o acquisition of water level fluctuation data in monitoring wells,
- o mineralogic characterization of site soils,
- o tracer testing of groundwater flow, and
- o acquisition and interpretation of aerial thermal sensing data.

Additional activities that are scheduled for 1984 include initiation of baseline water quality analyses and completion of several deep bedrock exploratory borings. Results of these investigations will be reported at a later date.

## 2. TOPOGRAPHY, PHYSIOGRAPHY, AND GEOMORPHOLOGY OF THE SITE

The West Chestnut Ridge Site is located near the southwest end of the DOE ORR. The site is generally bounded to the east by Tennessee Highway 95, to the north by Bear Creek Valley Road, and to the south and west by New Zion Patrol Road, which is a restricted-access DOE patrol road. This section presents discussion of site topography, physiography, and geomorphology.

### 2.1 SITE TOPOGRAPHY

The West Chestnut Ridge Site occupies upland terrain on Chestnut Ridge. The general site location is shown in Fig. 2.1. A topographic map of the site is shown in Fig. 2.2. The site area encompasses approximately 460 ha (1150 acres). Not all of the site is usable for waste disposal because of topographic constraints, groundwater conditions, and thin soils in portions of the site. Approximately 60 ha (150 acres) are under study for use as disposal area. Chestnut Ridge is a composite feature that typically includes three discontinuous ridge lines: the northwesternmost is the highest with crest elevations of approximately 320 m (1050 ft), the central ridge line is of intermediate crest height [285 m (940 ft)], and the southeasternmost and lowest of the three ridge lines typically has crest elevations of approximately 280 m (920 ft). Major valleys that carry perennial surface streams draining Chestnut Ridge occur to the north (Bear Creek Valley) and south (Bethel Valley). Elevations for the major valleys in the site vicinity are approximately 245 m (800 ft). Typical relief between valley floors and the crest of Chestnut Ridge is approximately 100 m (300 ft).

Surface runoff from the West Chestnut Ridge Site drains primarily into Ish Creek and an unnamed ephemeral stream. Smaller portions of the site runoff enter Raccoon Creek to the south, and Grassy Creek and Bear Creek to the north. The surface drainage system on the site is a weakly developed trellis drainage pattern typical of surface drainage patterns in areas underlain by dipping bedrock strata of alternating lithologies having variable resistance to weathering. Internal drainage via karst

- CARL -- COMPARATIVE ANIMAL RESEARCH LABORATORY
- EGCR -- EXPERIMENTAL GAS-COOLED REACTOR
- ORGDP -- OAK RIDGE GASEOUS DIFFUSION PLANT
- ORNL -- OAK RIDGE NATIONAL LABORATORY
- TSF -- TOWER SHIELDING FACILITY

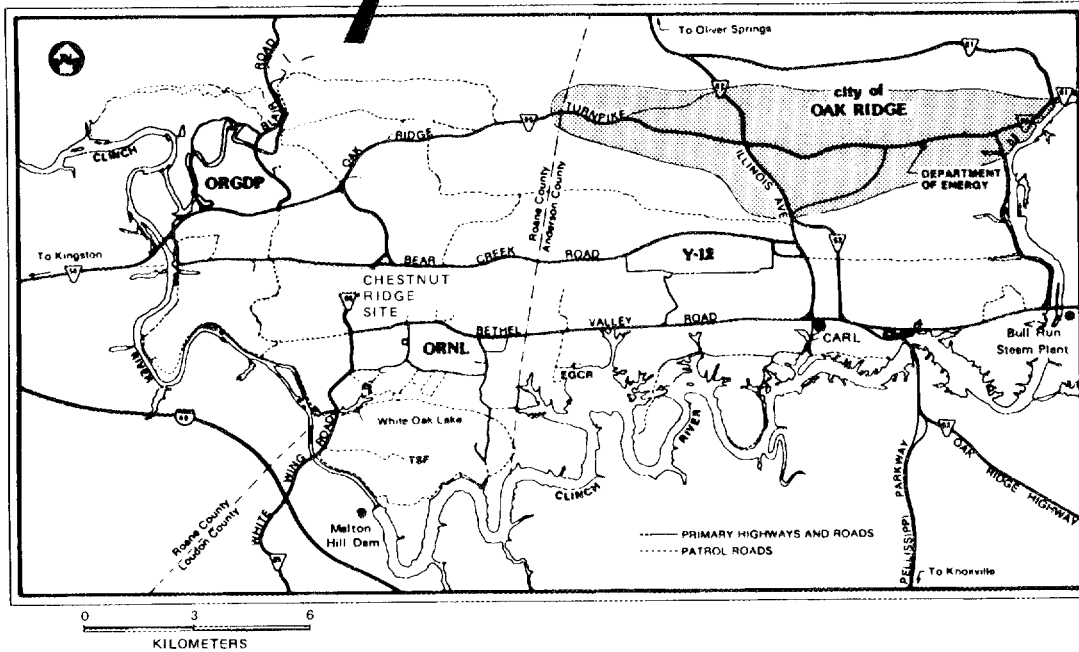
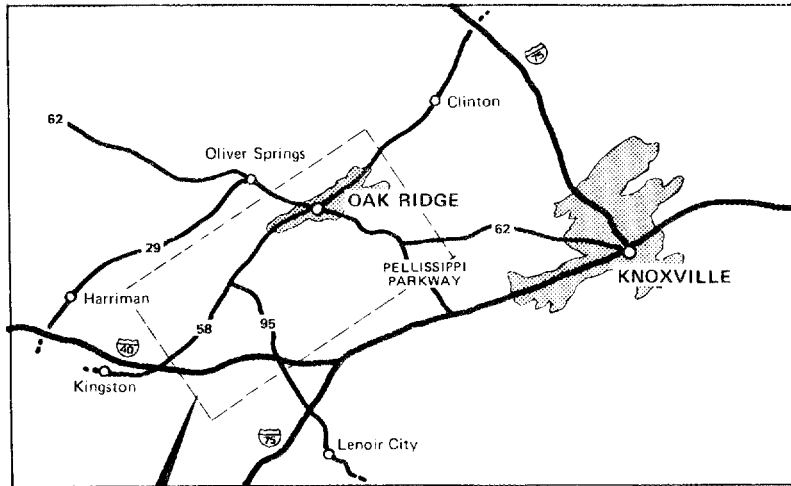


Fig. 2.1. Location of the West Chestnut Ridge Site.



Fig. 2.2. Topography of the West Chestnut Ridge Site.

features occurs in several zones on the site. The distribution of karst zones is discussed in a later section.

Slope angles on the site are variable, ranging from a few percent to more than 40%. Areas under investigation for use in waste disposal operations have slopes of less than 15%. A topographic profile through the site (Fig. 2.3) shows that the individual ridge lines which make up Chestnut Ridge have asymmetrical geometry. The northwest-facing slopes of the northern and middle ridge lines are steep (slopes range from 20 to 40%) while the southeast facing slopes are gentler (slopes ranging from <15 to about 20%). Ridge crests tend to be broad and gently sloping. The southern ridge line shows a reversal of this trend, with the southeast-facing slope on this ridge being the steeper slope.

## 2.2 PHYSIOGRAPHY AND GEOMORPHOLOGY

The ORR is located within the Appalachian Highland Physiographic Division of the eastern United States. Within the division, areas of distinctive bedrock lithology, stratigraphy, geologic structure, and geomorphic history are divided into physiographic provinces. A physiographic map of Tennessee is shown in Fig. 2.4. The site is located in the western portion of the Valley and Ridge Physiographic Province. The Valley and Ridge Province is characterized by alternating valleys and ridges that have been formed by the combined influences of the regional geologic structure and weathering and erosional processes.

The West Chestnut Ridge Site occupies an upland ridge area underlain by southeasterly dipping carbonate bedrock. As discussed in Sect. 2.1, Chestnut Ridge typically consists of three discontinuous ridge lines separated by valleys containing the local surface drainage system of first-order and second-order streams.

Active geomorphic processes which are occurring on the site include sheet erosion, localized gully erosion, soil creep on steeper slopes, and subsidence related to dissolution of the carbonate bedrock which is locally accompanied by subsurface sediment transport through open solution cavities near the bedrock surface. A map showing geomorphic features of the site is presented in Fig. 2.5. The surface drainage

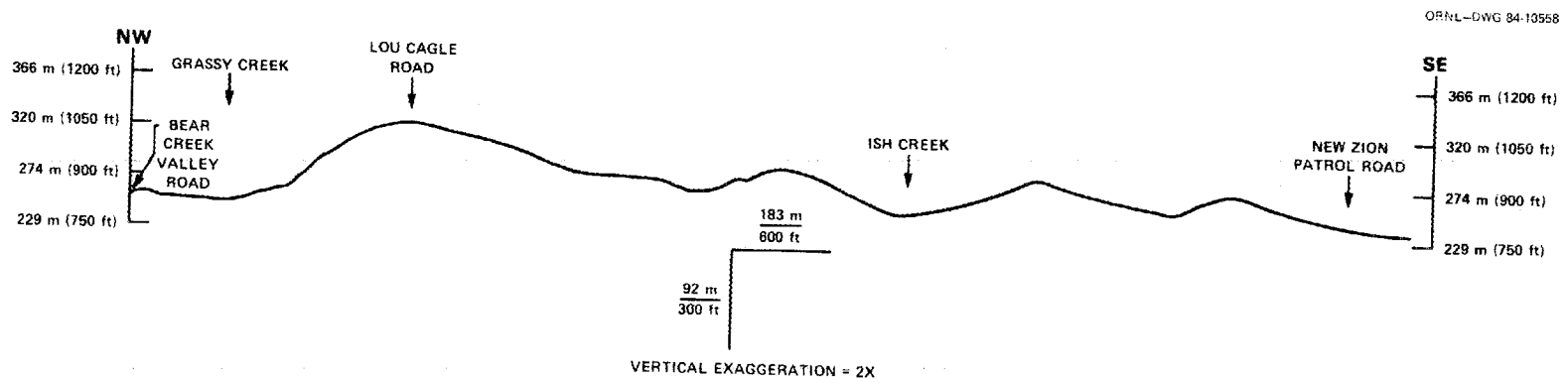
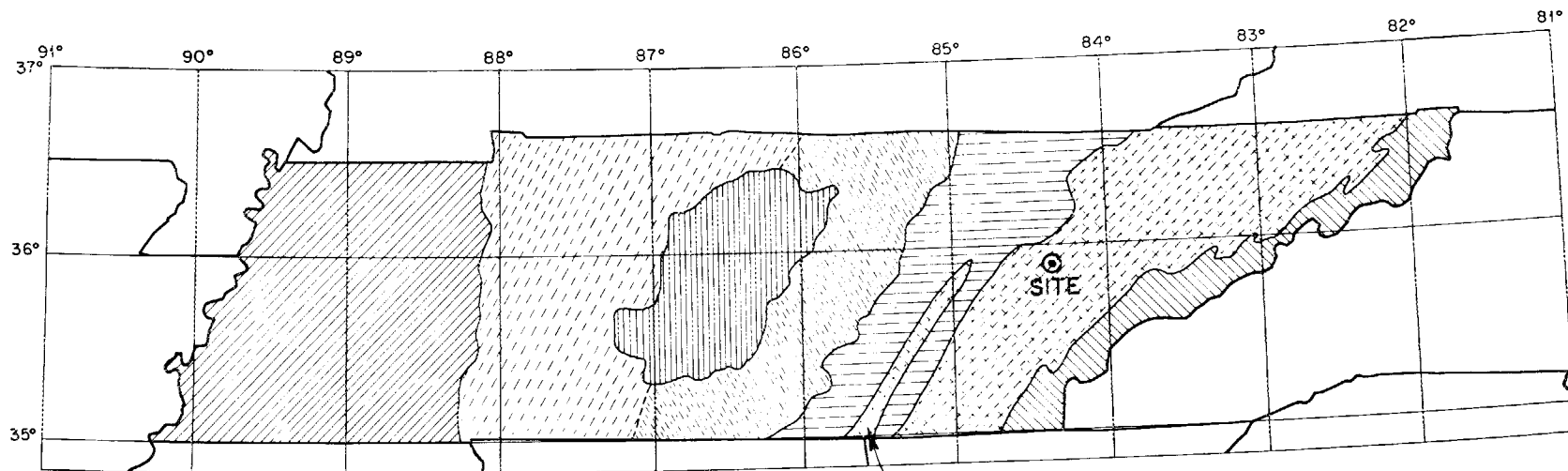


Fig. 2.3. Topographic profile crossing the site from northwest to southeast.



**PHYSIOGRAPHIC PROVINCES:**

-  MISSISSIPPI EMBAYMENT
-  WESTERN HIGHLAND RIM
-  EASTERN HIGHLAND RIM
-  CENTRAL BASIN

-  CUMBERLAND PLATEAU
-  VALLEY AND RIDGE
-  BLUE RIDGE

SEQUATCHIE VALLEY: OUTLIER OF VALLEY AND RIDGE

Fig. 2.4. Physiographic map of Tennessee.

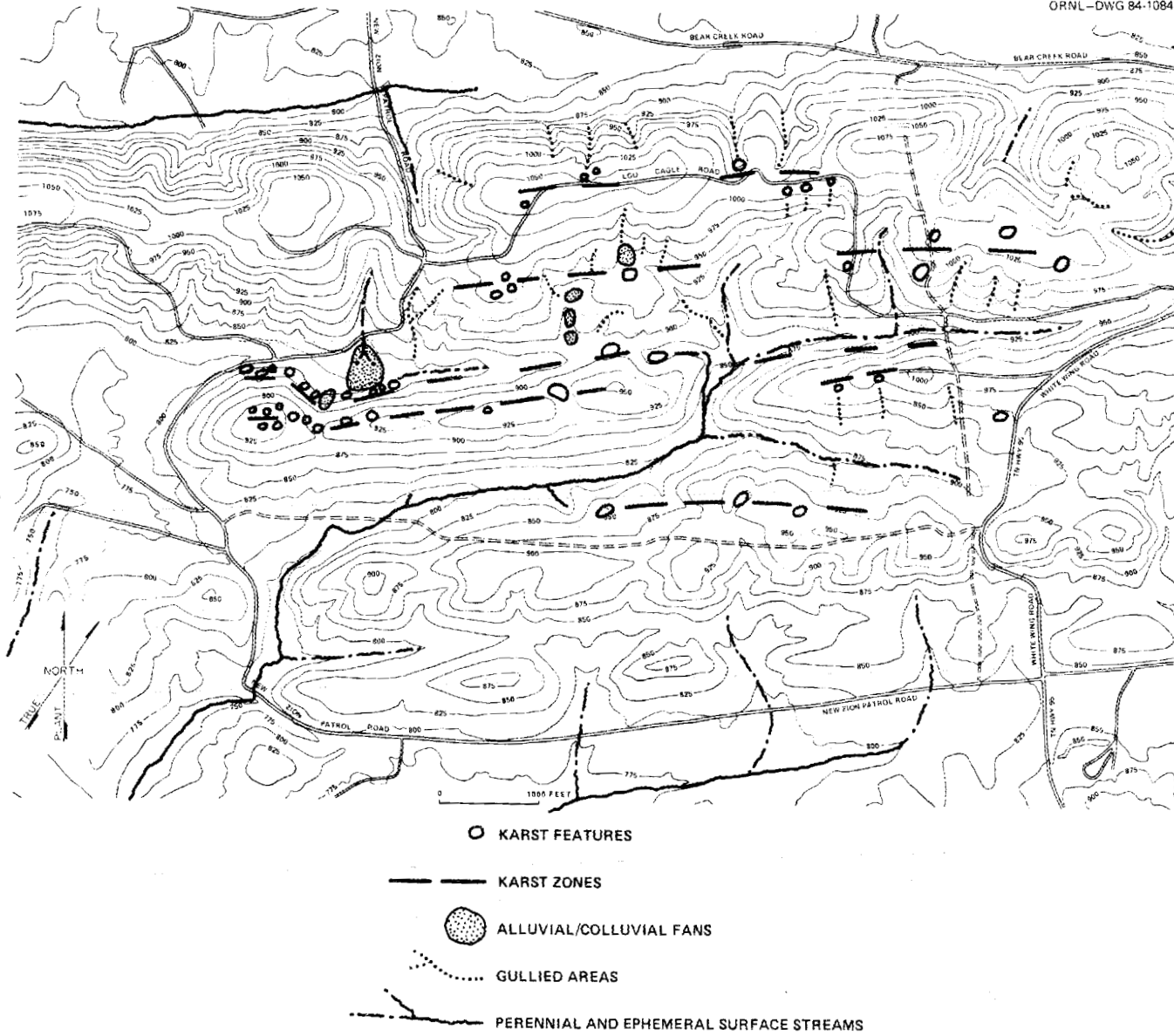


Fig. 2.5. Geomorphic features on the West Chestnut Ridge Site.

system for the site is shown, including perennial and ephemeral or wet season flow channels. Areas in which gully erosion has resulted in incision of local runoff channels are indicated as are recognized alluvial and colluvial deposits. The location of karst features that were observed in field mapping are indicated and five zones of karst occurrence are identified.

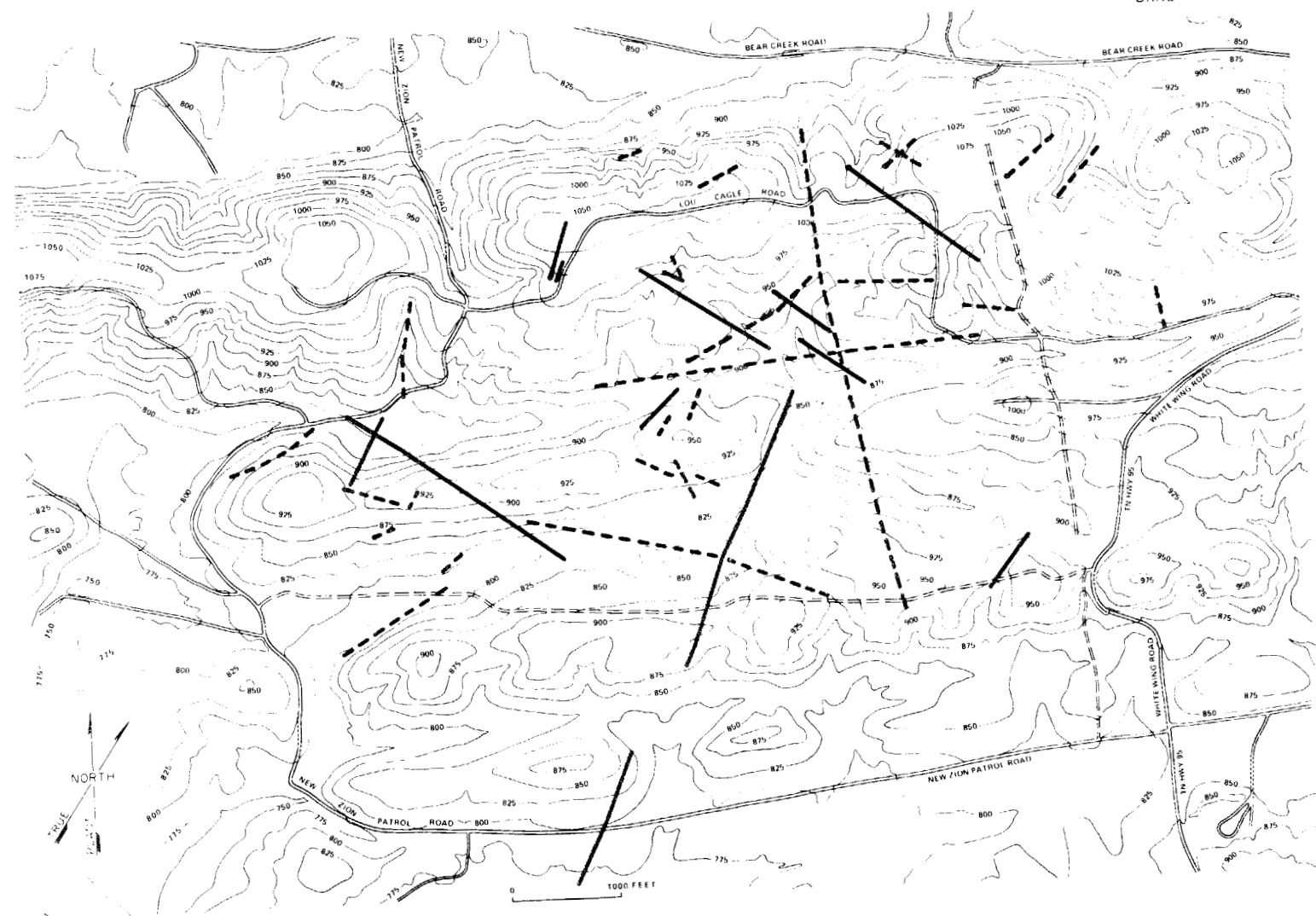
Sheet erosion results in a general lowering of the land surface by the gradual removal of residual soil particles through overland flow. Site soils are well drained and typically do not exhibit sheet runoff in their natural condition. Sheet runoff and sheet and rill erosion are likely to occur on site soils that are extensively disturbed by the removal of vegetation and topsoil. Erosion rate estimates are included in Sect. 4.4.

Gully erosion is caused by convergence of runoff into rills on sufficiently steep slopes and has occurred in several areas of the site. Some gullying may be attributed to agricultural practices in the area prior to government ownership, although, several of the ephemeral runoff channels occupy large ravines of natural origin. One gully that carries an ephemeral stream near New Zion Cemetery has deposited its sediment load as an alluvial fan which spreads across the valley bottom. Incision of the deeper dry valleys may reflect natural gully erosion caused by greater-than-present precipitation during prehistoric climatic variations.

Karst features of several varieties occur on the site in five zones that generally parallel the local and regional geologic strike. The correlation of these zones with bedrock geology is discussed in Sect. 3.2. Solution pan features have been observed in several areas. Solution pans are gentle sunken areas which have little or no actual topographic closure. Dolines are topographic depressions which have definite topographic closure. Several typical dolines occur on the site. One of the ephemeral surface streams on the site flows into a swallow hole that is an open karst throat. Seasonal surface flows from this stream are conducted into the groundwater system through this karst feature. In addition to these three classic types of karst features, a fourth geomorphic feature related to karst processes has been observed.

The northwest face of the middle ridge line has developed a hummocky slope shape, possibly by the ravelling of soil into bedrock cavities. An interesting juxtaposition of several ridge crest dolines and solution pans with gully erosion features has been observed. Lateral shallow flow in the soils apparently allows a portion of the water infiltrating the karst features to reemerge as surface runoff near the heads of the gullies. The significance of the karst zones to site geohydrology is discussed in Sect. 5.3.3.

Aerial photographs from several dates have been reviewed during the site investigations to gather information on site geology. Photolinear features and photogeologic information are plotted on the site topographic base map in Fig. 2.6. The photo features include linear vegetation patterns, visible linears, soil tonal patterns, and several crescent-shaped features which occur in a karst zone and are associated with subsidence on steep slopes.



————— FEATURES OBSERVED ON NOVEMBER 1939 PHOTOGRAPHS

- - - - - FEATURES OBSERVED ON MARCH 1977 PHOTOGRAPHS

Fig. 2.6. Photolinear features identified on aerial photography from November 1939 and March 1977.

### 3. GEOLOGY

This section presents geologic data and interpretation of site conditions based on the available information. The scope of site investigations which contribute to this section include

- o geologic field mapping of the site,
- o a preliminary seismic refraction study,
- o bedrock profiling by seismic refraction, and
- o subsurface investigations by exploratory drilling.

#### 3.1 REGIONAL GEOLOGIC SETTING

Bedrock underlying the ORR is comprised of interbedded clastic and carbonate rock units of Paleozoic age. A geologic map of the reservation is shown in Fig. 3.1. The regional structure is predominated by an imbricate arrangement of thrust faults which trend northeast and dip southeast. In the western portion of the Valley and Ridge Province the Rome formation typically forms the hanging wall (upthrust block) of the major thrust sheets.

A typical geologic cross section showing the geologic structure on a northwest to southeast transect across the ORR is shown in Fig. 3.2. The West Chestnut Ridge Site is located in the Whiteoak Mountain thrust sheet, so named because movement along the Whiteoak Mountain fault (Fig. 3.1) carried the bedrock beneath the site into the present configuration.

#### 3.2 STRATIGRAPHY AND AREAL GEOLOGY

The bedrock units which underlie the West Chestnut Ridge Site are predominated by carbonate rocks in the Conasauga and Knox Groups. A stratigraphic column, including the formations that occur on the site, is presented in Fig. 3.3. Estimated formation thicknesses and bedrock descriptions based on limited sample availability are included. The stratigraphic nomenclature adopted in this study uses the recognized formation names for the area (Rodgers 1953; Heller 1959; Swingle 1964). Departures from other stratigraphic descriptions apply in the cases of

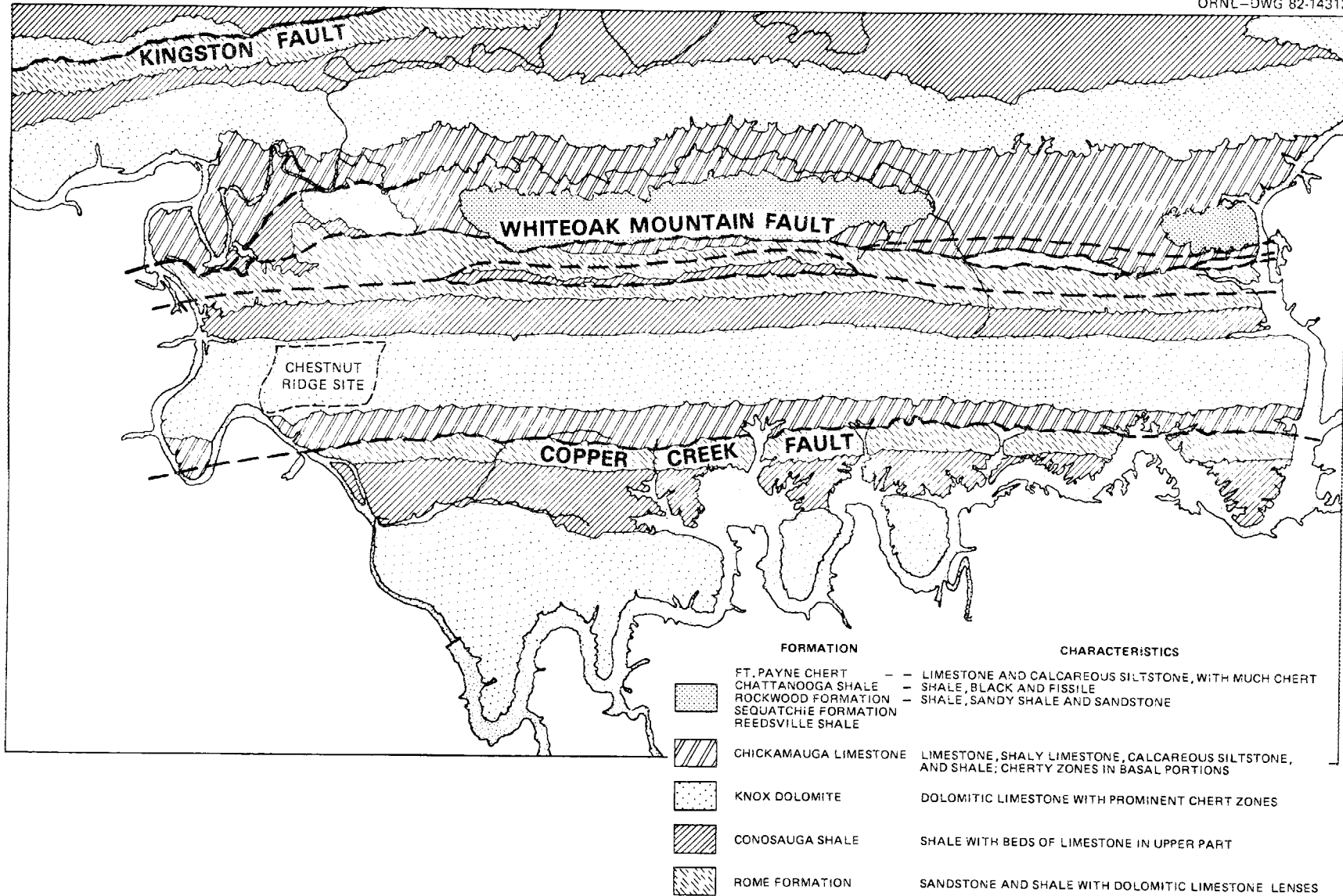


Fig. 3.1. Geological map of the Oak Ridge Reservation.

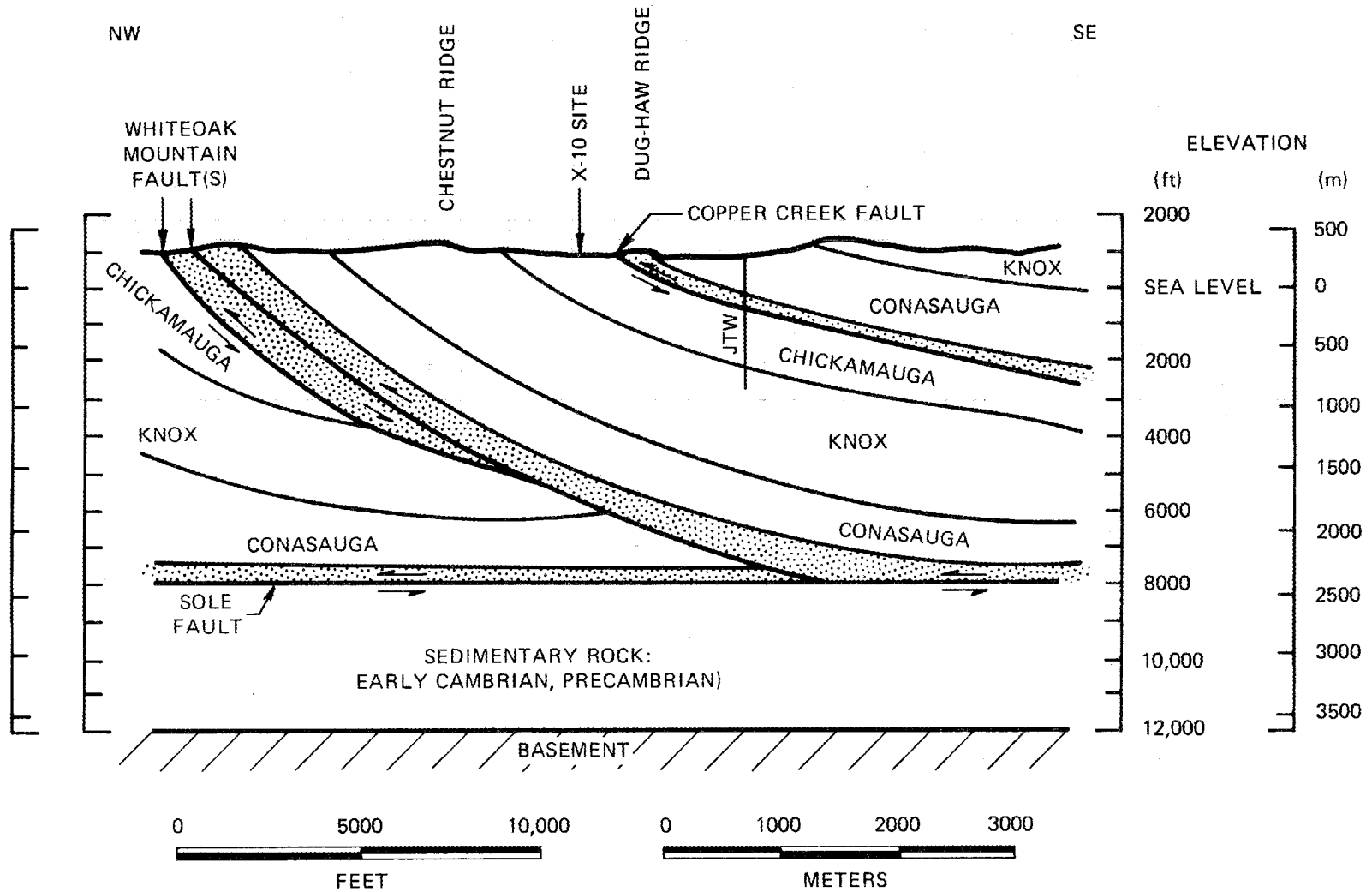


Fig. 3.2. Geologic cross section through the Oak Ridge Reservation.

Fig. 3.3. Stratigraphic Column of Bedrock Formations on the West Chestnut Ridge Site

System	Group	Formation	Estimated thickness	Description
Ordovician	Chickamauga	Undivided		Thin- to medium-bedded, cherty carbonate lithologies. Maroon mudstone and argillaceous limestones.
	Knox	Newala	275 m (900 ft)	Medium-bedded dolostones and limestones with variable chert content, scattered chert matrix sandstones. Abundant maroon mottling in carbonates. Thin soil development.
		"Longview"	15 m (50 ft)	Dense massive chert, bedded chert, and dolomoldic chert observed in residuum.
		Chepultepec Dolomite	215 m (700 ft)	Fine- to medium-grained, light to medium gray, crystalline dolostone, medium- to thick-bedded where observed, sandy in part, particularly near base. Minor maroon mottling appears near top. Thin to thick soil development.
Cambrian		Copper Ridge Dolomite	300 to 400 m (1000 to 1300 ft)	Medium- to thick-bedded, fine to coarse crystalline dolostone, medium to dark gray chert varies from massive porcellanous near base to blue-gray oolitic in upper 1/3 of the unit. Thin to thick soil development.
	Conasauga	Maynardville Limestone	60 to 90 m (200 to 300 ft)	Medium-bedded, light to dark gray, fine crystalline to oolitic limestone. Moderately thick soil development.

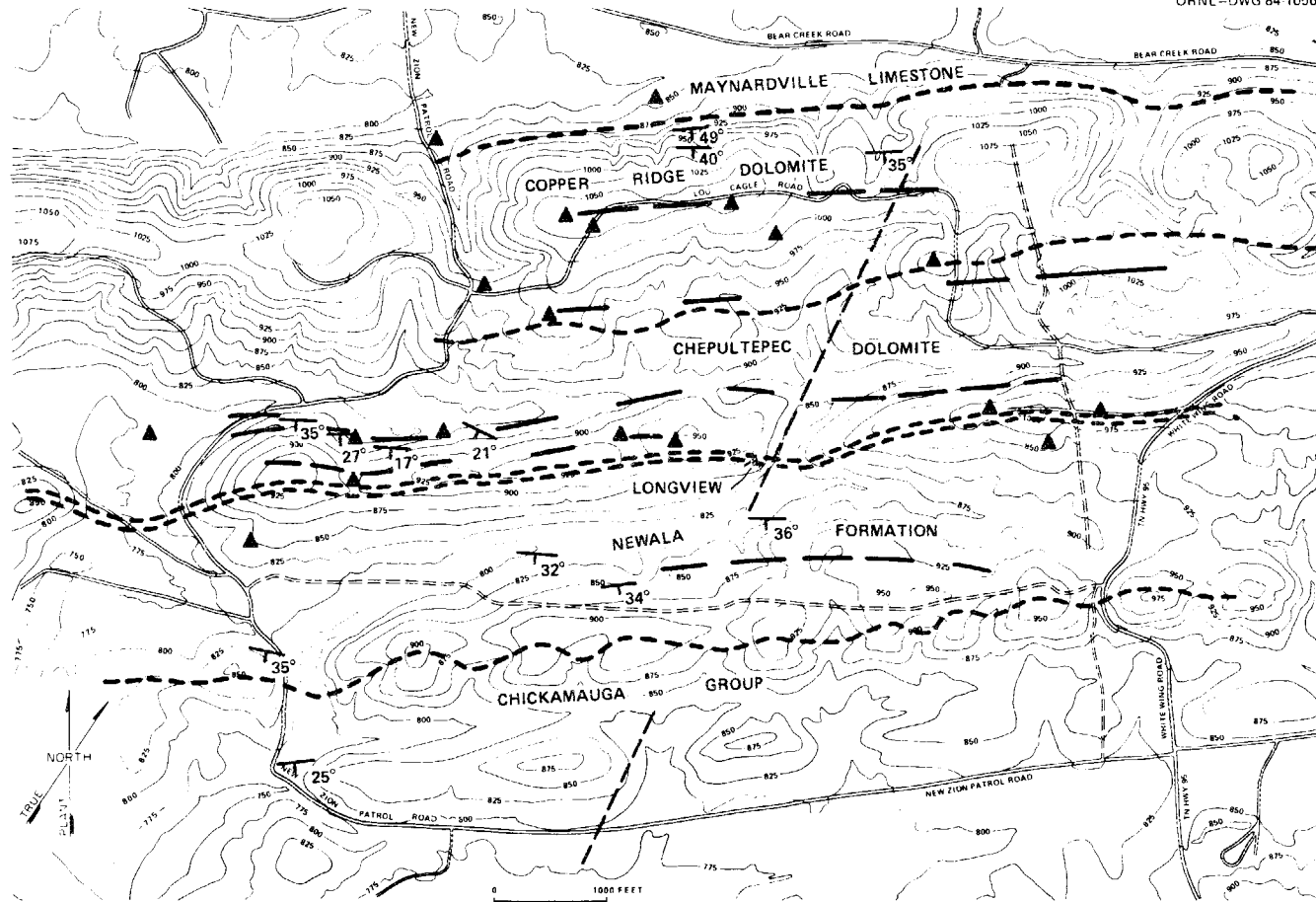
the Longview Dolomite and the Newala Formation. In the Chestnut Ridge strike belt the Longview is a bedded chert zone approximately 10 m thick, which is locally exposed by road cuts in the residuum. The Longview horizon is discontinuous and is not recognized as a mappable formation by the Tennessee Division of Geology (Brendt 1984). However, the heavy chert zone in soils is readily traceable for use in surface mapping and provides a control horizon at the top of the Chepultepec Dolomite. Elsewhere, the Newala Formation is recognized as the Kingsport and Mascot Formations. Generally thick soil development over the bedrock hampers extensive, detailed stratigraphic study. Inspection of rock chip samples from rotary drill holes in bedrock indicates that wide lithologic variations occur within each formation.

An areal geologic map of the site is shown in Fig. 3.4. The figure also shows locations of exploratory boreholes. Formation contacts are approximately located based on the identification of marker lithologies in residuum and rock chips from boreholes. The traces of the karst zones identified in Sect. 2.3 are also plotted on Fig. 3.4. The karst zones generally parallel the regional strike. The approximate location and orientation (N10°W) of a cross cutting structural feature identified on aerial photographs and in soil mapping is shown. This feature may be a tear fault or fracture zone related to differential movement of structural blocks within the Whiteoak Mountain thrust sheet.

### 3.3 STRUCTURAL GEOLOGY

Outcrops are sparse on the site; however, about a dozen strike and dip measurements were obtained during field mapping. The mean bedding strike is N57°E (range N45°E to N70°E) and the mean bedrock dip is 31° to the southeast (range 17° to 37°). The scarcity of rock outcrops on-site makes measurement of joint and fold orientations and other structural elements virtually impossible.

Since direct measurement of the orientation of structural features is not possible on the site, an alternative approach has been used to infer the orientations of bedrock structural features. The method used includes the compilation of bedrock data from other areas, orientation



- APPROXIMATE GEOLOGIC CONTACTS
- ALIGNMENT OF KARST ZONES
- ALIGNMENT OF A POSSIBLE FRACTURE ZONE
- ⊥ 37° STRIKE AND DIP OF BEDDING
- ▲ BORE HOLE LOCATION

Fig. 3.4. Areal geologic map of the West Chestnut Ridge Site.

data for linear erosional features in the Knox residuum, straight stream alignments, and the elongation of karst features and photolinear features. The underlying premise of this analytical approach is that penetrative faults, fractures, and joints in the carbonate bedrock provide locations for enhanced groundwater flow and are the features that control subsurface flow in the bedrock. Where structural or lithologic weaknesses are widened by dissolution of the rock, the overlying residuum can ravel or pipe into the flow conduit. Over prolonged time periods the progressive undermining of residuum by the underflow can carry substantial volumes of soil away, thus creating topographic expression along the trace of the feature (Parizek 1976). Supporting studies in the analysis include work performed by Smith and Gilbert (1983) and Crider (1981). Their studies are summarized below.

Bedding and joint orientations were measured by Smith and Gilbert (1983) at the Kerr Hollow quarry, which is excavated in the Newala Formation approximately 14 km (8.5 miles) northeast of the West Chestnut Ridge Site. Eighty-three planar orientations were measured, and the results indicate that the bedding orientation is fairly consistent at N48°E with a 35° dip to the southeast. Joint orientations at the Kerr Hollow quarry showed a wide scatter of northwest-dipping strike set joints and conjugate northeast- and southwest-dipping dip joints. Joint and fracture orientation maxima from Smith and Gilbert (1983) are tabulated in Table 3.1.

Crider (1981) collected bedrock joint and fracture orientation data in the Walker Branch Watershed, which lies on Chestnut Ridge approximately 7 km (4.4 mi) northeast of the West Chestnut Ridge Site. He compared joint and fracture orientations with photolinear data and derived hypothetical orientations for preferred groundwater flow paths. Joint and fracture orientation maxima from Crider (1981) are listed in Table 3.1.

Comparison of the maxima presented in Table 3.1 shows that, at the two study areas, different joint sets are prominent. However, if data groups are delineated from histogram plots, similarities in the overall joint and fracture orientations appear between the two data sets. Prominent joint sets occur in groups oriented approximately parallel to

Table 3-1. Comparison of bedrock joint and fracture orientations  
in two study areas on Chestnut Ridge

Maxima	Orientation ranges	
	Smith and Gilbert	Crider
Primary	N70°-80°E	N20°-25°W N30°-35°W
Secondary	N40°-50°W	N55°-60°E N40°-45°W N25°-30°W
Tertiary	N30°-40°E N60°-70°E	N10°-15°E N50°-55°E N75°-85°E N10°-15°W N60°-65°W N75°-85°W
Joint and fracture orientation groups		
	N60°E-N110°E	N75°E-N105°E
	N30°E-N50°E	N40°E-N60°E
	N20°W-N20°E	N15°W-N20°E
	N40°-50°W	N20°-45°W

strike, approximately north-south, approximately perpendicular to strike, and approximately east-west.

Orientations of photolinear features on the West Chestnut Ridge Site are grouped in four sets as follows:  $N20^{\circ}W$  to  $N30^{\circ}E$ ,  $N70^{\circ}$  to  $110^{\circ}E$ ,  $N50^{\circ}$  to  $60^{\circ}W$ ,  $N30^{\circ}$  to  $50^{\circ}E$ . Crider's data on photolinear orientation for Chestnut Ridge suggest groups with orientations as follows:  $N20^{\circ}$  to  $30^{\circ}E$ ,  $N40$  to  $55^{\circ}E$ ,  $N80^{\circ}$  to  $110^{\circ}E$ ,  $N40^{\circ}$  to  $50^{\circ}W$ . The major difference between the two data sets is that Crider's data do not show a strong north-south group, as does the West Chestnut Ridge Site study. This variation may be due to differences in imagery used or to the difference in results obtained by different observers. A comparison of Crider's data on fracture orientation based on straight stream segment analysis and an analysis of erosional topographic features on Chestnut Ridge between the Clinch River and Walker Branch shows strong similarities with maxima occurring in groups, as shown in Fig. 3.5 and summarized as follows:  $N10^{\circ}$  to  $40^{\circ}W$ ,  $N60^{\circ}$  to  $80^{\circ}W$ ,  $N0^{\circ}$  to  $10^{\circ}E$ ,  $N30^{\circ}$  to  $60^{\circ}E$ ,  $N80^{\circ}$  to  $90^{\circ}E$ .

Synthesis of this information leads to the following conclusions regarding bedrock fracture orientations.

1. Orientation measurements for bedrock joints and fractures can be divided into four groups or families (Table 3.1).
2. Measurements of photolinear features interpreted to be fracture traces yield generally similar information, though the results are variable between different study areas.
3. Erosional features and straight stream segments yield comparable orientation data when analyses for a detailed study area and a general study area are compared.
4. Cross-cutting structural features in the Chestnut Ridge strike belt generally occur in four orientation groups, as follows:
  - approximately parallel to bedding strike ( $N30^{\circ}$  to  $60^{\circ}E$ ),
  - approximately perpendicular to strike ( $N20^{\circ}$  to  $50^{\circ}W$ ),
  - approximately North-South ( $N10^{\circ}$ - $20^{\circ}W$ - $N20^{\circ}E$ ), and
  - approximately East-West ( $N60^{\circ}$ - $70^{\circ}E$ - $N110^{\circ}E$ ).
5. The prominence of a particular structural feature varies areally.

## CHESTNUT RIDGE TOPOGRAPHIC LINEARS

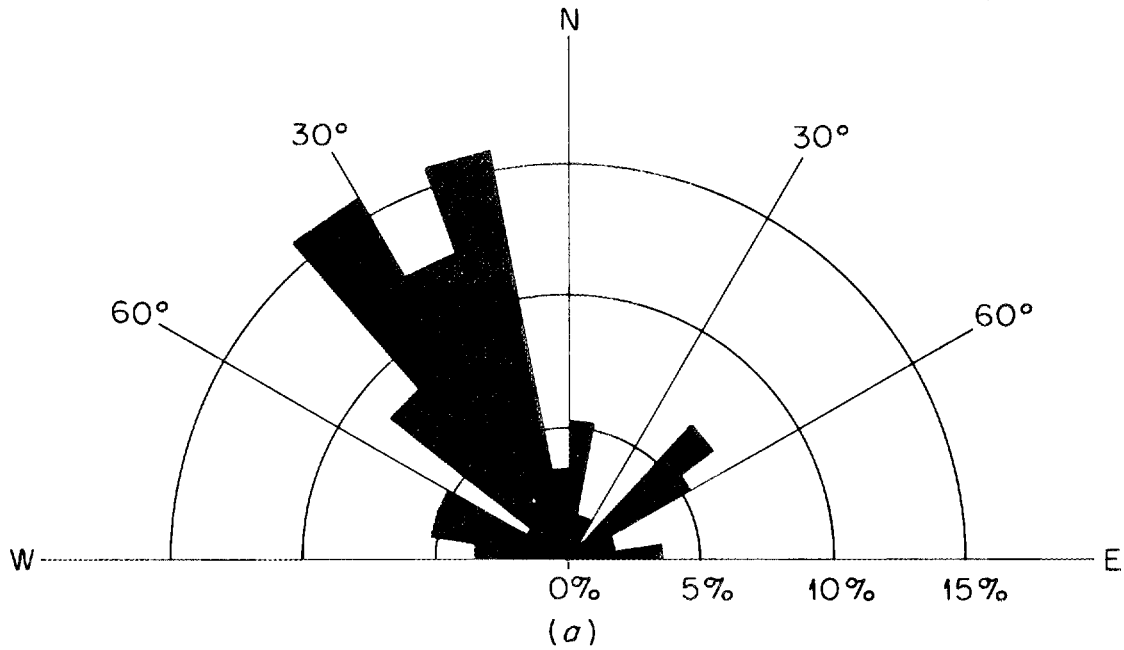
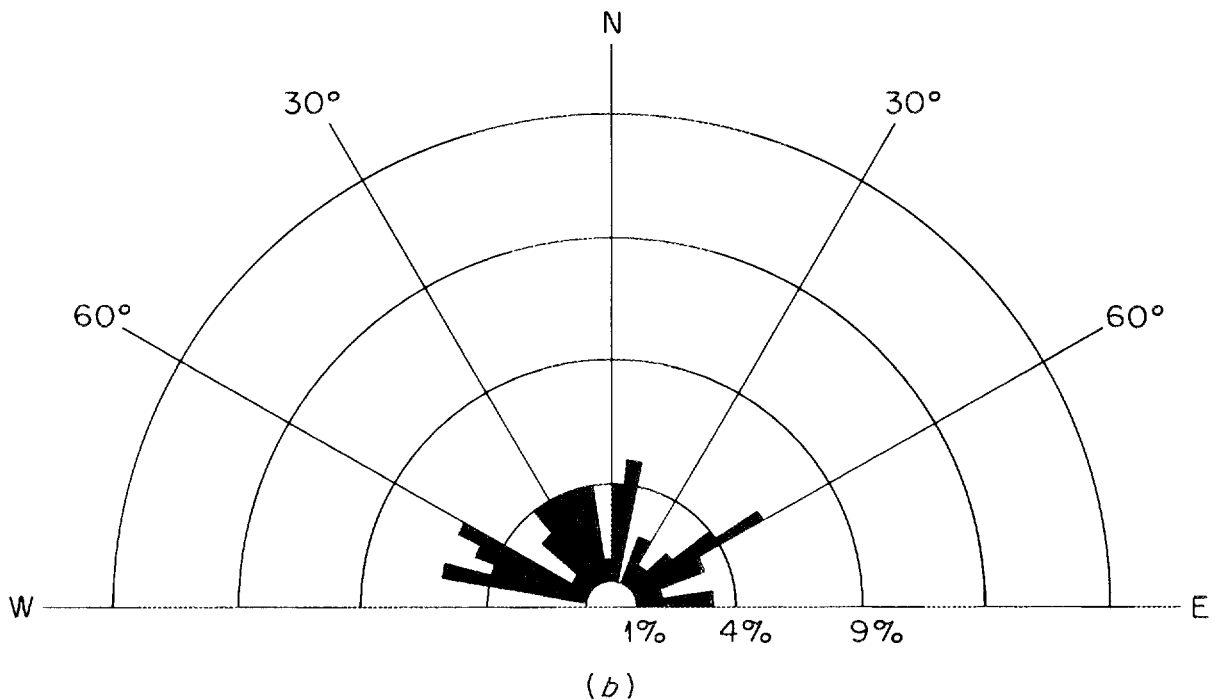
STRAIGHT STREAM SEGMENT ORIENTATIONS  
WALKER BRANCH WATERSHED

Fig. 3.5. Comparison of (a) topographic linear features and (b) straight stream segment orientations.

6. The detection of structural features in the residual soils by imagery interpretations and topographic analyses provides variable results, depending on the data quality, but does provide a useful tool in areas lacking bedrock outcrop.

### 3.4 BEDROCK CHARACTERISTICS

Bedrock investigations on the West Chestnut Ridge Site have been oriented toward evaluating the condition of bedrock and the extent of weathering. Bedrock investigations completed to date include

- o completion of 20 exploratory boreholes using the air rotary drilling technique to explore the weathered bedrock zone (geophysical logs were obtained from the bedrock exploratory boreholes), and
- o a seismic refraction profiling technique which provided data on bedrock conditions between borehole locations.

The criteria used in determining the drilling depths for the exploratory borings were to penetrate 9 m (30 ft) of continuous "sound" bedrock; however, if continuous rock was not encountered within 30 m (100 ft) of the first rock penetrated, the boring was terminated. Of the 20 bedrock exploratory borings completed, continuous rock was obtained in 13 borings, and more than 30 m (100 ft) of cavitose rock was encountered in 7 borings. Driller's logs for the bedrock borings are included as an appendix of the Woodward-Clyde report on subsurface characterization (1984).

Seismic refraction profiling of the bedrock surface was performed by personnel of the Tennessee Valley Authority. A detailed report of their work is in press (Staub and Hopkins 1984). The seismic refraction survey showed the elevation of the top of the refractive layer on 7.6 m (25 ft) spacings. The accuracy of the elevations is approximately  $\pm 3$  m (10 ft). In general, the data interpretation suggests that the weathered bedrock surface approximately coincides with the refractive surface. Over short intervals [40 m (130 ft)], relief on the refractive surface up to 10 m (30 ft) was measured in several areas. One of the profile lines which crossed the fracture trace (Sect. 3.2) where it

crosses the Copper Ridge Dolomite showed deeper weathering of bedrock. In general, the seismic profiling shows rather consistent elevation of the refractive surface within the study areas.

On the basis of data obtained during exploratory drilling activities and seismic profiling, the site bedrock conditions are defined as follows. Residual soils of variable thickness typically overlie a zone of cavitose carbonate bedrock with mud- and gravel-filled cavities. The thickness of this cavitose zone ranges from 0 to >30 m (0 to >100 ft). Vertical cavity dimensions reported by the driller range from 0.3 m to 5 m (1 to 16 ft). The configuration of the top of the zone of cavitose bedrock is approximated by the contours shown on Fig. 3.6. Residual soils above this zone are essentially devoid of carbonate minerals, so it also represents the approximate surface of carbonate rock.

As previously mentioned, in 13 of the exploratory boreholes at least 9 m (30 ft) of continuous bedrock was encountered. While 9 m of continuous rock drilled does not preclude the existence of underlying cavities, it suggests that the most active weathering zone has been penetrated. Figure 3.7 shows the approximate configuration of the top of the continuous rock based on drilling results. The stratigraphic distribution of boreholes that penetrated more than 30 m (100 ft) of cavitose bedrock and the configuration of the bedrock surface indicates that weathering is deepest in the Chepultepec Dolomite and in the upper 1/3 to 1/2 of the Copper Ridge Dolomite. Figure 3.8 shows a generalized geologic profile across the site. The figure includes the ranges obtained for the top of weathered and continuous bedrock zones and approximate formational contacts.

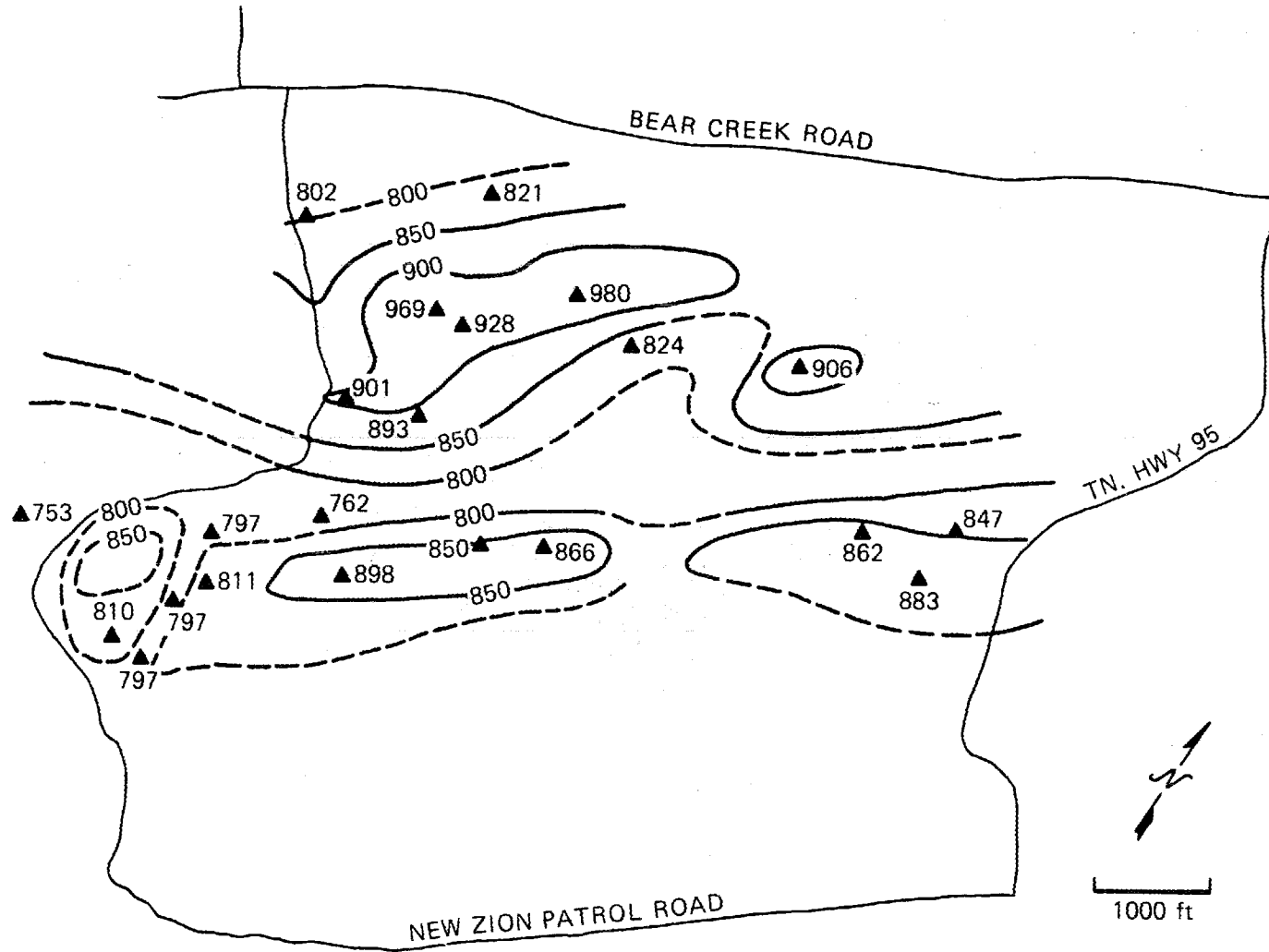


Fig. 3.6. Approximate configuration of the top of the weathered bedrock zone.

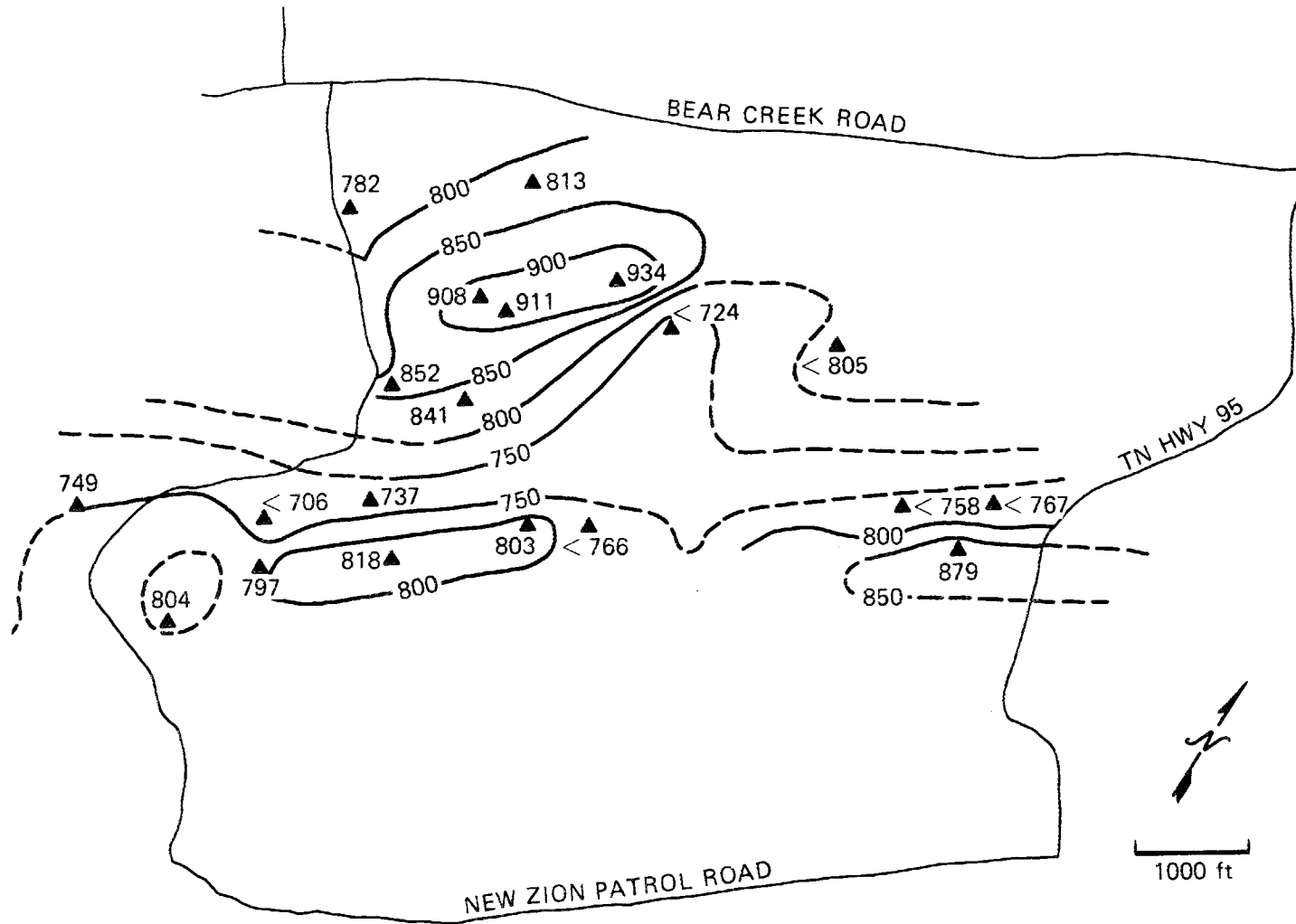


Fig. 3.7. Approximate configuration of the top of continuous bedrock.

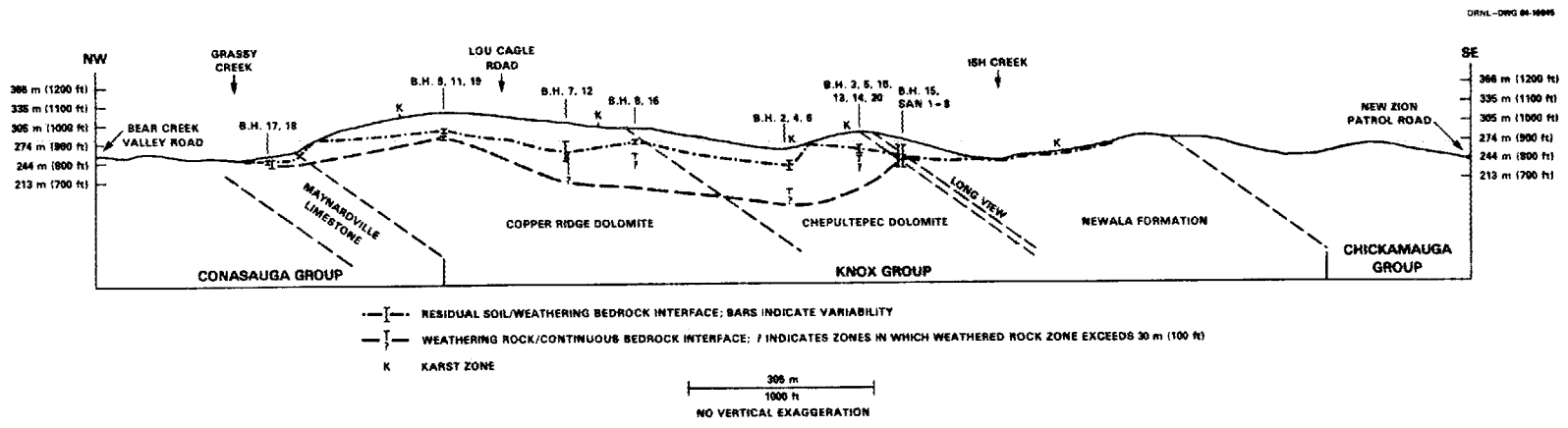


Fig. 3.8. Generalized geologic profile through the West Chestnut Ridge Site.



## 4. SOILS

Soil investigations performed in the site characterization include

- o soil mapping,
- o drilling and sampling to obtain samples for testing and to determine soil thickness,
- o physical testing of soils,
- o mineralogic testing, and
- o radionuclide adsorption testing.

Voluminous amounts of data have been obtained and are reported elsewhere (Woodward-Clyde 1984; Lee et al. 1984; Seeley and Kelmers 1984; Geotek 1981). The objective of this section is to present the salient aspects of the site soil characteristics.

### 4.1 PHYSICAL PROPERTIES OF SITE SOILS

This section summarizes the physical characteristics of Knox Group residuum. The discussion will include the mapping and classification of surficial soils, classification of subsurface soils, grain size characteristics, moisture and weight characteristics, and soil strength characteristics.

#### 4.1.1 Characteristics of Surficial Soils

Surficial soils on the site were mapped (Lee et al. 1984) as shown in Fig. 4.1. Table 4.1 identifies the soil types shown on the soils map. Soils mapped on the site are predominantly Paleudults, though areas of Entisols and Inceptisols were mapped where recent alluviation has occurred. Soil genetic classes identified during site mapping include soils formed by ancient alluvial processes, soils formed by residual weathering of bedrock, soils formed by Pleistocene alluvial/colluvial processes in the residuum, and recent alluvium. The range of the age of soil formation on-site extends from late Tertiary or early Pleistocene [ $10^6$  yr (soil No. 3)] to Holocene or Recent [PostEuropean settlement (soil No. 6)] (Lee et al. 1984). Soil forming and erosional processes

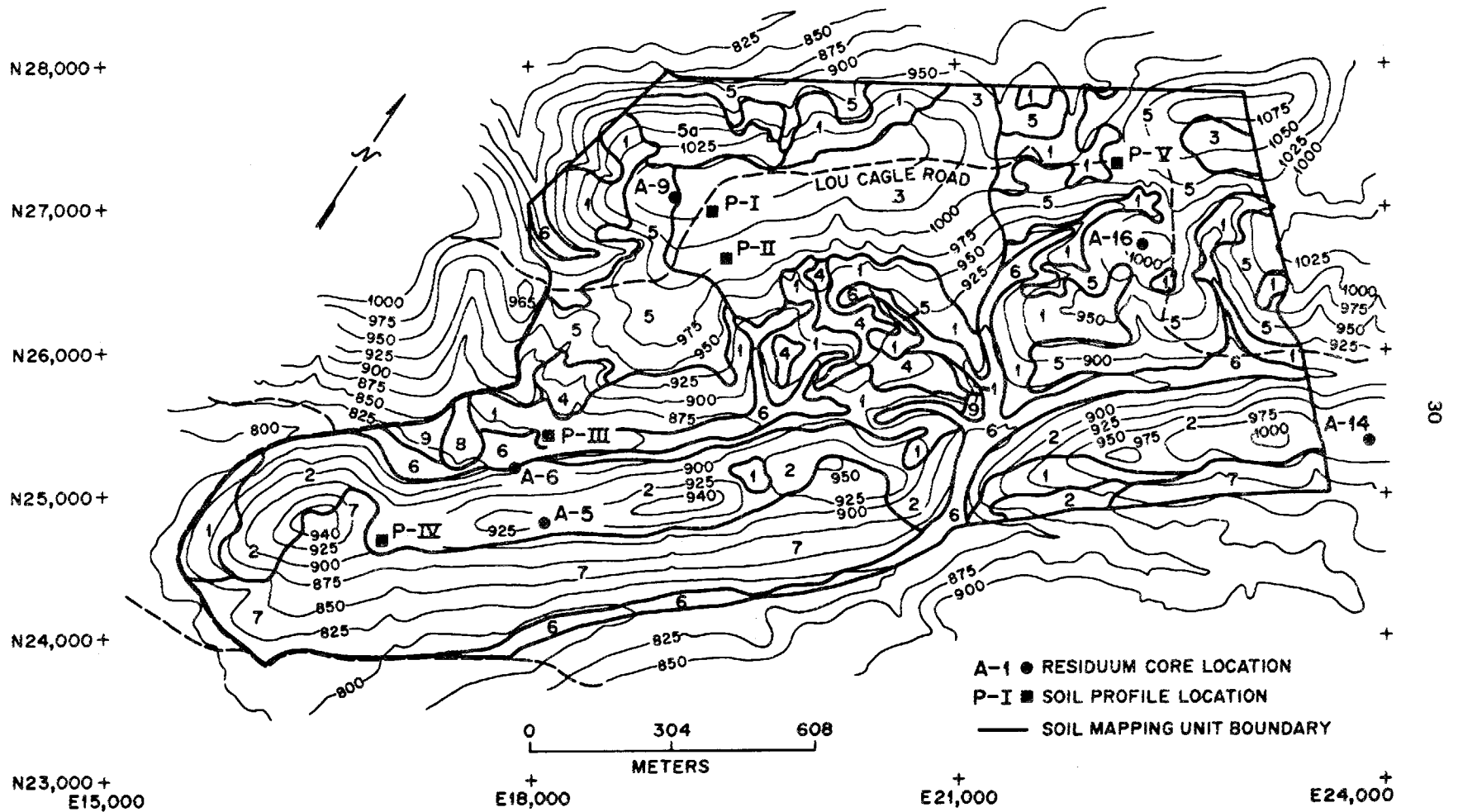


Fig. 4.1. Soil survey map of the West Chestnut Ridge Site.

Table 4.1. Classification of soils in the proposed Central Waste Disposal Area

Soil No.	Classification	Series
1	Fine loamy, siliceous, thermic, Fragic Paleudult	Shack
2	Clayey skeletal, mixed, thermic, Typic Paleudult	a
3	Fine loamy, oxidic, thermic, Typic and Rhodic Paleudults	Dewey and Decatur variants
4	Clayey, mixed, thermic, Paleudults	a
5, 5a	Clayey, mixed, thermic, Paleudults	a
6	Entisols and Inceptisols - undifferentiated	a
7	Fine loamy, siliceous and clayey, kaolinitic Typic Paleudult	a
8	Fine loamy, siliceous thermic, Paleudults	Holston
9	Fine loamy, siliceous, thermic, Paleudults	Etowah

a - Series is not determined.

Note: Soils 2, 5, 5a, and the clayey part of 7 would have been included in the Fullerton Series of past mapping. They are now variants because of mixed clay mineralogy, lack of sufficient chert in the family control section, or yellow mottling in the subsoil too close to the surface. These soils were also kept separate in order to evaluate whether individual dolomite formations gave rise to similar or dissimilar soils.

are discussed in Sect. 4.4. Residuum derived from each geologic formation on the site is distinct, as shown in Fig. 4.1 (Lee et al. 1984). Soil mapping corroborated the existence of a linear discontinuity trending north-south across the site. The feature identified in soil mapping coincides with the possible fracture trace identified on 1939 aerial photography and discussed in Sect. 2.2.

#### 4.1.2 Characteristics of Subsurface Soils

Particle size distribution analyses were performed on 115 subsurface soil samples (Woodward-Clyde 1984). Site soils are fine grained with 30 to 100% passing the No. 200 sieve (0.074 mm). The clay-size particle content (<0.002 mm) of soils tested ranged from about 10 to 70%. The sand and gravel content of residuum samples tested ranged from 0 to 50%. Some samples obtained from karst features tended to be sandy, with sand and gravel contents reaching as much as 80% in two such samples.

The site soils classify (Unified Soil Classification System) predominantly as highly plastic clays (CH) with traces to some fine to coarse sand and traces of chert gravel. The second most common classification encountered is low-plasticity clays (CL). Minor amounts of silts (ML, MH) and clayey sands and gravels (SC, GC) were encountered. Surficial soil samples commonly classify as low-plasticity clays. Consistent relationships between soil classification and bedrock stratigraphy are not readily apparent in soils tested. The sandy bedrock zone in the basal Chepultepec Formation did seem to result in a sandy soil at one of the test locations.

Physical properties of soils are summarized in Tables 4.2 and 4.3. Soil engineering parameters are included in the report on subsurface investigations (Woodward-Clyde 1984). Engineering tests included consolidation, compaction, triaxial shear, and unconfined compressive strength.

Site soils have very high moisture retention properties (Daniels and Broderick 1984). The percent saturation of soils vs depth below the ground surface is plotted in Fig. 4.2. This plot shows that the depth

Table 4.2. Summary of index and physical properties for Shelby tube samples

Index or physical property <sup>a</sup>	Units	Depths less than 3.0 m (10 ft)		Depths greater than 3.0 m (10 ft)	
		Range	Average	Range	Average
Initial water content	Percent	15.0 to 36.6	25.9	19.0 to 47.8	33.5
Initial volumetric water content	Percent	27.8 to 48.2	38.5	32.7 to 56.1	46.2
Liquid limit	Percent	41 to 87	66	46 to 101	69
Plasticity index	Percent	21 to 53	39	15 to 69	41
Initial liquidity index		-0.25 to 0.03	-0.06	-0.11 to 0.84	0.19
Percent chert	Percent	0.0 to 21.1	5.8	0.0 to 26.2	4.6
Percent fines	Percent	58.0 to 99.0	80.2	59.5 to 99.4	85.3
Specific gravity	g/cm <sup>3</sup>	2.66 to 2.82	2.73	2.68 to 2.84	2.74
Initial total unit weight <sup>b</sup>	lb/ft <sup>3</sup>	104.0 to 129.9	119.2	108.5 to 127.9	117.5 <sup>b</sup>
Initial degree of saturation	Percent	73.0 to 99.7	87.8	89.8 to 100.0	96.5

<sup>a</sup> Excluding data on samples from sink hole borings.

<sup>b</sup> Average value for all samples = 117.9 lb/ft<sup>3</sup> (18.52 kg/m<sup>3</sup>).

Table 4.3. Summary of index and physical properties from the engineering property test series

Index or physical property <sup>a</sup>	Units	Com- paction	Consoli- dation	Strength		Sat. Perm. series	M/S & Part. Sat. Perm. series	Part. Sat. Perm. series
				UU	CIU			
Initial water content	Percent	21.3	35.4	32.6	33.6	34.0	29.5	22.5
Initial volumetric water content	Percent		48.0	45.8	46.0	46.8	41.1 <sup>b</sup>	40.4
Liquid limit	Percent	59	62	71	65	62	71	60
Plasticity index	Percent	36	35	43	37	36	43	34
Initial liquidity index		-0.05	0.26	0.09	0.13	0.26	0.01	0.07
Percent chert	Percent	11.5	7.0	8.2	3.2	4.5	5.1	5.1
Percent fines	Percent	66.9	82.2	82.3	86.0	86.7	84.4	72.2
Specific gravity	g/cm <sup>3</sup>		2.75	2.74	2.76	2.73	2.74	2.71
Initial total unit weight <sup>c</sup>	lb/ft <sup>3</sup>		116.0	118.6	117.6	116.9	115.8 <sup>b</sup>	122.4 <sup>b</sup>
Initial degree of saturation	Percent		96.7	96.9	97.0	96.7	87.1 <sup>b</sup>	94.7
Initial void ratio			0.99		0.97	0.96	0.91 <sup>b</sup>	0.74 <sup>b</sup>
Average depth <sup>d</sup>	ft		51.1	17.7	20.5	62.8	9.9	

<sup>a</sup> Excluding data from sink hole borings.

<sup>b</sup> M/S test data is excluded.

ORNL-DWG 84-10833

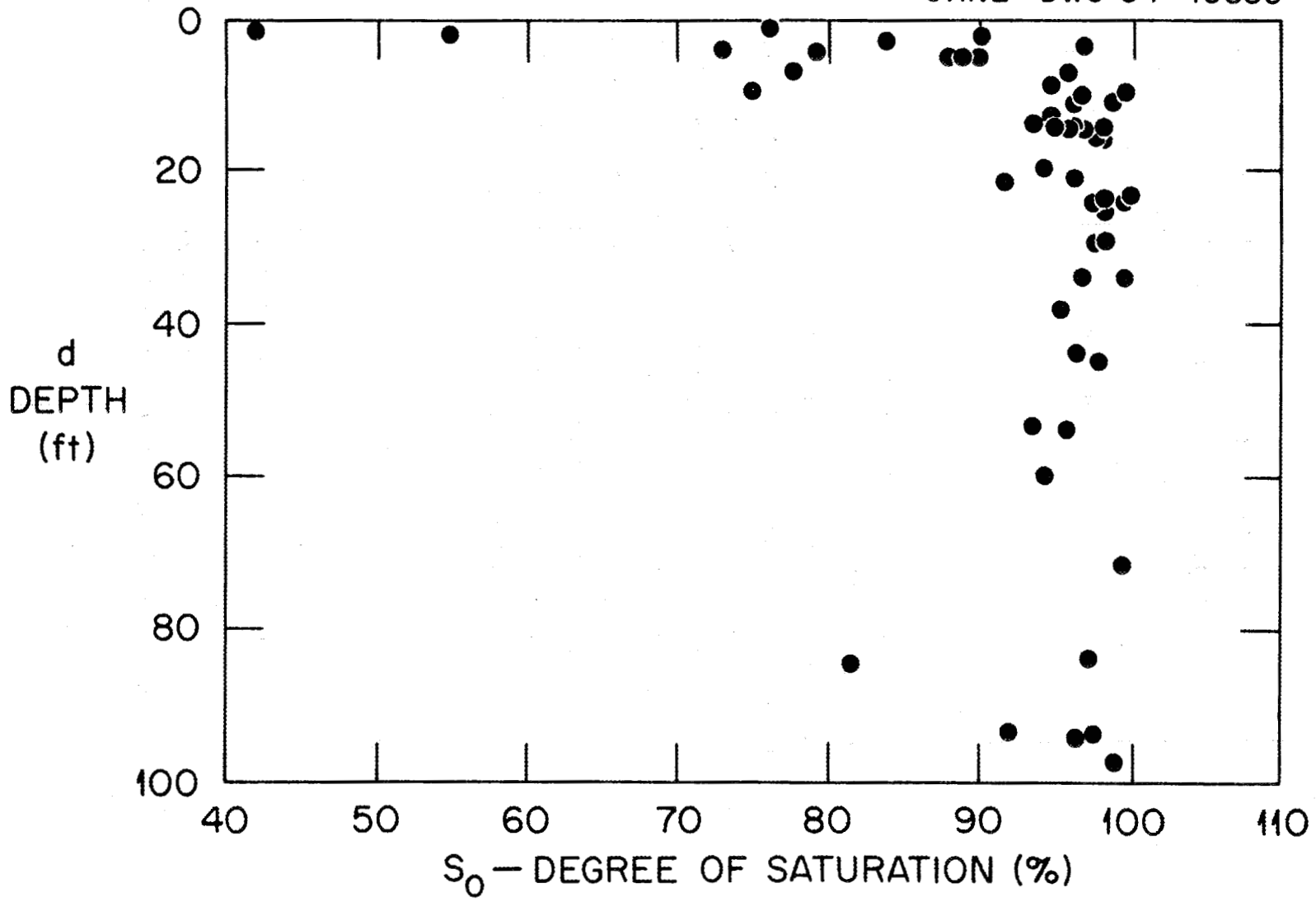


Fig. 4.2. Percent saturation vs soil sample depth.

of significant desiccation of the soils is approximately 3 m (10 ft). Samples used in this analysis were obtained during the dry season (September 1983). Below depths of 3 m (10 ft), the soils are typically >90% saturated.

Soil strength and the liquidity index for site soils show an inverse correlation. Figure 4.3 shows the general trends for the liquidity index ( $I_L$ ) and undrained shear strength ( $S_u$ ). The liquidity index is an expression of the soil's natural moisture content when sampled, compared to the moisture range under which the soil exhibits plastic behavior.

$$I_L = \frac{W - PL}{PI},$$

where

- W = the natural moisture content of the soil,
- PL = the plastic limit for the soil,
- PI = the plasticity index for the soil.

A liquidity index value of 0 indicates that the natural moisture content is below the plastic limit by an amount equal to the moisture range over which the soil exhibits plastic behavior. A liquidity index value of 1 indicates that the natural moisture content of the soil is equivalent to the liquid limit - the point at which the soil behaves as a liquid. Wide scatter occurs in the data as a result of vertical and lateral heterogeneity however, approximations of the variation of mean liquidity index and undrained shear strength with sample depth are shown in Fig. 4.3.

#### 4.2 GEOCHEMICAL CHARACTERISTICS OF SITE SOILS

Geochemical studies of Knox residual soils have included

- o physical characteristics of test specimens,
- o soil chemical analysis,
- o limited analyses of ground and surface waters,
- o measurement of radionuclide sorption and desorption characteristics for soils, and
- o column sorption tests.

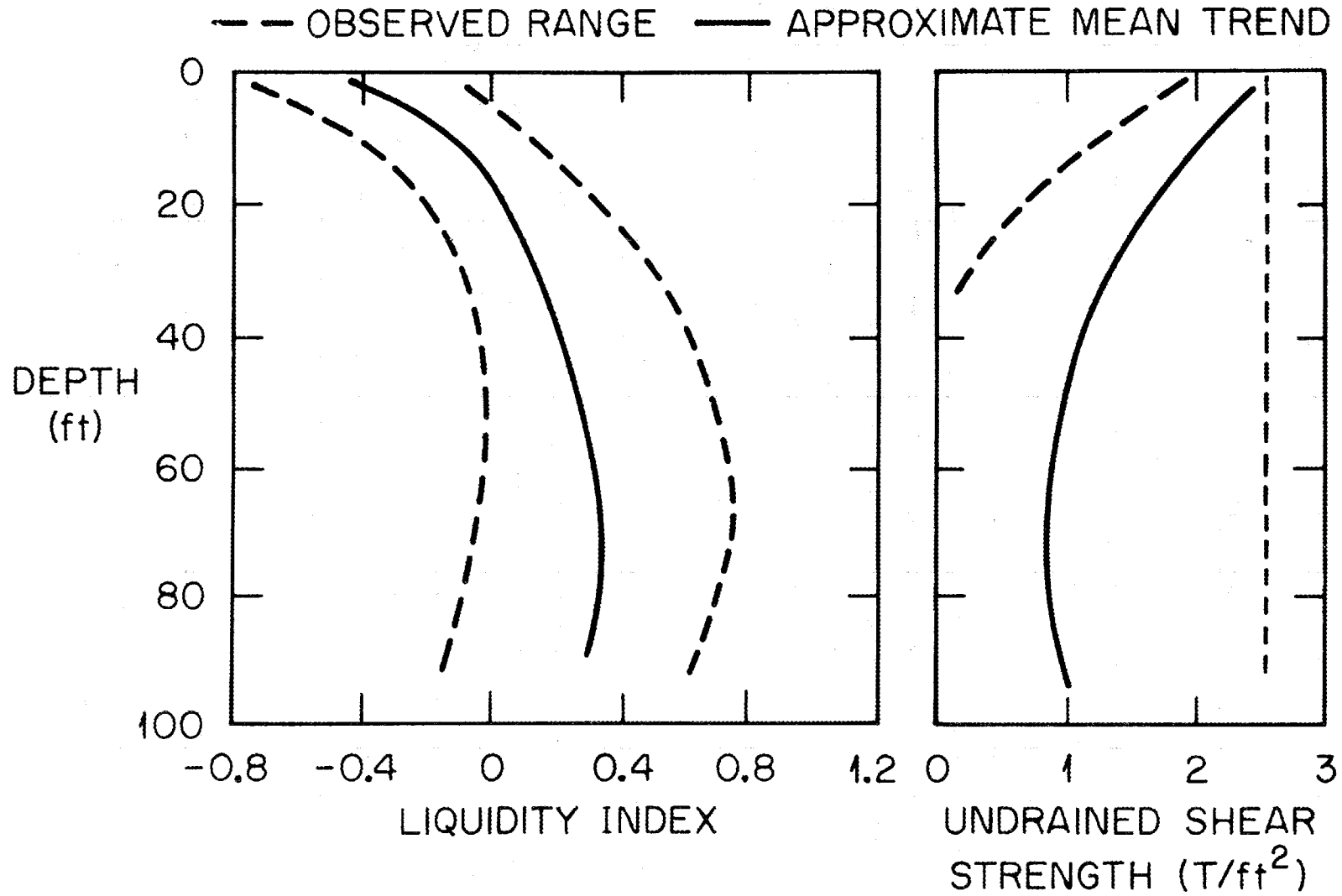


Fig. 4.3. Strength vs depth and liquidity index vs depth plots for Knox residuum on the West Chestnut Ridge Site.

Details of the soil geochemical testing are presented in Seeley and Kelmers (1984), and Lee et al. (1984). Results of selected portions of the soil geochemical study are summarized in this section. Samples were obtained from Copper Ridge Dolomite and Newala Formation residuum.

#### 4.2.1 Physical Characteristics of Test Specimens

Samples obtained for geochemical study were tested to determine the soil moisture content, particle size distribution, particle density, surface area, and mineralogy.

Gravimetric moisture contents ranged from approximately 18 to 31%, which are similar to those reported in Sect. 4.1. Particle size distributions for the study specimens indicate that the tested materials are fine silts and clays. Particle densities ranged from 2.7 to 3.1 g/cm<sup>3</sup>. One sample that had a surface area of 9.8 m<sup>2</sup>/g was apparently a fine silt composed primarily of quartz. The other samples had surface areas ranging from 32.71 to 46.54 m<sup>2</sup>/g and were composed, in descending abundance, of quartz, illite, and kaolinite (Sect. 4.4 presents additional discussion of soil mineralogy).

#### 4.2.2 Chemical Characteristics of Knox Residuum

Residual soils derived from weathering of the Copper Ridge Dolomite and the Newala Formation are heavily leached. They have carbonate contents ranging from 0.12 to 0.35% in the upper 10 m and decreasing to 0.03 to 0.04% with greater depth. The pH of water in equilibrium with residuum is mildly acidic. Elemental analyses of six soil samples are presented in Table 4.4. Uranium and radium values in the soils range from 3.9 to 8.0 µg/g and 2.28 to 4.71 pCi/g, respectively, with average values of 5.5 ± 2.5 µg/g and 3.4 ± 1.3 pCi/g, respectively.

#### 4.2.3 Chemical Characteristics of Soil Water and Surface Water

Data regarding the chemical constituents of soil waters in Knox residuum are based on analyses of soil waters recovered from a borehole

Table 4.4. Elemental Analyses of Knox Residuum from West Chestnut Ridge Site by ICP spectrometry (concentrations are  $\mu\text{g/g}$ , except Si)

Element	Newala Formation			Copper Ridge Dolomite		
	3 m (10 ft)	9 m (30 ft)	12 m (40 ft)	6 m (20 ft)	9 m (30 ft)	18 m (60 ft)
Ag	<4.5	<4.5	<4.5	<4.5	<4.5	<4.5
Al	80,000	110,000	95,000	97,000	26,000	99,000
B	37	31	40	<19	21	21
Ba	78	160	240	76	55	84
Be	1.9	5.1	8.3	2	1.8	3.9
Ca	150	1,400	2,200	350	96	1,100
Cd	7	7.3	7.8	7.1	4.6	5.6
Co	8	48	21	12	36	9.3
Cr	73	64	78	37	15	58
Cu	24	36	30	43	43	49
Fe	35,000	47,000	48,000	45,000	28,000	38,000
Ga	21	<18	<18	20	<18	22
Hf	25	34	34	27	19	28
K	18,000	20,000	2,900	11,000	6,100	14,000
Mg	7,000	8,200	9,700	3,700	2,100	5,000
Mn	140	1,800	1,200	330	2,000	540
Mo	33	51	41	23	27	35
Na	<1,000	<1,000	<1,000	<1,000	<1,000	<1,000
Ni	37	77	71	42	74	58
P	<83	<83	<83	<83	<83	<83
Pb	<65	<65	<65	<65	<65	<65
Sb	<35	<35	<35	<35	<35	<35
Se	<110	<110	<110	<110	<110	<110
Si(%)	32	28	27	31	40	31
Sr	15	24	28	19	6.3	16
Ti	3,700	3,300	2,300	3,000	1,300	3,100
V	80	65	86	88	31	93
Zn	250	480	410	310	26	360
Zr	120	120	120	120	120	120

Source: Seeley and Kelmers 1984.

in Knox residuum at another site on Chestnut Ridge and on synthetic soil water extracted from a composite soil sample of West Chestnut Ridge soils. Preoperational groundwater quality is being monitored and will be published under separate cover.

Soil pH measured on 1:1 soil-water mixtures ranged from 4.1 to 6.7 for surficial soils and from 5.0 to 6.7 for residuum samples (Lee et al. 1984). The pH of ground water obtained from a saturated zone in Copper Ridge Dolomite residuum at a site approximately 6.6 km (4 miles) north-east of this study area ranged from 5.7 to  $6.0 \pm 0.2$ . The pH of a synthetic soil water prepared by mixing a composite soil sample with deionized water was 6.65. Anion and elemental analyses of soil waters show very low values for bicarbonate, chloride, calcium, radium, and silicon. Values for most other parameters were below detection limits for the method used. Table 4.5 shows the analytical results of soil water analyses. The results for natural and synthetic soil water are similar.

Surface waters on the site were low in dissolved constituents on the dates sampled. Temperature, specific conductance, and pH are shown in Table 4.6. (Surface water sample stations correspond to gaging stations - Sect. 6 contains a map showing these locations.) Data in Table 4.6 for September suggest that under low flow conditions waters at stations 1, 2, 3, and 7 receive water which has circulated through weathering bedrock (higher pH and conductance), while water at stations 4, 5, and 6 apparently emanate from sources in the residuum. Under the higher flow conditions of April there is lower contrast between most stations, with the exceptions of stations 1 and 7, which retain high pH and conductance values. Elemental analyses show that calcium and magnesium concentrations are higher in surface waters than in soil waters on the site. The reason for this and the higher pH is that two of the three surface streams on the site receive a portion of their flow from a bedrock aquifer that contributes calcium and magnesium from the gradual dissolution of dolomite and results in the neutral to slightly alkaline pH of the water.

Table 4.5. Dissolved constituents in Knox residuum soil waters  
(concentrations are in  $\mu\text{g/ml}$ )

	Offsite borehole	Synthetic soil water
Anions		
$\text{SO}_4^{-2}$	<4	1
$\text{NO}_3^{-3}$	<4	1
$\text{NO}_2^{-}$	<2	
$\text{F}^{-}$	<1	<1
$\text{Cl}^{-}$	2-24	1
$\text{Br}^{-}$	<5	<1
$\text{PO}_4^{-3}$	<4	<1
$\text{HCO}_3^{-}$	9-12	0.152
$\text{CO}_3^{-}$	0	0
Cations		
Ag	<0.018	0.0407
Al	<0.058	0.104
As		<0.64
B	<0.076	<0.076
Ba	0.029-0.094	0.009
Be	<0.0013	<0.0013
Ca	0.5-2.1	<4
Cd	0.029	<0.009
Co	<0.013	<0.013
Cr	<0.023	<0.023
Cu	<0.032	<0.032
Fe	<0.02	<0.02
Ga	<0.07	<0.07
Hf	0.043	<0.04
K	<4, <0.5	<4
Mg	0.17-1.1	0.162
Mn	0.14-1.5	0.008
Mo	<0.027-0.034	<0.027
Na	2.8-15	0.678
Ni	<0.11	<0.11
P	<0.33	<0.33
Pb	<0.26	<0.26
Se	<0.43	<0.43
Si	3.3-3.5	2.33
Sr	<0.016	<0.016
Ti	0.024-0.026	0.056
V	<0.015	<0.015
Zn	<0.010	
Zr	0.064-0.065	<0.016

Source: Seeley and Kelmers 1984.

Table 4.6. Surface water physiochemical parameters

	Sample station						
	1	2	3	4	5	6	7
	Water temp.(°C)						
4/18/83	9.6	10.1	11.7	10.5	11.1	10.5	10.6
9/11/83	21.5	20.5	23.4	21.3	21.7	22.3	18.4
	Specific Conductance μS/cm						
4/18/83	125	92	50	63	66	26	195
9/11/83	282	229	164	27	54	41	288
	pH						
4/18/83	7.5	6.7	6.3	6.5	6.5	5.9	8.4
9/11/83	7.1	7.3	7.2	6.3	7.0	6.0	7.4

Source: Seeley and Kelmers 1984.

Based on testing performed to date, the Knox soil, rock, and water system seems to be divisible into zones similar to those used in the soil and bedrock characterization. A conceptual model of the site geochemical character includes two zones: the residual soils which have been deeply leached, have mildly acidic pH and low carbonate content; and a zone influenced by the presence of weathering carbonate rock that has generally neutral to alkaline pH and higher Ca, Mg, and soluble carbonates. The contrast between the two zones is expressed by the pH and specific conductance values measured at surface water stations (Table 4.6). The two zones undoubtedly interfinger extensively in the weathering bedrock zone.

#### 4.3 RADIONUCLIDE SORPTION AND DESORPTION CHARACTERISTICS OF KNOX RESIDUUM

Two variations of the conventional batch contact method were used to measure radionuclide sorption isotherms and apparent concentration limits in site soil/ground water systems (Seeley and Kelmers 1984). The two approaches were used because of the unbuffered nature of the Knox residuum soil/water system, which allowed significant pH changes to occur during the test. A few desorption tests were performed to explore sorption-desorption equilibrium. Two column sorption tests were performed to provide a preliminary evaluation of radionuclide multiple speciation effects on the sorption characteristics.

Details of these studies are reported in Seeley and Kelmers (1984) and the results are summarized here. Sorption ratios ( $R_s$ ) obtained for site soils using 5 mg/L initial solution concentrations are summarized in Table 4.7. An increase in the initial solution concentration results in a decrease in the sorption ratio for each radionuclide tested. The ranges in sorption ratio variations for each radionuclide tested under ambient pH conditions (pH was allowed to vary as radionuclide concentration was increased) are shown in Figs. 4.4 through 4.11. Solution pH values ranged from 7 to 4, and pH decreased as initial radionuclide concentration increased. The sorption data obtained under ambient conditions give some indication of how soils in the

Table 4.7. Summary of radionuclide sorption data

Radionuclide (valence)	pH	$R_S$ values <sup>a</sup>	
		Range	L/Kg
U (+6) ( $UO_2^{+2}$ )	5.6 $\pm$ 1.0	Average	3.2E3
		High	2.5E4
		Low	2.5E2
Sr(+2)	6.0 $\pm$ 0.6	Average	6.9E2
		High	1.6E3
		Low	2.0E2
Cs(+1)	5.4 $\pm$ 0.7	Average	3.3E3
		High	1.1E4
		Low	1.1E2
Co(+2)	6.0 $\pm$ 1.0	Average	1.6E3
		High	7.9E3
		Low	7.1E1
Eu(+3)	5.0 $\pm$ 0.7	(one only)	
		High	6.1E4
		Low	6.4E1
Th(+4)	4.0 $\pm$ 0.7	(one only)	
		High	1.1E4
		Low	5.4E0
Tc(-1)	5.1 $\pm$ 0.2	(one only)	
		High	1.6E0
		Low	1.0E0
I(-1)	5.8 $\pm$ 0.6	Average	1.8E-1
		High	1.8E0
		Low	1.4E-2

<sup>a</sup> $R_S$  values are derived from contacts with low initial concentrations of the radionuclide (5 mg/L).

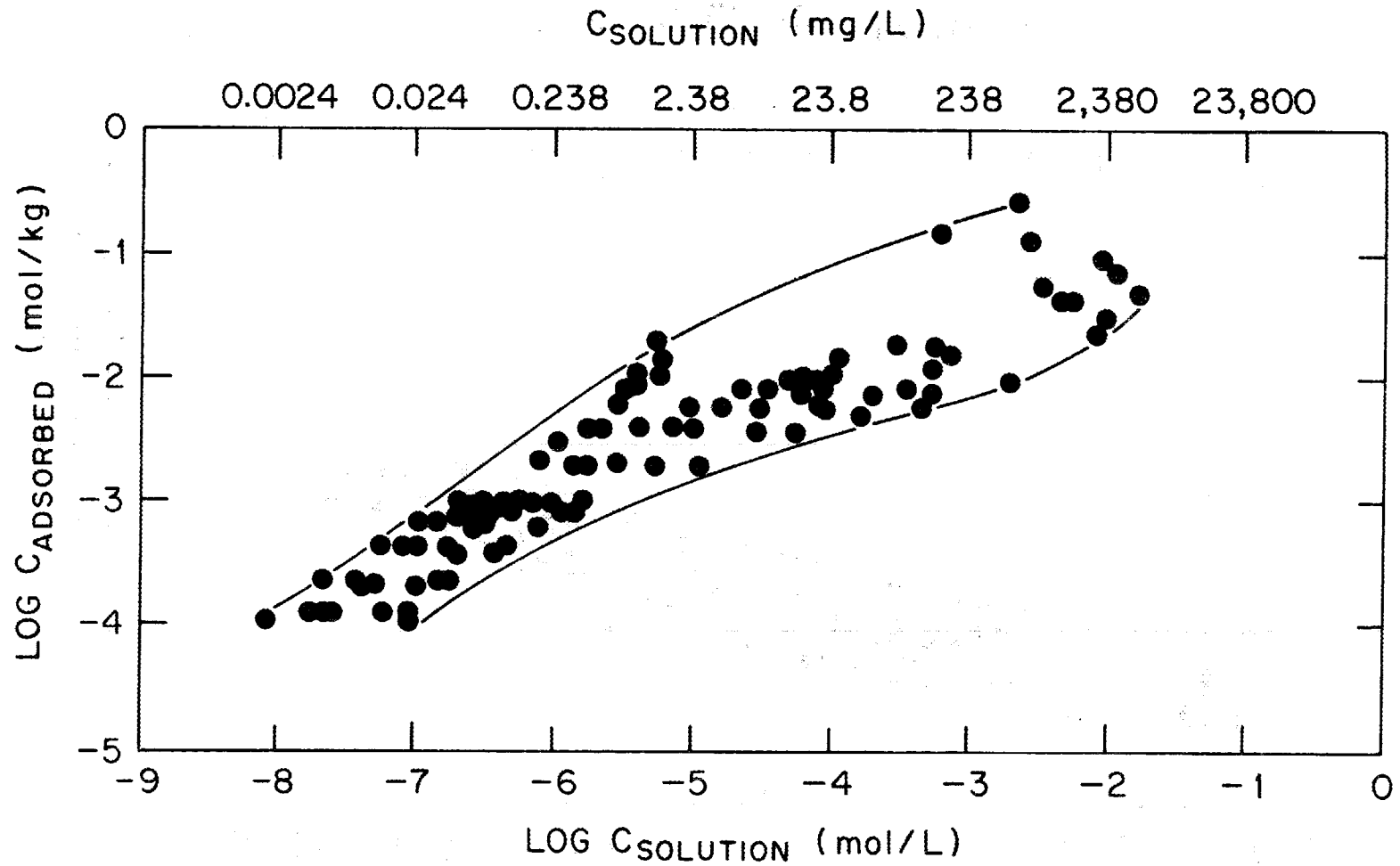


Fig. 4.4. Range of uranium (VI)  $R_S$  values for six soil samples - ambient pH conditions.

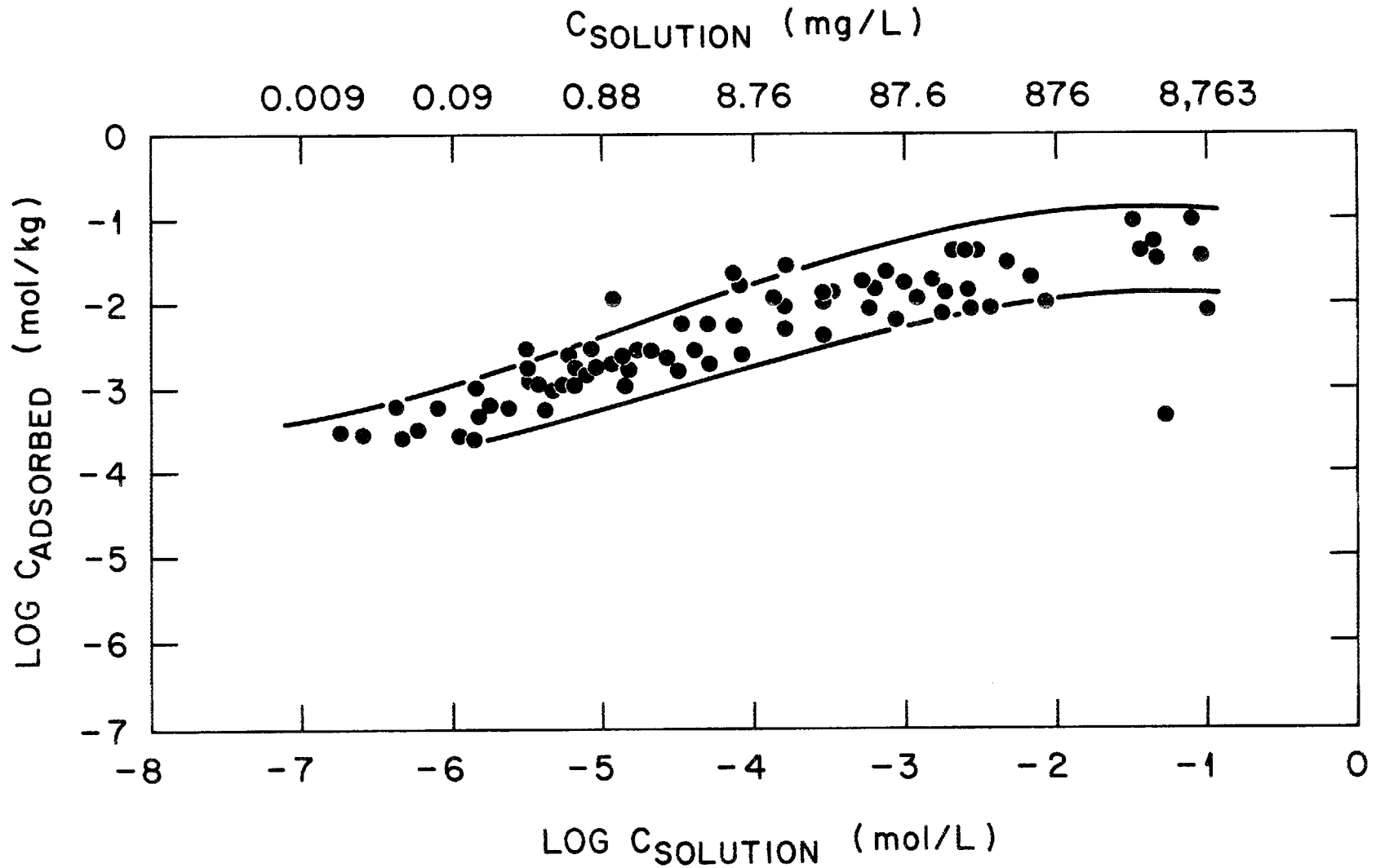


Fig. 4.5. Range of strontium  $R_s$  values for six soil samples - ambient pH conditions.

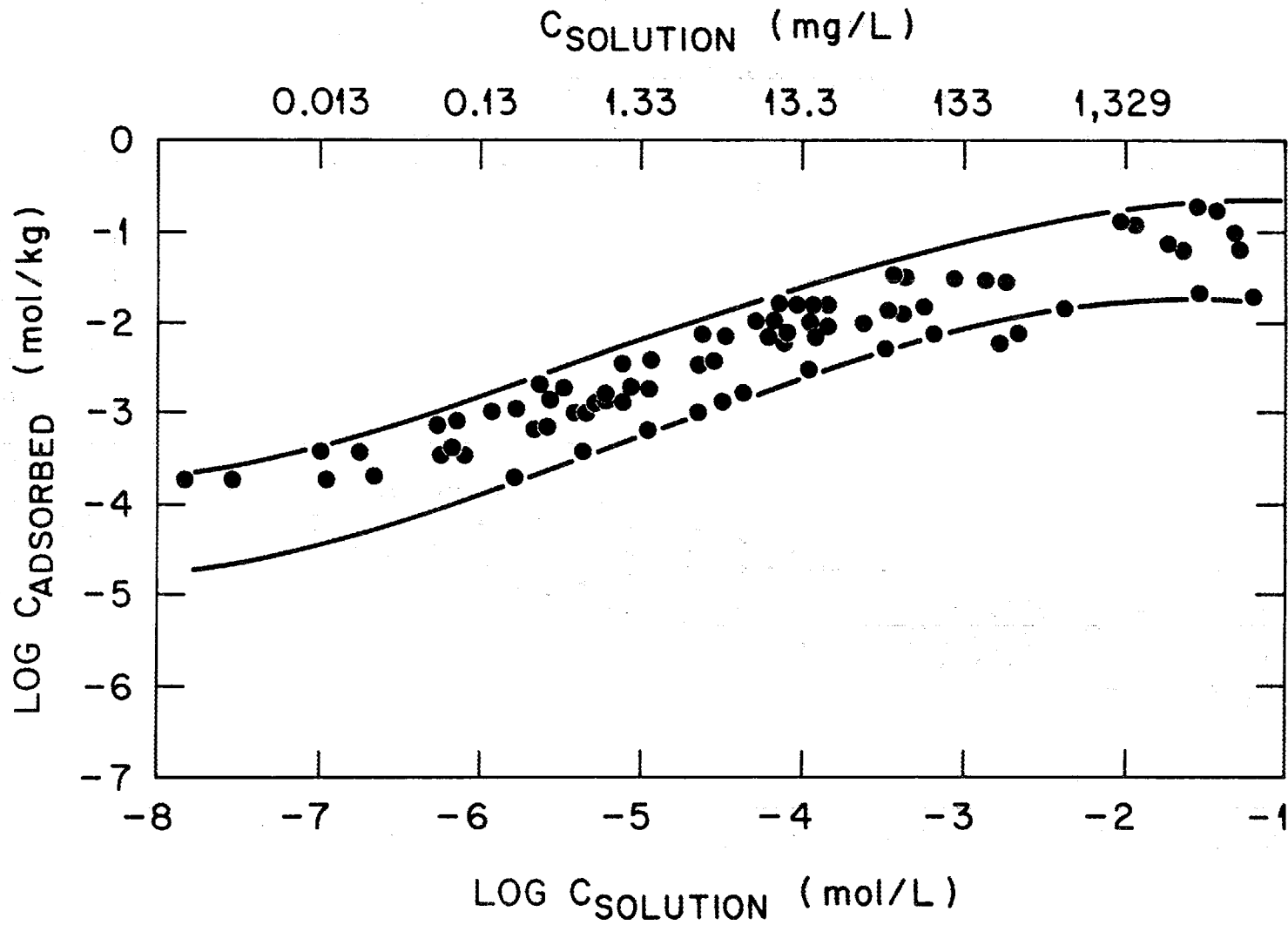


Fig. 4.6. Range of cesium  $R_s$  values for six soil samples - ambient pH conditions.

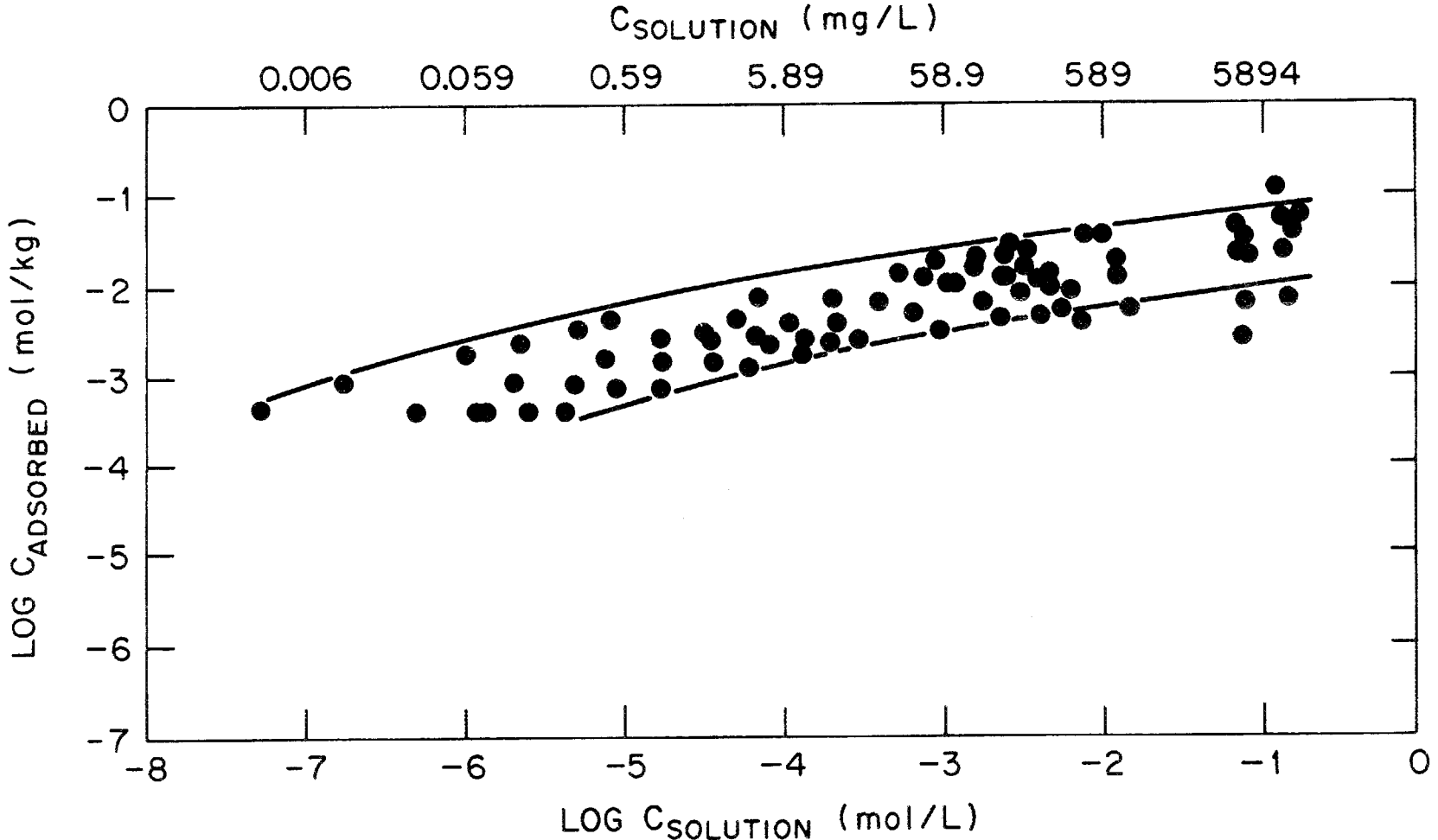


Fig. 4.7. Range of cobalt  $R_S$  values for six soils samples - ambient pH conditions.

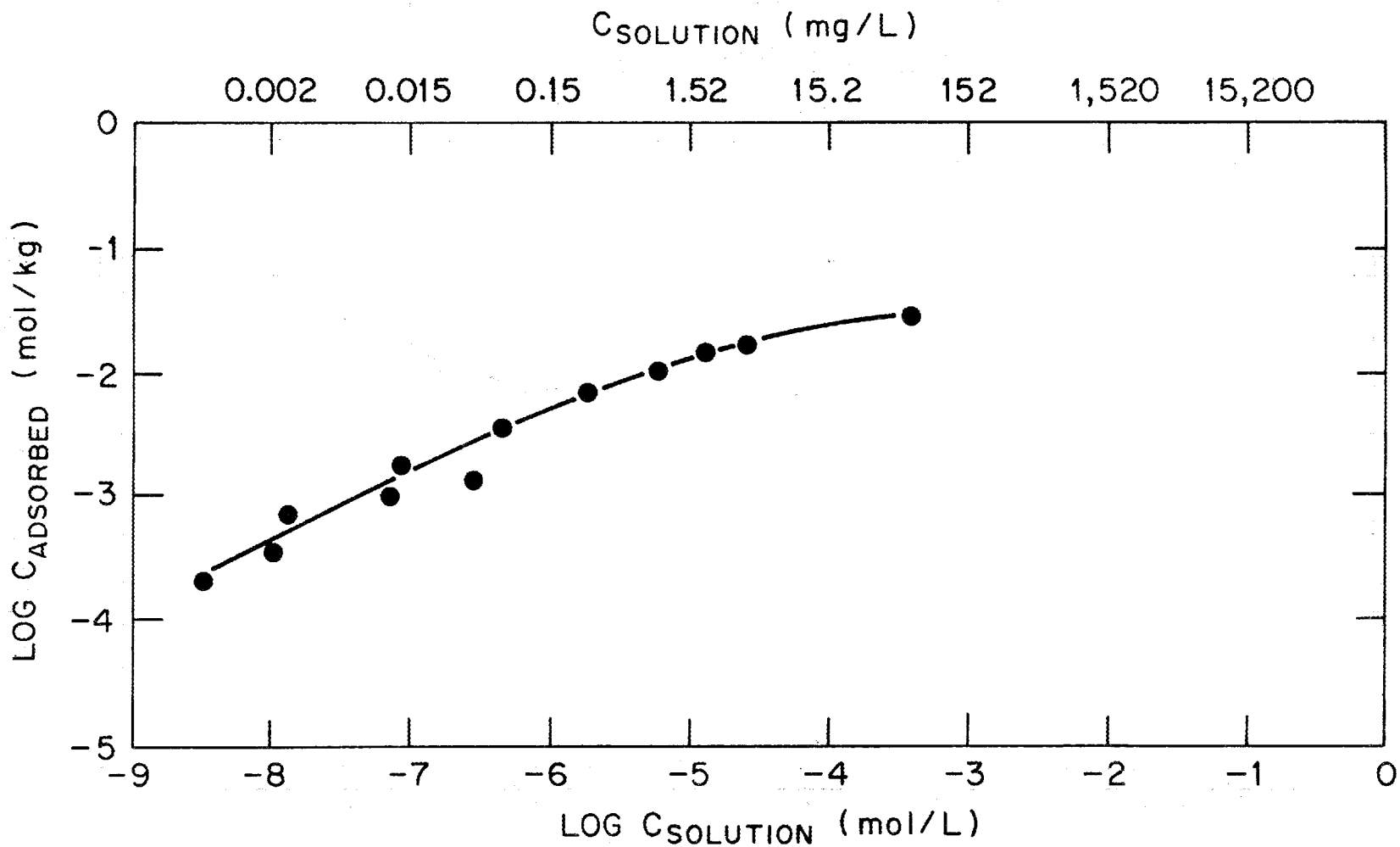


Fig. 4.8. Europium  $R_s$  values for one soil sample - ambient pH conditions.

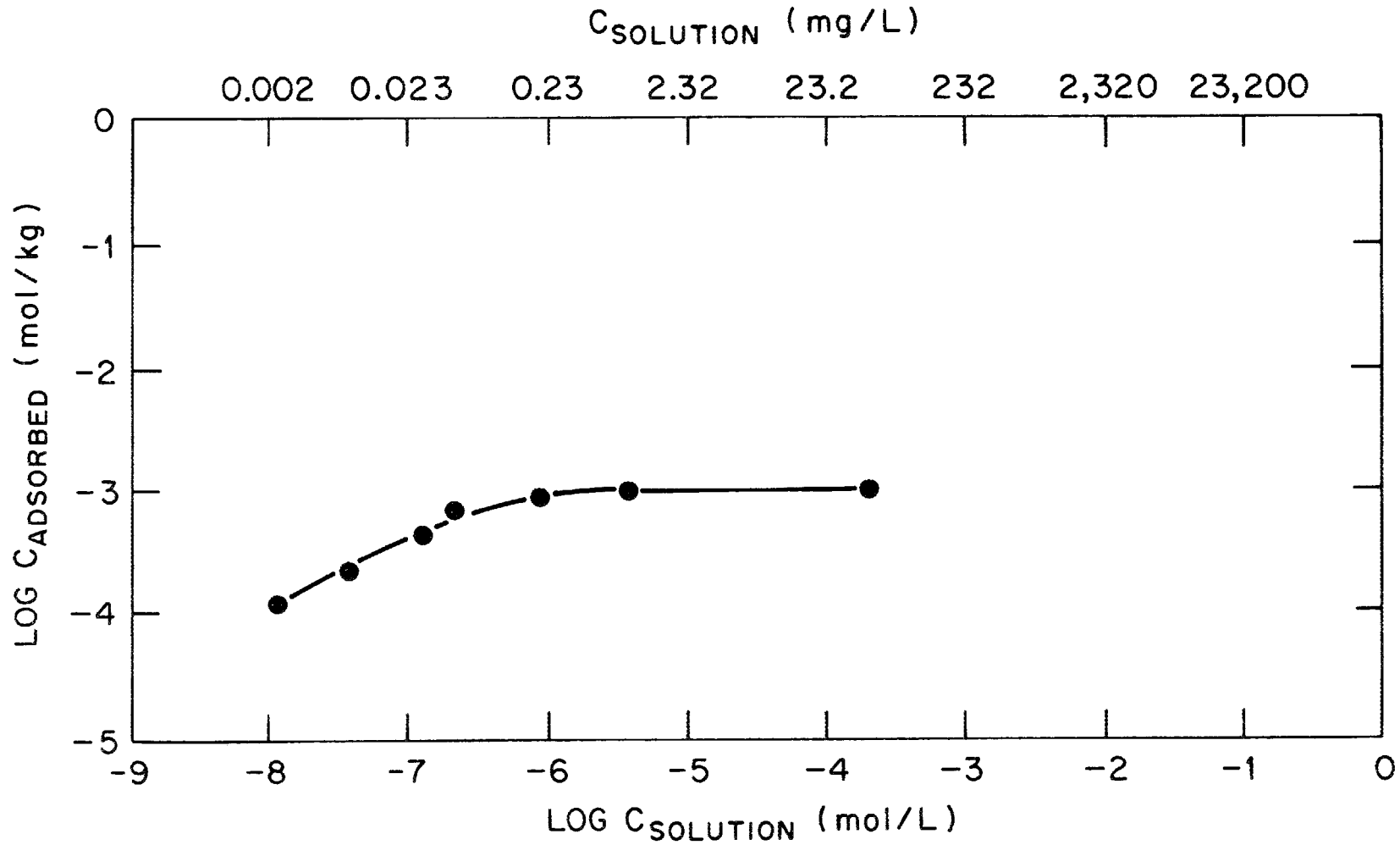


Fig. 4.9. Thorium  $R_s$  values for one soil sample - ambient pH conditions.

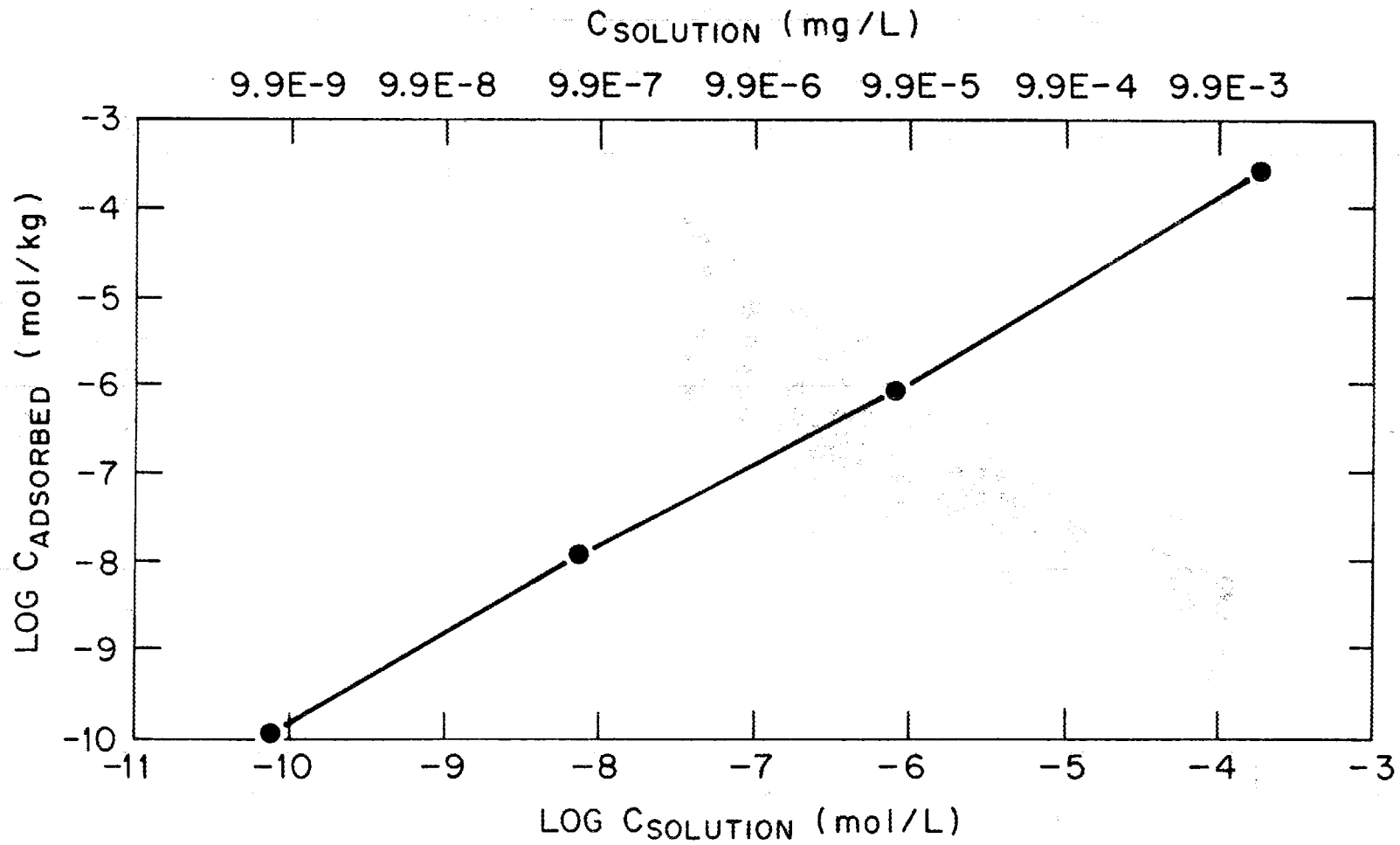


Fig. 4.10. Technetium  $R_S$  values for one soil sample - ambient pH conditions.

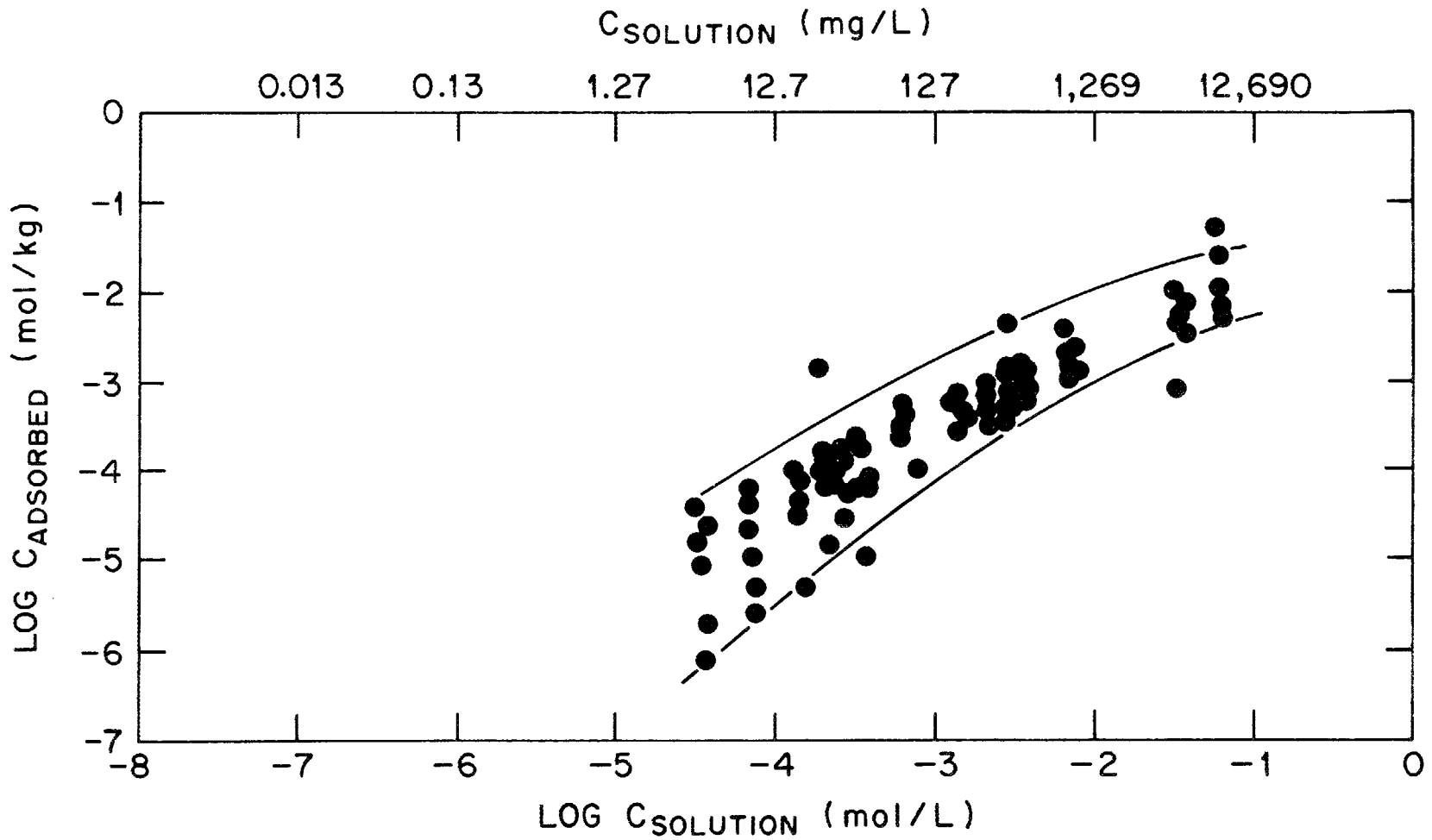


Fig. 4.11. Range of iodine  $R_s$  values for six soil samples - ambient pH conditions.

natural condition may respond to chemical changes induced by waste leachate infiltration.

Sorption-desorption characteristics for U(VI) in the soil/synthetic groundwater system indicate that steady state conditions exist and that  $R_S$  values obtained are a close approximation to distribution coefficients ( $K_d$ ) for site soils.

Tests performed to evaluate the influence of system pH on radionuclide sorption ratios showed that, in general, sorption ratios for cationic radionuclides increase with increases in pH for given radionuclide concentrations.

Sorption ratios determined using the soil water and soil system reflect the behavior of radionuclides dissolved in the clean natural system. Leachates which are generated from waste materials are very likely to contain a broad spectrum of anionic and organic substances as major dissolved constituents. Very limited testing has been performed to evaluate the effects of complexation and chelation of radionuclides in the Knox residuum. The effect of sulfate on strontium sorption was tested and can be summarized as follows. At low initial strontium concentrations and sodium sulfate concentrations of 0.5 and 5 M,  $R_S$  values were decreased by factors of  $10^2$  and  $10^3$ , respectively, due in part to competition between Na and Sr for exchange sites. Formation of  $SrSO_4$  apparently establishes maximum Sr concentration limits of 90 and 800 mg/L, respectively, for 0.05 and 0.5 M sulfate concentrations in the solution. Without the sulfate the solubility limit for Sr was  $68,000 \pm 12,000$  mg/L.

The effect of organic complexing or chelating agents on radionuclide sorption characteristics was evaluated using 0.01 and 0.05 M EDTA or citric acid in solutions for uranium sorption tests. Both complexing agents resulted in the reduction of  $R_S$  values by approximately two orders of magnitude at low initial uranium concentrations, and by one order of magnitude at high initial uranium concentrations. Transport of radionuclides in chemically complexed forms can result in migration rates much higher than those expected based on the results of tests using radionuclides in solution as dissociated ions. This fact emphasizes the importance of minimizing complexing compounds in the waste stream and keeping wastes dry to minimize dissolution and migration.

Two column sorption tests have been performed using Knox residuum. Each column was loaded with 3.0 g of a composite soil sample. The soil occupied approximately 10 cm (4 in) of the total column length, had a void volume of approximately 3.5 ml, and a flow of approximately 0.1 ml/H was established through the soil.

In one column, a uranium solution was placed on top of the column of settled soil and a downflow of synthetic groundwater was applied for 10 days (approximately 7 void volumes through the soil). No alpha activity was counted in the effluent samples, and upon extrusion and sampling of the soil alpha activity was found in only the top 1 cm of soil. This result confirms high  $R_s$  values for uranium as determined by batch testing.

In the other column, a solution containing strontium, cesium, and iodine was placed on the top of the soil. Difficulty was encountered in maintaining a constant flow rate, however, the following observations were made. Strontium and cesium activity was detected in effluent water after one void volume of flow. After approximately one week of flow, iodine activity was detected in the effluent solution. Upon extrusion of the soil column, the major fraction of total activity (Sr and Cs) was located in the top 25% of the column; the second 25% of the column contained small amounts of Sr, Cs, and I; and the bottom 50% contained only I activity. The initial arrival of Sr and Cs is possibly due to the formation of colloids, which were transported with the first void volume of flow. The test confirmed weak retardation behavior for I and strong retardation for most of the Sr and Cs.

#### 4.4 SOIL MINERALOGY

Preliminary information on the mineralogy of Knox residuum is presented in Seeley and Kelmers (1984), based on powder X-ray diffraction (XRD) analyses without thermal treatments or selective cation and polar organic saturation of the samples. The results of the analyses published by Seeley and Kelmers (1984) are presented in Table 4.8. In this analysis the predominant minerals present in the residuum are quartz and illite, with lesser amounts of kaolinite. One sample was predominantly

Table 4.8. Preliminary mineralogical data

Parent material	Sample depth (m)	Surface area (m <sup>2</sup> /g)	Crystalline phases		
			Major	Intermediate	Minor
Kingsport Formation	3	37.13	Quartz	Illite	
	9	46.54	Quartz	Illite	Kaolinite
	12	43.76	Quartz	Illite	
Copper Ridge Dolomite	6	33.56	Quartz	Illite	Kaolinite
	9	9.80	Quartz		Illite
	18	32.71	Quartz	Illite	Kaolinite

quartz silt and had a much lower surface area than the other samples which contained larger percentages of clay.

A more detailed study of soil mineralogy has been prepared by Lee et al. (1984), including analyses of surficial soils and residuum. The following discussion includes excerpts from the report prepared by Lee et al. (1984). Three diagnostic horizons from each of four soil profiles, and six residuum core samples, were selected for mineralogical analyses. The location of soil profiles and core samples tested are shown in Fig. 4.1. The coarse fractions (gravel and sand) of the samples were comprised of different types of cherts, iron/manganese oxide nodules, and quartz.

The samples had high clay contents (except surficial A and E horizons) and low pH and base saturations. The clay fractions were composed of varying amounts of kaolinite, mica, vermiculite, hydroxy-interlayered vermiculite, amorphous iron/aluminum oxide, gibbsite, and quartz. The aluminum hydroxy-interlayered vermiculite is the major component in surface horizons, but kaolinite becomes dominant in subsurface horizons of the soils. The degradation of kaolinite and the formation of aluminum hydroxy-interlayered vermiculite and iron/aluminum oxides are pronounced chemical weathering processes in the surface soils. The aluminum interlayering of vermiculite reduces cation exchange and the selective sorption capacities of soils.

Standard methods of clay mineral analysis were used, and detailed discussion of the methods is included in Lee et al. (1984). The results of studies performed on surficial soil profiles and on residuum are summarized below.

#### 4.4.1 Surface Soil Horizons

Soil horizons developed in the Knox are quite complex because of the fact that these soils were not simply developed on top of stable Knox residuum. There is substantial evidence that material derived from the Knox group has been transported laterally by running water, downhill by gravity (as colluvium), washed into fractures in the rock, disrupted by farming, etc. The character of Knox soils is likely to change

abruptly, both vertically and horizontally. Such differences can be observed even in the walls of a single pit. Surface soil samples were obtained from test pits excavated in four locations.

The soil in profile I has developed on old alluvium over residuum of the Copper Ridge Dolomite. The soil has a dark reddish-brown color in surface horizons and a dark red color in diagnostic subsurface horizons. The texture of the soil varies from clay loam to silty clay loam (Table 4.9). The proportion of chert fragments is low (1 to 7%) in the profile. The soil is relatively porous down to 120 cm (48 in) with many 1 to 2 mm Fe/Mn nodules.

The soil in profile II has developed on old silty alluvium over sandy residuum that is probably weathered from sandstone strata, which start at 80 cm (31.5 in) below the soil surface. The mixed zone of the two lithologies contains lag gravel of weathered chert. The surface horizons have a dark brown color and the subsurface horizons have a dark red color with many blackish Fe/Mn nodules. The texture of the soil changed from loam to clay loam and sandy clay loam, reflecting translocation of clays and differences in lithology within the soil profile.

Profile III was taken from a low footslope between two drainage-ways; the soil has developed on a cherty colluvium parent material. The soil varies from grayish brown to yellowish red, and fragipan is developed near a fluctuating perched water zone (2 Btx/Ex horizon). The soil has a loam to clay loam texture and contains 12 to 30% coarse chert fragments.

The soil in profile IV has developed on cherty dolomite residuum weathered from the Longview Dolomite formation. The soil is brown in surface horizons and yellowish red to red in subsurface horizons. A drastic increase of clay content and decrease of chert content were observed from the surface horizons to the subsurface horizons.

Soil pHs ranged between 5.3 to 4.1, except the A and 2Bt3 horizon of profile I, where the pHs were 6.0 and 6.7, respectively. The higher pHs are possibly the result of lime applications in the past. The pHs in 1M KCl solution were lower than in H<sub>2</sub>O because of the exchangeable acidity, Al plus H, in the soils.

Table 4.9. Physical and chemical properties of selected samples from surface soil profiles

Profile	Horizon	Depth cm	Color Wet	pH 1:1 H <sub>2</sub> O	Gravel fraction (<2 mm) (%)	Size distribution of <2 mm		
						Sand	Silt (%)	Clay
I	A	0-15	5YR3/2	6.0	3	20	52	28
	Bt1	46-69	2.5YR3/6	4.9	7	15	53	32
	2Bt3	92-120	2.5YR4/6	6.7	5	15	49	36
II	A	0-15	7.5YR3/2	5.2	6	27	47	26
	Bt2	58-80	2.5YR3/6	4.4	3	24	41	35
	2Bt4	110-150	2.5YR3/6	4.1	<1	60	17	23
III	E	0-15	10YR4/2	5.3	12	34	46	20
	Bt2	39-60	7.5YR4/4	4.3	19	34	37	29
	2Bt1	115-150	7.5YR5/6	4.6	13	42	43	15
IV	A	0-15	10YR4/3	5.1	27	30	51	19
	E	15-48	10YR5/4	4.5	45	55	27	18
	Btz	80-150	2.5YR4/8	4.8	3	27	14	58

Exchangeable Al concentration varied from 1 to 20.2 mmol/Kg and was relatively lower in surface horizons of the profiles (Fig. 4.12). A subsurface horizon of profile IV had the highest concentration of the labile Al. The Al concentration increased with decreasing exchangeable Ca in the soils. The Mg concentration showed a similar trend with Ca but varied less drastically within soil profiles.

#### 4.4.1.1 Gravel and Sand Morphology

Chert comprises the dominant grains found in the coarser-than-sand size fraction. Several chert types were observed, including massive, oolitic, dolomoldic, porous, and a few banded grains. In many cases the chert showed evidence of extensive alteration to clay and/or Fe/Mn nodules. In most cases, more than one chert type was found in a single horizon. Chert grains up to 4.0 cm (1.6 in) across were observed; *small* ✓ however, some of these had obviously been broken and larger gravels and cobbles are likely to be encountered at the site.

Iron/manganese nodules are an important constituent of the soils in several specimens, in some cases comprising more than 50% of the specimen. ✓ Included in this category are thoroughly stained chert and rock fragments. An interesting feature of a significant number of these Fe/Mn nodules is the fact that they are magnetic. ✓ These magnetic grains are shown by (XRD) to contain the minerals maghemite and hematite. In general, the amount of maghemite is greatest in the uppermost horizons of each pit. Lesser amounts of maghemite were detected with a hand magnet in some of the lower soil horizons, but usually only in trace amounts.

#### 4.4.1.2 Clay and Silt Mineralogy

In the selected soil profiles from the West Chestnut Ridge Site, the clay fractions are composed of varying amounts of kaolinite, hydroxy-interlayered vermiculite (HIV), vermiculite, mica, iron oxides, gibbsite, and quartz (Table 4.10). Kaolinite is the most abundant clay mineral in the subsurface horizons and HIV is the most abundant clay in

ORNL-DWG 84-10499

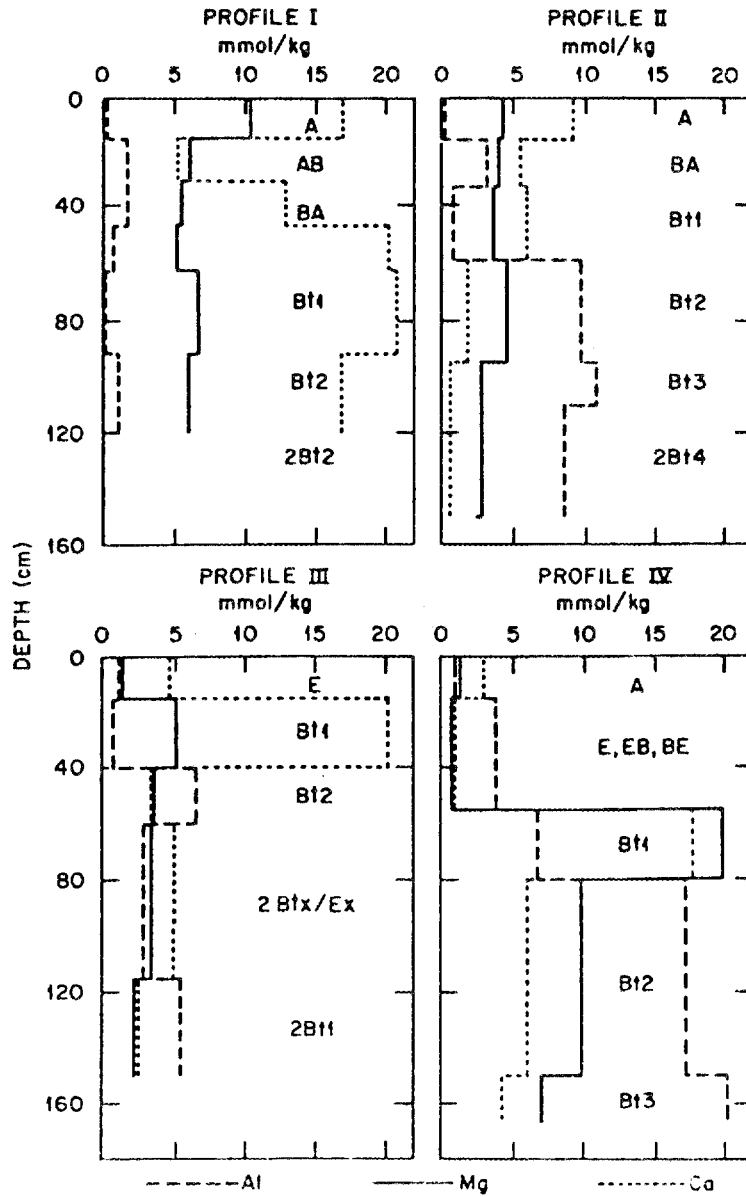


Fig. 4.12. Distribution of KCL (1M) exchangeable Al, Mg, and Ca in the soil profiles.

Table 4.10. Mineralogical composition of the clay fractions (<2 $\mu$ m) from selected horizons of surface soil profiles<sup>a</sup>

Profile	Horizon	Fe <sub>2</sub> O <sub>3</sub> <sup>b</sup>	Al <sub>2</sub> O <sub>3</sub> <sup>b</sup>	Gibbsite	Kaolinite (%)	Mica	Vermiculite	HIV <sup>c</sup>	Others <sup>d</sup>
I	A	6.5	1.9	1.0	20	5	11	30	Qtz
	Bt1	8.3	1.1	2.0	30	5	10	25	Qtz
	2Bt3	8.4	0.8	trace	35	6	13	15	Qtz
II	A	5.8	1.5	2.0	20	11	10	25	Qtz
	Bt2	7.2	0.7	0.2	35	12	9	20	Qtz
	2Bt4	9.2	0.9	0	40	13	9	10	Qtz.C.
III	E	4.0	1.6	1.0	10	10	9	25	Qtz
	Bt2	5.1	0.8	1.0	20	14	10	10	Qtz
	2Bt1	4.0	0.8	0.7	20	13	13	15	Qtz
IV	A	5.0	1.7	3.5	10	10	9	40	Qtz
	E	4.5	1.3	3.0	10	12	9	40	Qtz
	Bt2	6.0	0.7	0	40	18	10	5	Qtz

<sup>a</sup>105°C oven-dry weight basis.

<sup>b</sup>CBD extractable free oxides.

<sup>c</sup>HIV = Aluminum hydroxy-interlayered vermiculite estimated from XRD intensity.

<sup>d</sup>Qtz = quartz, C. = cristobolite.

the surface horizons (A and E). Mica, vermiculite, and quartz are the next most common minerals. Amorphous iron and aluminum oxides, gibbsite, and crystalline iron oxides (hematite and maghemite) and minor (<10%) components.

The mineralogical composition of the silt (50-2  $\mu\text{m}$ ) fractions of the 12 soil samples from four soil profiles were determined by XRD. The silt fractions were composed of >80% quartz grains and <10% mica. There were trace amounts of kaolinite and iron oxide minerals in the silt fractions.

#### 4.4.2 Residual Soils

Six samples from five borehole cores were selected for characterization. Selected properties and depths of the residuum sections taken are given in Table 4.11.

The residuum sample from borehole A-5 was red clay mixed with a small amount of yellowish weathered shale, siltstone fragments, and small amounts of gravel-size chert. The reddish clay was chosen for analysis because it was the major constituent in the section. The sample selected from core A-6 was yellowish red and had a clay loam texture with a large quantity of gravel-size cherts. The A-6 sample appeared to be colluvium rather than in situ residuum. Two sections were chosen at different depths from core A-9. The sample (denoted as A-9s) from the 23.6 to 24 m (77.4 to 78.7 ft) section was a weathered, very pale brown shale with clay texture; the other sample (A-9d), from the 29.6 to 30.0 m (97.1 to 98.4 ft) section, was a reddish-brown dolomite residuum with a clay texture.

The sample from the A-14 core had many small [ $<1$  cm (0.4 in)], very pale brown, weathered shale fragments in yellowish-red residuum matrix. The texture of the sample was clay with <15% of silt plus sand. The sample from A-16 had a reddish matrix containing yellowish brown, weathered siltstone fragments coated with black manganese oxides on the edges of the fragments.

The pH of the residuum ranged between 5.0 to 6.7, which is slightly higher than the pH of the surface soils developed from them (Table 4.9).

Table 4.11. Physical and chemical properties of selected samples from borehole residuum cores

Core No.	Depth (m)	Color wet	pH (1:1 H <sub>2</sub> O)	Gravel (>2 mm) (%)	Size distribution of <2 mm			KCl (1 M) exchangeable		
					Sand	Silt (%)	Clay	Ca	Mg m mol/Kg	Al
A-5	13.2-13.7	2.5YR4/6	5.0	1	<1	26	73	1.3	0.9	1.2
A-6	20.6-21.0	5YR5/6	6.7	42	27	40	33	3.8	3.3	0.1
A-9s	23.6-24.0	10YR7/4	6.3	14	7	33	60	2.8	2.2	0.1
A-9d	29.6-30.0	5YR4/4	6.6	<1	11	5	84	3.8	3.1	<0.1
A-14	11.6-12.0	5YR5/5	5.1	1	4	10	86	0.6	0.3	1.3
A-16	27.0-27.5	5YR4/4	5.4	1	5	32	63	1.4	1.2	0.4

As was suggested by pHs, the A-6, A-9s, and A-9d samples had high exchangeable Ca and Mg but very low exchangeable Al in 1 M KCl solution. The other samples had higher exchangeable Al but they were lower than in the surface soils studied.

#### 4.4.2.1 Gravel and Sand Morphology

The dominant mineral in the coarse fraction is chert. The largest size noted was about 2.5 cm (1 in); however, much greater dimensions are typically observed in the field. The chert occurs in several types, including massive (sometimes porcelaneous), oolitic, dolomoldic, porous, etc. More than one type of chert occurs in what appears to be a single grain. The chert has been weathered or altered in different ways, sometimes resulting in the development of clay minerals and various Fe/Mn oxides which diffused into porous zones in the chert. In some cases, the different chert components undergo different types of alteration. For example, some oolitic cherts that appear to be partially replaced by Fe/Mn oxides also appear to be releasing fresh, unaltered grains of quartz from within the oolites.

Most of the quartz grains found in the residuum are in the sand-size range; however, a few larger grains occur and clusters of authigenic (post depositional-formed in place) quartz crystals occur in the gravel fractions. Numerous dark brown to almost black grains were found in this fraction and represent Fe/Mn oxide nodules or coated grains.

A few pieces of siltstone (or fine sandstone), which are presumed to have derived from beds of these lithologies in the dolostones were observed.

In general, material observed in the sand-size fraction is similar to that observed in the gravel fraction; however, quartz and Fe/Mn nodules are present in greater amounts and in some specimens are the dominant phases. Some of the Fe/Mn nodules may have originally been part of larger particles that were disaggregated during sample preparation and handling.

Many quartz grains are relatively well rounded, although a complete range of "roundness," from angular to well rounded, was observed. Many

of the quartz grains exhibit frosted surfaces, which are interpreted as a characteristic of windblown material.

#### 4.4.2.2 Clay and Silt Mineralogy

In the residuum samples, kaolinite is the dominant mineral of the clay fractions, ranging from 30% to as much as 55% (Table 4.12). Other mineral components include mica, vermiculite, quartz, and amorphous iron/aluminum oxides. Amorphous iron/aluminum oxide coatings constituted less than 8% of the clays, but they effectively reduced the cation exchange coefficient (CEC) of the clays. After removal of the oxides by citrate-bicarbonate-dithionite (CBD) treatment, the CEC of the clays increased more than 50% (Table 4.13).

The clay mineral assemblage found in samples from residuum cores was less complex than the surface soil mineral assemblage. The primary minerals present included kaolinite, mica, and vermiculite with lesser amounts of Fe and Al oxides, quartz, and HIV was found in only two samples of the six samples tested.

Mineralogy of silt fraction (50 to 2 m) of the residuum core samples is very simple, consisting of >90% quartz and <10% mica.

### 4.5 SOIL PROCESSES

Active soil processes on the West Chestnut Ridge Site include soil formation, by continued weathering of the dolomite bedrock, and soil movement by erosion, soil creep on steeper slopes, and subsidence in zones of karst formation.

#### 4.5.1 Carbonate Rock Weathering Rates

Residual soils are formed by chemical alteration, dissolution, and the removal of soluble constituents of the parent rock material, leaving the insoluble mineral constituents. The rate of carbonate rock dissolution has been found to be nearly constant in time, with variation due to climatic variations (Colman 1981). Carbonate rock weathering rates have

Table 4.12. Mineralogical composition of the clay fractions (2 $\mu$ m) of selected samples of residuum cores<sup>a</sup>

Core No.	Fe O	Al O	Kaolinite	Mica	Vermiculite	Others <sup>b</sup>
A-5	7.1	0.8	35	20	26	Qtz HIV
A-6	5.6	0.7	35	19	20	Qtz HIV
A-9s	2.7	0.4	30	26	8	Qtz
A-9d	5.4	0.6	55	17	6	Qtz
A-14	5.3	0.8	35	20	12	Qtz
A-16	5.6	0.6	45	14	15	Qtz

<sup>a</sup>105° oven-dry weight basis.

<sup>b</sup>Qtz = quartz,; HIV = aluminum hydroxy=interlayered vermiculite estimated from XRD intensity.

Table 4.13. Cation exchange capacities of the clay fractions of residuum before and after citrate-biocarbonate-dithionite (CBD) treatments

Residuum	A-5	A-6	A-9s	A-9d	A-14	A-16
	(m mol Ca/kg)					
Before CBD	85	70	40	45	75	65
After CBD	225	180	80	70	115	140

been measured indirectly, in other regions, by long-term monitoring of chemical constituents leaving a watershed in stream discharge or by use of microerosion meters (Jennings 1983). Uncertainties result from either approach. Atkinson and Smith (1976) demonstrated a correlation between carbonate rock removal rate and annual watershed runoff. Table 4.14 shows some carbonate rock weathering rate data and indicates that the range in estimates for temperate climates approaches the order of magnitude [25 to 200 mm/1000 yr (1 to 8 in/1000 yr)].

Using data from Atkinson and Smith (1976) and Schmidt (1982), the present rate of carbonate rock weathering for east Tennessee is estimated to lie in the range of 30 to 40 mm/1000 yr (1.2 to 1.6 in/1000 yr).

An important unknown for estimating the age of residual soil masses is prehistoric climate changes which may have increased or decreased the rate of soil formation. Consensus has not been reached on the variance of average annual precipitation during the Pleistocene epoch from present precipitation patterns. Estimates range from essentially present average precipitation (Sellers 1965) to 2 to 3 times the present average precipitation. A 2- to 3-fold increase in runoff for the site area would indicate a range of carbonate removal for the site of 60 to 90 mm/1000 yr (2.4 to 3.5 in/1000 yr). If the higher weathering rates are used to estimate the age of Knox residuum formation, one would estimate that formation of the thicker masses of residuum of > 30 m (100 ft) encountered on the Chestnut Ridge Site has occurred over a period of at least  $3.3 \times 10^4$  to  $3.3 \times 10^5$  years. If the present estimated rate of rock weathering is used, the estimate of soil formation of 30 m (100 ft) of residuum is  $7.5 \times 10^5$  to  $1 \times 10^6$  years.

#### 4.5.2 Soil Erosion Rates

Soil is removed from the land surface primarily by water erosion in East Tennessee. The types of water erosion include sheet and rill erosion and gully erosion. The Universal Soil Loss Equation (ULSE) was developed to estimate the quantity of soil lost to sheet and rill erosion. Factors included in estimating soil erosion by the USLE are: the rainfall erosivity index, the soil erodibility index, slope length and gradient, and soil management factors.

Table 4.14. Rates of chemical weathering of limestone in temperate climates (mm/10<sup>3</sup> yrs)

Region	Rate	Source
Florida	35	Atkinson & Smith 1976
N. England	25-45	Sweeting 1960
England	51-106	Goodchild 1890
Mammoth Cave, Ky.	40-100	Schmidt 1982
Temperate region average	57	Embleton & Thornes 1979

Major slopes on the site are occupied by soils of the Fullerton series variants (soil types 2, 4, 5, and 7), with lesser areas occupied by soil of the Shack series (soil type 1). Northwest-facing slopes are steeper (30 to 40%) than southeast-facing slopes (15 to 20%) and the areas under consideration for use as disposed tracts have slopes of <15%.

Table 4.15 shows annual soil erosion estimates for Fullerton, Shack, and Dewey and Decater variant soils in their natural wooded condition, and for the Fullerton and Dewey and Decater soils under grassland conditions. These are used to estimate the erosion potential of the developed area of the site after revegetation. Factor K was obtained from the Soil Survey of Anderson County (1981), and all other factors were obtained from tables in Dunne and Leopold (1978). It is also noted that the values used for slope gradient and length lie in the range of extrapolation beyond the range of demonstrated applicability because of the long, steep slopes which occur on parts of the site.

The estimates shown in Table 4.15 show the effects of vegetation type on soil erodibility. The estimated annual soil erosion from the Fullerton variant soils on a 15% slope increases by a factor of 13, depending on whether the cover is woodland or grassland. This fact indicates that to minimize the impact on soil stability for the overall site a minimum of area clearing should accompany site development. Terracing to reduce slope length is also an effective approach to reduce erosion. Steeper slopes on the site should remain wooded.

The credibility of the USLE estimates for these soils is questionable because of the well developed internal drainage system of the soils. Monitoring of a small watershed on the northern slope of Chestnut Ridge for a period of 3 years detected only 1 runoff event, which was produced by a precipitation event of 5 cm (1.96 in) in 24 hr (West & Mann 1982).

Conversion of the erosion rate data to erosional downcutting yields estimates as follows. For the Fullerton variant soils in 15% slopes with woodland cover, the USLE estimates erosional downcutting on the order of 30 mm/1000 years (1.2 in/1000 yr). For 40% slopes the rate of erosional downcutting is estimated at 230 mm/1000 years (9.1 in/1000 yr).

Table 4.15. Estimated Annual Soil Erosion Potential of West Chestnut Ridge Site Soils

	R	K	LS <sup>a</sup>	C	P	A metric tons/ha annual
<u>Woodland Cover</u>						
Fullerton var. (75-100% Canopy)						
15% slope 152 m long	200	0.28	5.5	.001	0.8	0.55
40% slope 152-183 m long	200	0.28	35	.001	1.0	4.39
Shack series 30-35% slope						
92 m long	200	0.28	15	.001	0.9	1.69
Dewey and Decater variants						
15% slope 152 m long	200	0.24	5.5	.001	0.8	0.47
20 % slope 105 m long	200	0.24	7.5	.001	0.8	0.65
<u>Grassland Cover</u>						
Fullerton var. 15% slope						
152 m long	200	0.28	5.5	0.013	0.8	7.18
Dewey and Decater variants						
15% slope 152 m long	200	0.24	5.5	0.013	0.8	6.15

<sup>a</sup> Values are extrapolated beyond the demonstrated reliable range.

These estimates are not considered highly reliable though they tend to compare favorably with the estimates of residual soil formation based on carbonate rock weathering rates.

#### 4.5.3 Karst Processes

Other active soil processes include soil creep and frost heave movements on the steeper slopes, and soil movement through karst processes. The rates of soil creep and frost heave are slow. The process of karst soil movement can be slow downwarping at the soil surface by plastic deformation of the soil mass or rapid motion accompanying shear failure of the soil over open cavities.

Karst features observed on the site typically have very gentle slopes associated with them, which suggest that they have either formed by gradual downwarping or that they are very old features. The exception to this condition on the site is in the karst zone of the middle Chepultepec Dolomite, which contains several steep sided, obviously recent features. All the karst features on the site have some hydrologic function because they are infiltration areas for precipitation.

Soil characteristics in the karst features were investigated in boreholes in three karst features. Soil strength characteristics within the karst features do not lie outside the range of variation for local soils lying outside of the karst features.

The development of the karst zones on-site results from dissolution of the dolomite bedrock accompanied by downward displacement of the overlying soil mass to fill voids. Under natural conditions, metastable conditions can develop, with open voids occurring in the zone of weathering rock. Extreme weather conditions (alternating droughts and extreme precipitation events) or tectonic events (earthquakes) may cause the metastable soils to move downward into voids. Extreme water table fluctuations can cause bridged soils to collapse. Most sinkhole collapses that are investigated are attributed to hydrologic causes.

Human activities have also been attributed with inducing sinkhole development (Newton 1976). The typical human activities that induce sinkhole development are excessive well pumping or dewatering which

cause extreme depression of the water table and induced recharge through the soil mass by overirrigation or ponding of water at the land surface. The implications of this information with regard to the West Chestnut Ridge Site are that site development activities should minimize aquifer drawdown and the ponding of water at the ground surface.

In view of the apparent age and topographic character of the Knox residuum, one must conclude that during recent geologic time the soils have been stable or that karst movement has been largely by plastic deformation. Just as there appears to be an inherent stability to most of the residuum, there is an inherent uncertainty in predicting when karst processes may accelerate. ✓



## 5. SITE GEOHYDROLOGY

Characterization studies performed to define geohydrologic parameters for the West Chestnut Ridge Site include:

- o field and laboratory testing of soil permeability,
- o field measurement of bedrock permeability,
- o laboratory measurement of soil moisture characteristics and permeability under unsaturated conditions,
- o monitoring of water table fluctuations in observation wells, and
- o aerial thermal sensing to identify groundwater emanations.

### 5.1 PERMEABILITY OF SOIL AND ROCK

#### 5.1.1 Soil Permeability

The soil permeability determines the rate of water migration from the land surface to the water table and determines water movement within saturated zones in the soil mass. Soil permeability can be measured in the field or in the laboratory. Laboratory test values typically yield much lower permeability values than field tests because in the field the macropore system can be tested, while the small size of laboratory test specimens usually results in tests of fine-grained samples.

A total of 39 falling head field permeability tests were performed. Each test interval was 0.61 m (2 ft) long. At each of 20 test sites coinciding with the test boring locations, two tests were performed; one at a depth of approximately 2.5 to 3 m (8 to 10 ft), and the other at depths ranging from 6 to 12 m (20 to 40 ft). At one site a test was not possible in the deeper test range because of the shallow bedrock condition.

The permeability tests were performed by Woodward-Clyde Consultants (1984) and the following summary is excerpted from their report. Table 5.1 contains a summary of all the field permeability test data and all the laboratory saturated permeability test data. The field and laboratory data are concentrated at three typical depths: 3 m (10 ft), 12 m (40 ft), and 21 to 30 m (70 to 100 ft). These depths were selected

during the design phase of the field and laboratory investigations and do not reflect a change in either soil composition or depositional history. An inspection of Table 5.1 reveals a general tendency for permeability to decrease with depth, and also a general tendency for a reduction in the scatter of permeability data with depth.

Table 5.1. Summary of field and laboratory soil permeability test results

Typical depth and type of test	Mean permeability (cm/s)	Mean $\pm$ 1 std. deviation (cm/s)
3 m (10 ft)		
- field tests	$6.1 \times 10^{-6}$	$7.9 \times 10^{-5}$ to $5.0 \times 10^{-7}$
- lab tests	$3.2 \times 10^{-6}$	$7.9 \times 10^{-5}$ to $1.3 \times 10^{-7}$
12 m (40 ft)		
- field tests	$2.0 \times 10^{-6}$	$2.0 \times 10^{-5}$ to $2.0 \times 10^{-7}$
- lab tests	$1.0 \times 10^{-7}$	$2.5 \times 10^{-7}$ to $4 \times 10^{-8}$
21-30 m (70-100 ft)		
- field tests	no data	no data
- lab tests	$6.3 \times 10^{-8}$	$5.0 \times 10^{-8}$ to $7.9 \times 10^{-8}$

The values of mean and standard deviation were calculated by assuming the log of permeability is a normally distributed random variable.

Depth of 3 m (10 ft). The following observations can be drawn from data obtained in the upper 6 m (20 ft).

- o Twelve laboratory test and 21 field permeability tests were conducted within this depth range.
- o The range of the laboratory and field data is approximately the same and covers approximately four orders of magnitude.
- o The average laboratory value of permeability is  $3.2 \times 10^{-6}$  cm/s and compares with the average field value of  $6.1 \times 10^{-6}$  cm/s.

- o There does not appear to be any statistical correlation between lab and field permeability data at a given site, even at approximately the same depth.

The last observation suggests that large variations in permeability occur over short distances. The laboratory testing program indicates that the observed variations in permeability cannot be correlated with index properties. Thus, the differences in permeability are probably associated with differences in soil structure.

Depth of 12 m (40 ft). The range of this field data is somewhat smaller than that for the field data from the shallower depths, and the average value of  $2.0 \times 10^{-6}$  cm/s is about one-third of the average value from shallow depths. The range of the three laboratory permeability determinations is very small compared to the range of field data. This may be the result of the limited number of tests, and of the bias in the laboratory tests at this depth and deeper caused by choosing samples at or close to the groundwater level.

Depth of 21 to 30 m (70 to 100 ft). These data include eight laboratory tests with permeabilities ranging from  $4 \times 10^{-8}$  cm/s to  $1 \times 10^{-7}$  cm/s, with an average value of  $6.3 \times 10^{-8}$  cm/s. These very low values are believed representative of the more plastic, finer, less cherty soils close to or below the water table. Soils in this depth interval are expected to have lower porosity than overlying soils because of the greater overburden pressures at depth.

#### 5.1.2 Permeability of Weathered Rock

Weathered rock was generally supported by steel casing in the bedrock exploratory borings, and no packer tests or falling head permeability tests were conducted in the weathered rock. The permeability of the weathered rock zone was determined from the well pumping test in the weathered bedrock zone aquifer in the Chapultepec Dolomite.

At the time of testing the aquifer thickness was approximately 10 m (30 ft), the transmissivity was approximately  $9.3 \times 10^{-4}$  m<sup>2</sup>/min (0.01 ft<sup>2</sup>/min), and the permeability of the zone was  $1.7 \times 10^{-4}$  cm/s.

### 5.1.3 Permeability of Unweathered Rock

Twenty-three packer permeability tests were performed in unweathered rock. The permeabilities were zero (no flow measured) in 10 out of 23 tests. The remaining 13 tests gave relatively high permeability values ranging from  $8.5 \times 10^{-6}$  cm/s to  $> 1.0 \times 10^{-3}$  cm/s. A representative value of permeability for those tests which had a permeability greater than zero was about  $1 \times 10^{-4}$  cm/s. The permeability estimates for the weathered rock were about  $2 \times 10^{-4}$  cm/s, which is a value very close to that estimated from the packer tests on sound rock. It is evident that the sound rock, as defined herein, is not necessarily impermeable. The permeability measured in the unweathered rock is attributed to flow in fractures and/or open bedding planes.

## 5.2 MOISTURE-SUCTION AND PERMEABILITY-SUCTION CHARACTERISTICS OF RESIDUUM SAMPLES

Moisture-suction and permeability-suction characteristics of selected residuum samples were determined by Daniels and Broderick (1983). Details of the method used are contained in their report. The scope of their work and results are summarized as follows:

- o twelve moisture-suction tests were performed to develop plots of soil suction vs percent saturation,
- o two permeability tests on unsaturated samples were performed to develop curves relating permeability to soil suction,
- o two permeability tests on saturated samples of soil were also performed to provide data on the permeability of the soils at 100% saturation, and
- o plots of permeability vs soil suction were prepared using (1) moisture-suction curves, (2) measured permeabilities at full saturation, and (3) theoretical relationships that relate permeability-suction curves to moisture-suction curves.

### 5.2.1 Results of Moisture-Suction Tests

Data given for soil suctions >10 m (30 ft) of water were obtained using thermocouple psychrometers. Soil suctions of <10 m (30 ft) of water were measured with tensiometers. There is considerable scatter in the data for the soils tested. The moisture-suction test results are summarized in Fig. 5.1 as a range of behavior for the soils tested. The soil suction at equivalent percent saturations can vary by about one order of magnitude near saturation and by more than three orders of magnitude at 70% saturation.

### 5.2.2 Results of Permeability Tests Performed at <100% Saturation

Permeability tests were performed on two samples at less than total saturation conditions. The soil samples were initially dried to reduce the degree of saturation and then were moistened when the permeability tests began. Initially, thermocouple psychrometers were used to measure the soil suctions at various points in the soil columns. When the soil suctions could no longer be measured with psychrometers, the psychrometers were removed and tensiometers were inserted. More than usual scatter in the data was observed, and considerable smoothing of results was required. The variable nature of the soil, and particularly the variations in gravel content from one part of the sample to another, are thought to be the cause of the scatter in measurements. The permeabilities measured on saturated samples for the two tests were  $7.2 \times 10^{-7}$  cm/s and  $2.8 \times 10^{-8}$  cm/s.

The test results showed considerable variability in moisture-suction and permeability-suction behavior of site soils. For this reason Daniels and Broderick (1983) recommended upper, mid-range, and lower-bound curves for moisture-suction and permeability-suction.

1. The three moisture-suction curves plotted in Fig. 5.1 provide a good representation for most of the test results. Because the soils at this site are already close to saturation below a

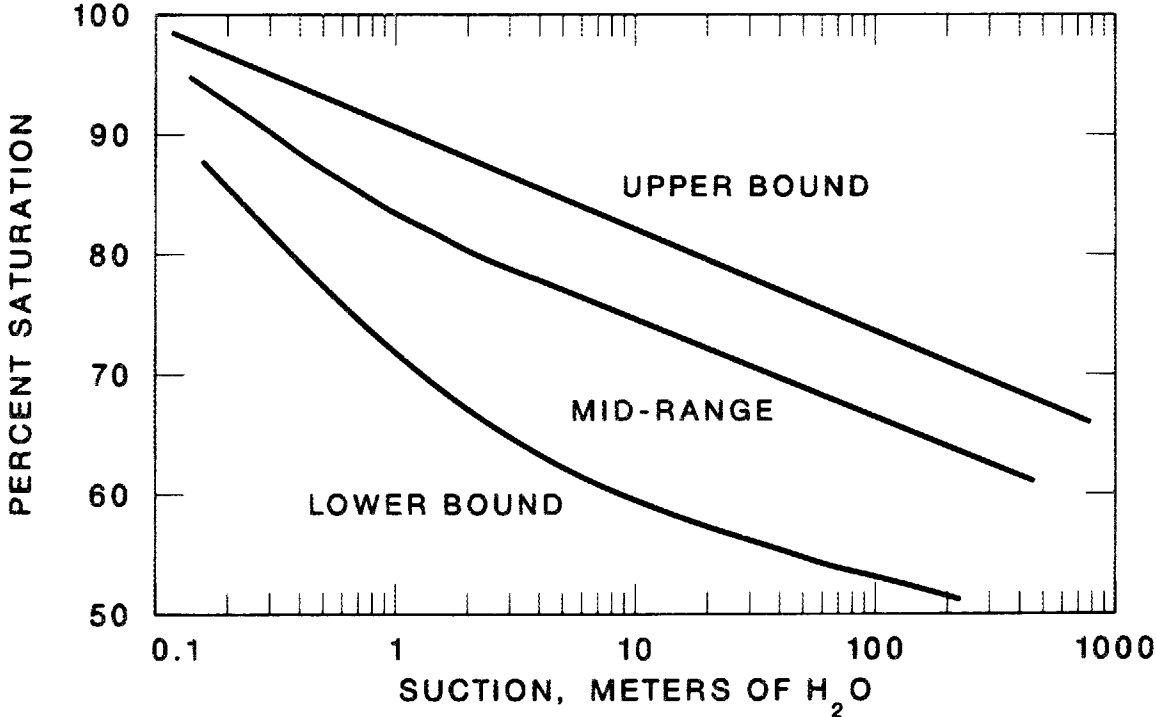


Fig. 5.1. Recommended moisture-suction curves.

depth of a few meters, it might be appropriate to assume zero suction at 100% saturation. However, dry soils will not reach full saturation at zero suction if they are gradually moistened (high positive water pressure, or back pressure, is required to achieve full saturation).

2. The relative permeability-suction relations tabulated in Table 5.2 are recommended for use in analysis. The relative permeability at any suction is multiplied by the permeability at full saturation to obtain the permeability at a particular suction. The permeability at full saturation is best determined from a combination of laboratory tests, field tests, and geohydrological studies.

### 5.3 GROUNDWATER FLUCTUATIONS AND FLOW PATHS

Groundwater fluctuations were measured periodically in wells completed in residual soils and bedrock. Groundwater flow paths and approximate rates were tested in one flow zone by dye tracer testing.

#### 5.3.1 Groundwater Fluctuations

At each of 19 locations, paired observation wells were installed to allow measurement of water levels in soils and bedrock. At one site the subsurface conditions allowed installation of the soil observation well only. The depth to the water was measured in each well with varying frequency beginning October 5, 1983. Eight water level recorders were installed during early April 1984 to provide continuous records of water levels at eight selected locations. The well hydrographs are included in Appendix A.

Several general observations can be made upon inspection of the hydrographs. These are stated below.

- o Seasonal fluctuations of <1 to 15 m (15 to 45 ft) have been observed in some of the wells. ✓
- o Not all of the wells show seasonal fluctuations. ✓

Table 5.2. Recommended range of values for curves of relative permeability versus soil suction

Soil suction (meters of water)	Relative permeability		
	Upper bound	Mid-range	Lower bound
0	1	1	1
0.1	$6 \times 10^{-1}$	$2 \times 10^{-1}$	$4 \times 10^{-1}$
0.2	$5 \times 10^{-1}$	$1 \times 10^{-1}$	$8 \times 10^{-2}$
0.5	$3 \times 10^{-1}$	$4 \times 10^{-2}$	$1 \times 10^{-2}$
1	$2 \times 10^{-1}$	$2 \times 10^{-2}$	$3 \times 10^{-3}$
2	$1 \times 10^{-1}$	$1 \times 10^{-2}$	$9 \times 10^{-4}$
5	$4 \times 10^{-2}$	$4 \times 10^{-3}$	$1 \times 10^{-4}$
10	$2 \times 10^{-2}$	$1 \times 10^{-3}$	$4 \times 10^{-5}$
20	$1 \times 10^{-2}$	$5 \times 10^{-4}$	$1 \times 10^{-5}$
50	$6 \times 10^{-3}$	$1 \times 10^{-4}$	$2 \times 10^{-6}$
100	$3 \times 10^{-3}$	$8 \times 10^{-5}$	$5 \times 10^{-7}$
200	$8 \times 10^{-4}$	$2 \times 10^{-5}$	$1 \times 10^{-7}$
500	$1 \times 10^{-4}$	$5 \times 10^{-6}$	$2 \times 10^{-8}$

Note: These data correspond to the curves shown in Fig. 5.1.

- o Wells screened in the residuum tend to respond more rapidly to precipitation events than do the bedrock wells.
- o Bedrock and residuum wells located in topographic low areas respond together and typically show very rapid fluctuations. These wells show small seasonal fluctuations - their hydrographs are a series of precipitation event responses.
- o Water levels in several of the wells are strongly controlled by the presence of discrete permeable zones in the weathered bedrock or soil zones.
- o Monitoring records indicate that beneath the upland portions of the site two saturated zones exist: one in soil and one in the weathered bedrock and bedrock zones. The similarity in fluctuations in the two zones varies widely.
- o Hydrographs for bedrock wells located in the same general lithostratigraphic interval tend to show similar behavior.
- o The major feature on all the well hydrographs was the response to a series of large precipitation events which occurred during late April and early May 1984.

### 5.3.2 Maximum Water Table Elevations

In the lower elevation areas of the site the water table rises to within <1m of the ground surface. Figures 5.2 and 5.3 show the relationship between the topographic location of wells and the maximum observed water elevation. These plots include the well responses of early May 1984.

### 5.3.3 Groundwater Flow Paths

The transmission of water through site soils and bedrock occurs rapidly, as shown by the rapid well responses to precipitation events. Precipitation that falls at rates below the vertical infiltration capacity of the residuum infiltrates through the residuum into the bedrock aquifer. When the vertical infiltration capacity of the residuum is exceeded during a precipitation event, lateral quickflow occurs in the

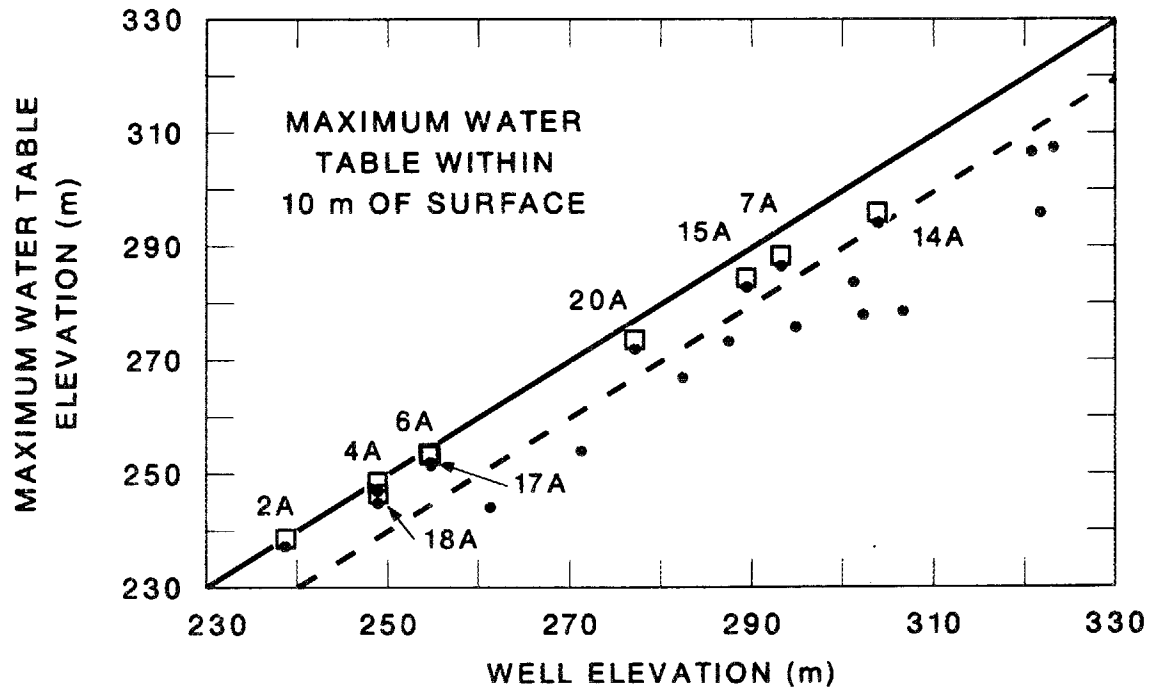


Fig. 5.2. Well elevation vs maximum water table elevations, soil wells.

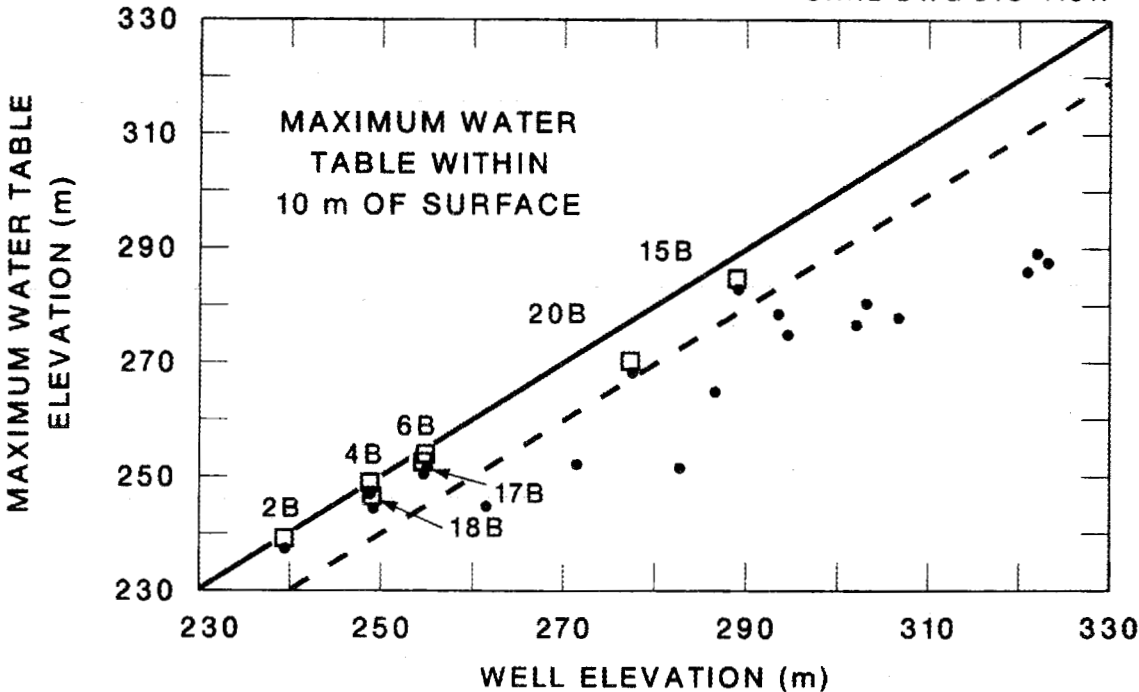


Fig. 5.3. Well elevation vs maximum water table elevations, bedrock wells.

upper soil horizons and ephemeral surface flow occurs where the quick-flow emerges to the surface. This phenomenon may occur several times during the winter and spring seasons. These events also cause the infiltration of saturated pulses through the residuum. At least three such events are apparently recorded in well hydrographs for wells on the crest of the ridge. The late April and early May rains caused widespread saturation of the surface soils accompanied by rapid rises of the water tables at depth. During well monitoring, air was observed blowing from several of the wells completed in the residuum, indicating that a vapor lock condition had formed with a saturated infiltration pulse trapping air in the residuum.

Water movement in the weathered bedrock and bedrock aquifer is strongly controlled by the locations and orientations of cavities. The primary orientations of cavity systems are controlled by the local bedding orientation and the orientation of penetrative joints and fractures, which are widened by dissolution. The influence of stratigraphic controls on groundwater movement has been demonstrated on the site by performance of a tracer test in the ephemeral stream located in the middle portion of the Chepultepec Dolomite. The dye tracer test is reported in detail in Appendix B. Dye tracer was introduced into the aquifer by way of a disappearing stream and was detected in surface water approximately 1.5 to 3 km (0.9 to 1.9 mi) away. The flow path apparently followed a narrowly confined cavity system southwest from the point of injection to a cross-cutting valley. From there the flow path apparently followed the cross-cutting feature south toward the Clinch River. A portion of the discharge from this flow system enters the Clinch River at the watershed outlet. Inconclusive evidence was found suggesting flow southwest along strike approximately 3 km (1.9 mi) to the Clinch River. Attempts to pull the dye tracer into an observation well by pumping the well were unsuccessful. The inability to pump tracer into the nearby well may be due to lack of hydraulic connection between the well and a confined cavity or due to insufficient pump capacity. The travel rate within the traced flow path is on the order of 240 to 380 m/d (780 to 1250 ft/d). Flow in this portion of the site is thought to represent the upper bound of groundwater movement for the site.

Within both the soil and bedrock aquifers, flow is from the higher topographic areas toward the lower areas. Gradients indicate flow toward the nearest perennial surface water features. Apparent water divides are located beneath the ridges on the site. In the Copper Ridge Dolomite outcrop belt, the groundwater divide appears to coincide with the topographic divide. In the Longview/Newala Ridge, the groundwater divide does not coincide with the topographic divide but tends to occur approximately 100 m (300 ft) southeast of the ridge crest. ✓

Groundwater from the Longview Formation apparently flows down dip and/or through fractures into the upper Chepultepec Dolomite. Flows from the middle and upper Copper Ridge Dolomite (the southeast face of the ridge) apparently flow down dip and down gradient to the Chepultepec Dolomite. The actual groundwater flow paths in the bedrock and weathered bedrock zones are expected to resemble rectangular or trellis drainage patterns. Flow probably follows long runs parallel to strike and is diverted by shorter cross-strike channels to other strike-controlled zones or to emanation in a surface stream. Lateral flow in solution channels beneath Chestnut Ridge may follow discrete zones for distances >0.5 km. This observation is based on the general alignment of karst features along strike, and the locally well-developed karst features apparently related to discrete zones [12 karst features aligned along strike in 650 m (2100 ft)] on the West Chestnut Ridge Site and further northeast on Chestnut Ridge. The appearance of the dye tracer in a surface stream demonstrates that the flow system tested discharges to surface water. ✓

Lateral flow paths may also occur in residuum where predominantly gravelly zones have formed by the weathering of bedded cherts or where sandy zones in bedrock persist in the residuum. The lateral extent of such flow has not been demonstrated. ✓

On the West Chestnut Ridge Site, the karst zone in the upper Chepultepec Dolomite shows the most recent activity (steep-sided sink-holes) and acts as a collector and discharge pathway for groundwater, which flows down dip out of the Copper Ridge Dolomite. Electromagnetic (EM) terrain conductivity has been used in portions of this zone to locate preferential groundwater flow paths (Pin and Ketelle 1983).

Strike-parallel and strike-perpendicular conductivity anomalies were mapped at the western end of the West Chestnut Ridge Site. The strike-perpendicular portion of the EM conductivity anomaly coincides with the discharge pathway of the dye tracer test. The strike-parallel portion of the EM conductivity anomaly was initially thought to represent the discharge path which the dye tracer would follow; however, the dye was not detected in a well placed in that feature.

## 6. SURFACE WATER HYDROLOGY

The primary objective of hydrologic studies emphasizing surface waters is to support analysis of the water budget for the West Chestnut Ridge Site and to provide a basis for testing and analyzing hydrologic simulations in support of pathways analyses. The data that have been collected include biweekly measurement of flows at temporary monitoring sites between July 1982 and September 1983; continuous precipitation measurements beginning in December 1982; and continuous stream flow monitoring, instrumented and operated since October 1983, at five locations where either a flume or weir has been constructed. In addition, limited water quality analyses have been made for a few surface water samples. Results of these studies are reported in detail by Huff et al. (1984), Elmore et al. (1984), and Huff and Frederick (1984), but for the sake of brevity are summarized here to provide a general characterization of the surface water hydrology of the site. A map of the initial hydrologic study sites is presented in Fig. 6.1, which is taken from Huff et al. (1984). The present hydrologic study sites are shown in Fig. 6.2, which is taken from Huff and Frederick (1984).

### 6.1 PRECIPITATION

There are three general sources of information available to characterize precipitation at the West Chestnut Ridge Site: data from the Oak Ridge weather station, which is 13 km (8 mi) to the east and is operated by the National Oceanic and Atmospheric Administration; records taken at Walker Branch Watershed, which is 5 km (3.1 mi) to the east of the site; and data collected since December 1982 at a central location on the site (Fig. 6.2). Normal annual precipitation at the Oak Ridge weather station is 1336 mm (52.6 in). During the past 14 years, annual precipitation has averaged 1456 mm (57.3 in) at the weather station and 1398 mm (55.0 in) at Walker Branch Watershed. Precipitation at the West Chestnut Ridge rain gage is approximately the same as that at Walker Branch, and thus both these sites appear to average about 4% less precipitation than the Oak Ridge weather station. A comparison of monthly

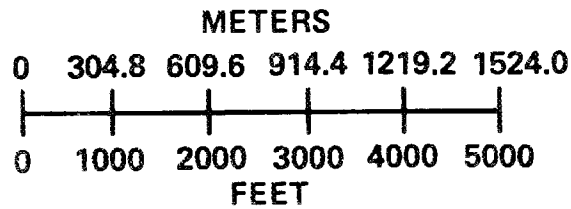
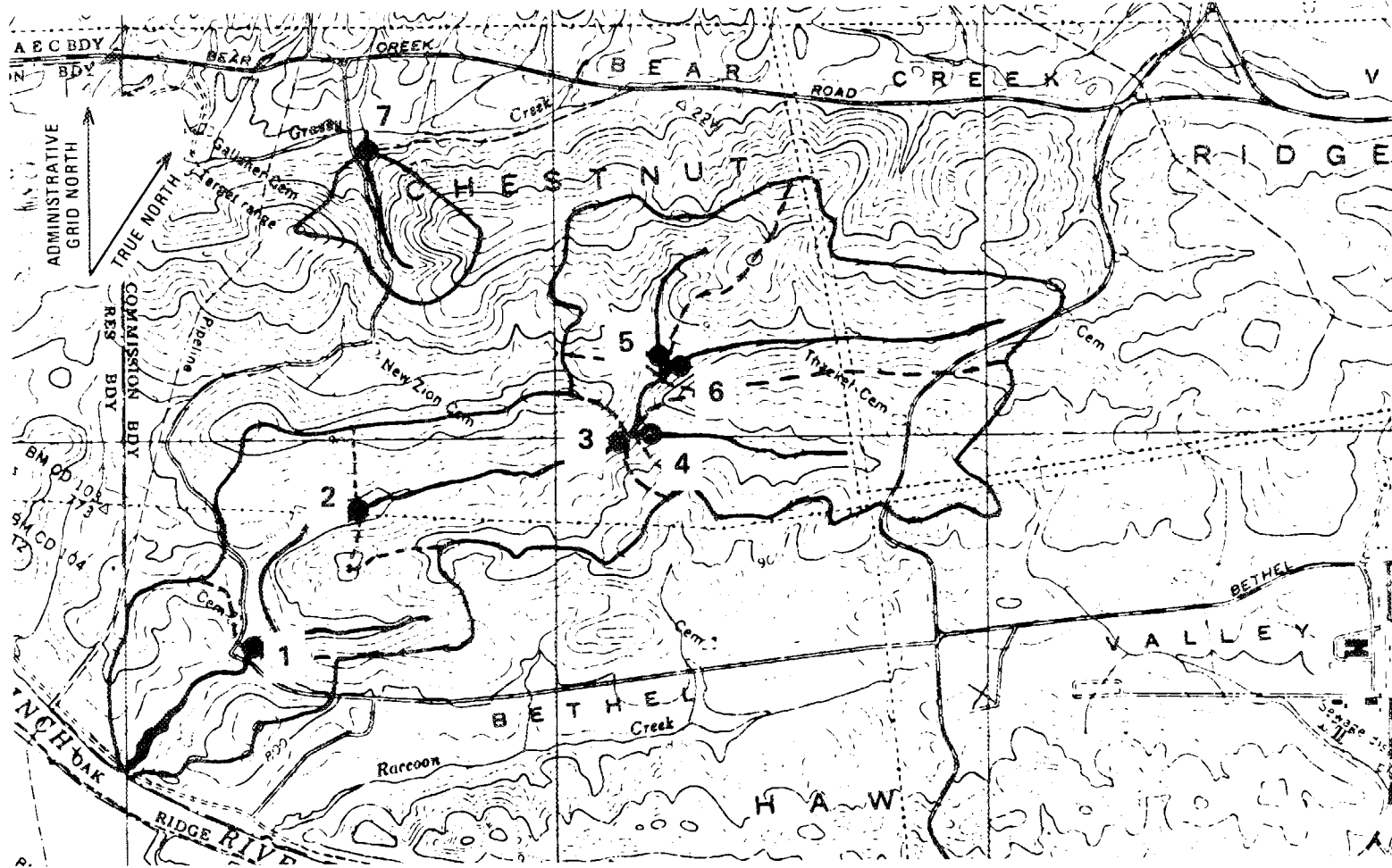


Fig. 6.1. Drainage area for Ish Creek (CWDF) and location map for seven temporary stream flow monitoring points.

CWDF HYDROLOGIC STUDIES

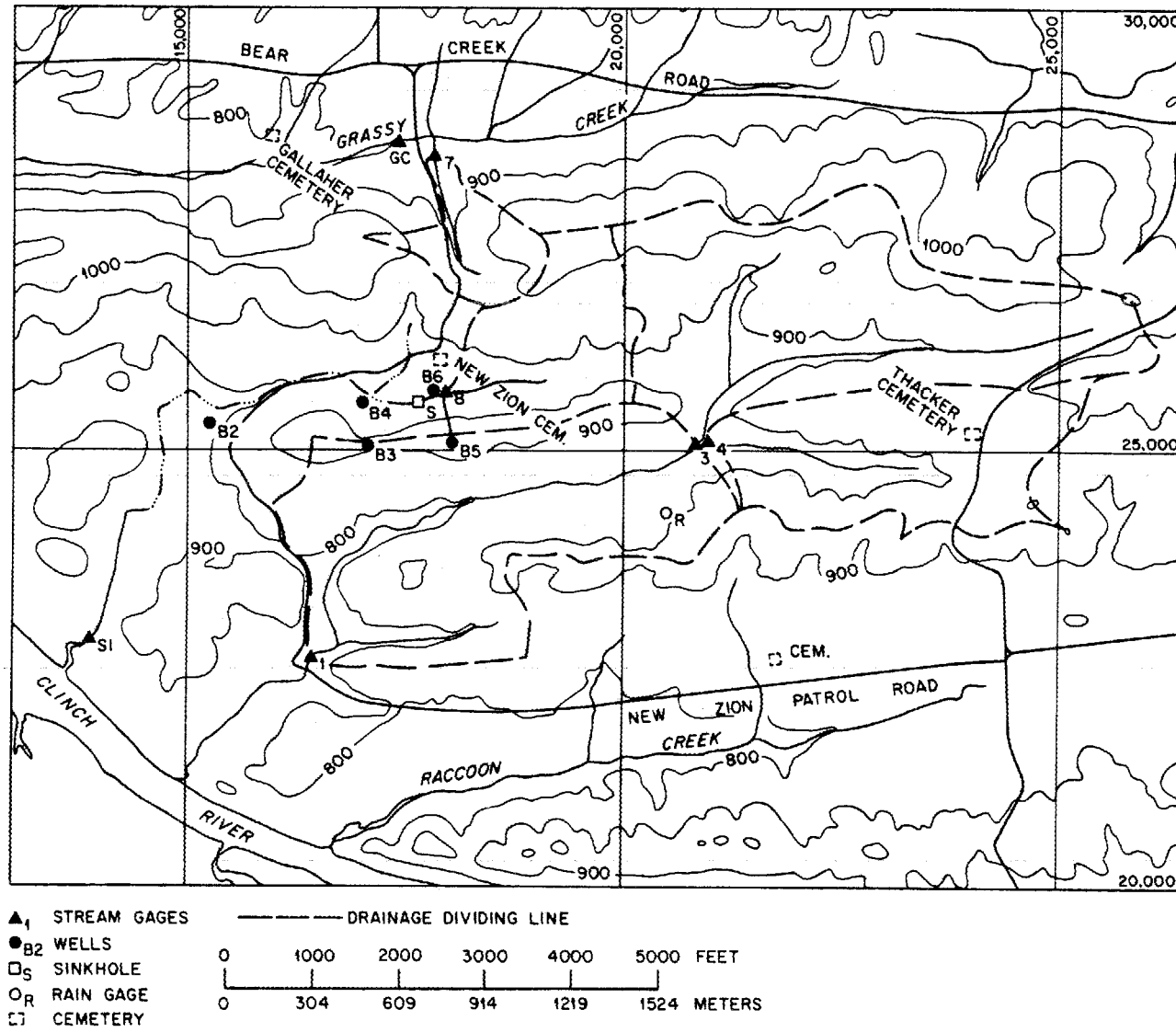


Fig. 6.2. Location map and drainage areas for continuous stream flow discharge measuring stations, recording rain gage, and selected groundwater monitoring wells.

totals among the three sites for calendar year 1983 is given in Table 6.1. Generally, precipitation is evenly distributed during the year, although October is normally the driest month. A summary of rainfall frequency for various durations is presented in Table 6.2. These values may be used to design runoff control and monitoring installations for the small areas planned for use in the site.

## 6.2 SURFACE WATER FLOWS

Flow measurements were made at approximately biweekly intervals between July 1982 and September 1983. Details are reported by Elmore et al. (1984) and Huff et al. (1984). Measurements were summarized in estimated time-weighted annual flow at each of the seven sites shown in Fig. 6.1, and are given in Table 6.3. However, it should be noted that the estimation procedure ignores the true dynamic nature of the system and probably biases the results toward underestimation. Thus, the values should be used only to evaluate relative differences among sites and not as an absolute measure of the water budget. Given this qualification, it appears that site 1 represents an area where flow is higher per unit area than at the other sites. This may result from the different geologic unit underlying site 1, as compared to those at other locations. It is likely that more of the subsurface flow is forced to the surface in this area than at the other sites, thus making it more suitable for a permanent long-term monitoring point for flow and water quality. Although the maximum observed flow rates shown in Table 6.3 are not representative of storm event conditions, the low flow values are probably good measures of minimum flows to be expected at the site. The variability of flow per unit area, together with the fact that some of the catchments exhibit zero flow for extended periods, is indicative of underlying solution features that capture and transmit flow. Work by Hollyday and Goddard (1979) has shown this to be true in the same geologic formation in another location (Dandridge, Tennessee), which is about 80 km (50 mi) northeast of the site.

Beginning in October 1983, continuous flow monitoring at the five locations shown in Fig. 6.2 was initiated. Each of these sites has a

Table 6.1. Comparisons of monthly precipitation at the West Chestnut Ridge Site (WCRS), Walker Branch Watershed (WBW) and Oak Ridge Townsite (ORT) weather stations for calendar year 1983.  
All values are in millimeters

Month	WCRS	WBW	ORT	Normal
Jan.	40.82	37.92 <sup>a</sup>	44.45	133.35
Feb.	111.71	110.30 <sup>a</sup>	111.25	133.10
March	57.84	53.71	65.28	138.43
April	163.05	162.24	162.56	106.93
May	150.61	163.48	175.26	89.41
June	56.15	67.08	64.26	100.08
July	68.12	41.78	61.21	144.02
Aug.	25.88	37.64	32.51	97.79
Sep.	34.80	48.01	52.58	84.84
Oct.	125.74 <sup>a</sup>	113.44	116.33	69.09
Nov.	136.87	135.17	148.59	102.87
Dec.	170.78 <sup>a</sup>	173.03	176.53	136.14
Total	1142.4	1143.8	1210.8	1336.0

<sup>a</sup> Missing data estimated from nearby records.

Table 6.2. Rainfall (inches) vs frequency on areas up to 10 miles<sup>2</sup> in Anderson and Knox counties, Tennessee

Frequency (yrs)	Minutes <sup>a</sup>					Hours <sup>b</sup>				
	5	10	15	30	60	2	3	6	12	24
2	0.43	0.65	0.80	1.14	1.5	1.8	2.0	2.4	2.8	3.3
5	0.50	0.78	0.98	1.43	1.9	2.4	2.5	3.0	3.6	4.2
10	0.56	0.89	1.12	1.65	2.2	2.7	2.9	3.5	4.1	4.8
25	0.64	1.03	1.30	1.89	2.5	3.0	3.4	3.9	4.7	5.5
50	0.71	1.15	1.45	2.11	2.8	3.4	3.7	4.7	5.3	6.1
100	0.77	1.26	1.60	2.36	3.1	3.8	4.0	4.9	5.7	6.6

<sup>a</sup> 2 yr and 100 yr; 5 min, 15 min, and 60 min data from maps in NWS HYDRO-35 (1977). All other "minute" data calculated using appropriate equation from the publication is listed as footnote b.

10 min: (0.59) (15 min) + (0.41) (5 min)  
 30 min: (0.49) (60 min) + (0.51) (15 min)  
 5 yr: (0.278) (100 yr) + (0.674) (2 yr)  
 10 yr: (0.449) (100 yr) + (0.496) (2 yr)  
 25 yr: (0.669) (100 yr) + (0.293) (2 yr)  
 50 yr: (0.835) (100 yr) + (0.146) (2 yr)

<sup>b</sup> Interpolated from maps in USWB TP 40 (1961).

Table 6.3. Summary of intermittent flow measurement data for July 15, 1982, to July 11, 1983

Station	Contributing area (km <sup>2</sup> )	Flow rate					
		Annual mean		Maximum		Minimum	
		(L/s)	(cm) <sup>a</sup>	(L/s)	(cm/d) <sup>b</sup>	(L/s)	(cm/d) <sup>b</sup>
1	2.44	38.9	50.3	139.0	0.49	1.33	0.005
2	1.94	21.8	35.4	78.7	0.35	0.82	0.004
3	1.45	14.0	30.4	49.7	0.30	0.33	0.002
4	0.54	3.2	18.7	10.9	0.17	0.00	0.000
5	0.25	1.9	24.0	6.8	0.24	0.32	0.011
6	0.52	3.9	23.6	14.9	0.25	0.00	0.000
7	0.14 <sup>c</sup>	1.6	36.0	4.4	0.27	0.39	0.024

<sup>a</sup> Flow rate computed as centimeters of runoff from the contributing watershed area.

<sup>b</sup> Flow rate computed as cm/d runoff from the contributing watershed area.

<sup>c</sup> The area for site 7 has been revised from earlier estimates by Elmore, et al. (1984) and Huff, et al. (1984).

flume or weir that has been calibrated by direct field measurement of corresponding stage height and flow over a broad range of conditions. A brief synopsis of the monthly results of all five sites is given in Table 6.4, which includes values of recorded daily maximum and minimum flows as well as mean monthly values. The period represented in the summary is November 1983 to April 1984, although data collection is ongoing. Note that some data are missing at sites 4, 7, and 8. More comprehensive and detailed data are available and are summarized by Huff and Frederick (1984), but are too voluminous to include here.

Peak flow rates for selected recurrence intervals have been estimated for the site by Huff et al. (1984), and values are summarized in Table 6.5. For comparison purposes, the peak instantaneous flow at site 1 on May 7, 1984 was estimated at 5,900 L/s (193,515 G/min) (by rating curve). Flow at other sites on that date are not available. The May 7 value at site 1 corresponds to a recurrence interval of approximately 7 years for peak flow, based on the flood frequency curve shown in Fig. 6.3, assuming the general regional relationship applies.

### 6.3 WATER BUDGET ESTIMATES

Continuous records of surface water data collected to date are of insufficient length to allow direct calculation of a site water budget. However, it is possible to compare precipitation and runoff volumes by subbasin for monitoring sites where data are sufficient. Such comparisons allow estimation of combined evaporative loss, deep seepage and groundwater losses, and change in soil moisture storage. Table 6.6 presents monthly comparisons of precipitation volume, runoff volume, and runoff as a percent of precipitation. General relationships and studies of interception losses for deciduous (mixed hardwood) forest cover suggest that dormant season losses are expected to be about 6 to 11% of precipitation, depending on the number of storm events. Once the basins are fully recharged from summer and autumn moisture deficits, one would expect most of the net precipitation to reappear as runoff. Using simulations developed for other nearby watersheds (based on the Thornthwaite-Mather technique for determining evapotranspiration),

Table 6.4. Monthly flow data (L/s) for monitoring stations on the West Chestnut Ridge Site

	Nov. 1983	Dec. 1983	Jan. 1984	Feb. 1984	Mar. 1984	Apr. 1984
CWDF 1						
Monthly mean	23.7	93.2	45.4	50.1	73.2	49.6
Instantaneous max.	1750	1010	132	346	682	281
Instantaneous min.	1.2	14	9.6	9.6	14	14
CWDF 3						
Monthly mean	6.82	41.7	21.8	25.6	39.4	32.5
Instantaneous max.	185	283	71	150	318	e130
Instantaneous min.	0.6	5.7	4.4	3.2	6.4	8.1
CWDF 4						
Monthly mean	2.23	14.9	8.55	10.1	12.0	8.30
Instantaneous max.	>48	>48	22	>48	>48	>48
Instantaneous min.	0.03	2.8	2.3	1.5	2.7	1.8
CWDF 7						
Monthly mean	0.68	3.82	2.50	2.62	4.05	3.33
Instantaneous max.	10	21	7.2	14	31	13
Instantaneous min.	0.1	0.8	0.7	0.7	1.0	1.8
CWDF 8						
Monthly mean	0.87	7.11	4.16	4.97	8.50	6.79

Note: Fragmentary stage record at CWDF 8 is adequate to allow reasonable estimates of mean daily discharge, but except for NO FLOW prior to Nov. 27, instantaneous maximum and minimum values cannot be reliably determined. Maximum flow probably exceeded 48 L/s on March 28.

Table 6.5. Estimated frequency of peak discharges on Ish Creek

Recurrence interval (year)	Peak estimated flows <sup>a</sup> (L/s)		
	Station 1	Station 2	Station 3
2	3,440	2,900	2,320
5	5,720	4,840	3,890
10	7,480	6,340	5,120
25	12,000	8,430	6,820
50	14,200	10,200	8,280

<sup>a</sup> Approximate standard error of estimation is 50%. Table taken from Huff et al. (1984).

# GUMBEL PROBABILITY DISTRIBUTION

ORNL-DWG 82-18446

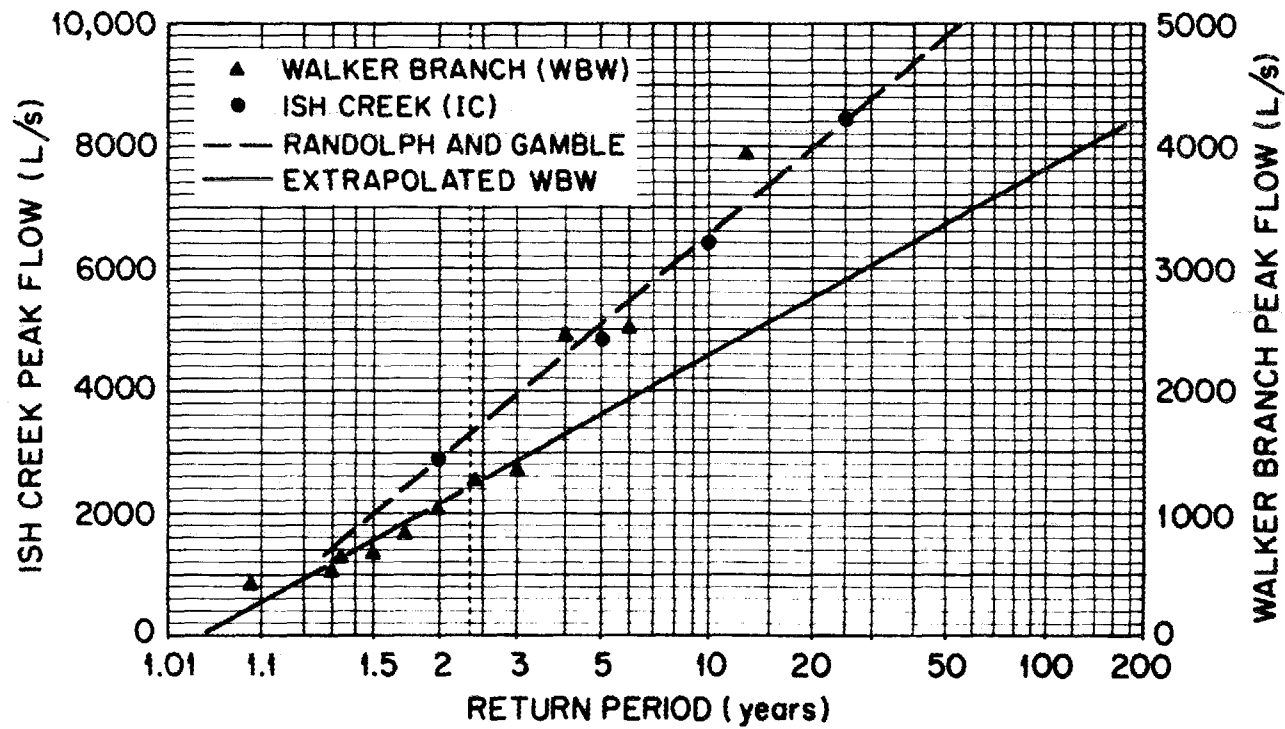


Fig. 6-3. Flood frequency curves for Walker Branch and Ish Creek, based upon the Gumbel extreme-value frequency distribution

Table 6.6. Precipitation - Runoff comparison at West Chestnut Ridge flow measuring sites

	<u>Nov. 1983</u>	<u>Dec. 1983</u>	<u>Jan. 1984</u>	<u>Feb. 1984</u>	<u>Mar. 1984</u>	<u>Apr. 1984</u>	<u>Nov. 1983- Apr. 1984</u>
	Precipitation, mm						
	136.87	170.78	62.91	92.84	115.84	102.63	682.07
	Runoff, mm						
CWDF 1	25.20	102.29	49.79	51.44	80.35	52.67	361.74
CWDF 3	12.20	77.15	40.30	44.23	72.90	58.15	304.93
CWDF 4	10.63	73.26	42.12	46.33	58.92	39.53	270.79
CWDF 7	12.61	73.12	47.88	46.93	77.43	61.74	319.71
CWDF 8	7.13	60.48	35.41	39.55	72.30	55.84	270.71
	Runoff/rainfall ratio						
CWDF 1	0.18	0.60	0.79	0.55	0.69	0.51	0.53
CWDF 3	.09	.45	.64	.48	.63	.57	.45
CWDF 4	.08	.43	.67	.50	.51	.39	.40
CWDF 7	.09	.43	.76	.51	.67	.60	.47
CWDF 8	.05	.35	.56	.43	.62	.54	.40

estimates have been made for evaporative losses for the period of November 1983 through April 1984. Respective values as a fraction of rainfall are: 0.16, 0.10, 0.16, 0.11, 0.43, and 0.35. Thus, if storage changes and groundwater losses were negligible, the expected runoff ratios for the November-April period would be 0.84, 0.90, 0.84, 0.89, 0.57, and 0.65. Comparison of these estimates against observed values given in Table 6.6 shows that observed values are considerably lower than expected values except for March. When the runoff ratios between various other sites and site 1 are compared, the results suggest that 25 to 30% of the runoff at other sites is lost to deep seepage or ground water flow across topographic boundaries. This is consistent with earlier results showing large variability in runoff per unit area for the various subbasins. However, given the short period of records available for analysis, such conclusions must be considered as speculative and usable only with due caution.



## REFERENCES

- Allen, P. N., J. P. Bell, T. R. Butz, G. O. Irurhe, C. S. Lide, A. G. Payne, R. M. Pritz, T. R. Putney, Gilbert Commonwealth Engs. & Cons. 1980. Draft Alternatives Document for the Oak Ridge Solid Waste Disposal Facilities Feasibility Study, ORNL-5693, Oak Ridge National Laboratory, Oak Ridge, Tenn.
- Atkinson, T. C. and D. I. Smith, 1976. "The Erosion of Limestones," in the Science of Speleology ed. T. D. Ford and C. H. D. Cullingford, Academic Press, pp. 151-177.
- Brakensiek, D. C., H. B. Osborn, and W. J. Rawls, 1979. "Field Manual for Research in Agricultural Hydrology," Agricultural Handbook No. 224, U.S. Department of Agriculture, pp. 88-97.
- Brendt, W., geologist with the Tennessee Division of Geology. 1984. Personal communications with R. H. Ketelle, Oak Ridge National Laboratory, Oak Ridge, Tenn.
- Colman, S. M. 1981. Rock Weathering Rates as Functions of Time, Quaternary Research, Vol. 15, pp. 250-264.
- Crider, D. V. 1981. "Structural and Stratigraphic Effects on Geomorphology and Groundwater Movement in Knox Dolostone Terrane," Masters Thesis, University of Tennessee, Knoxville.
- Daniels, D. E., and G. Broderick. 1983. "Results of Moisture-Suction and Permeability Tests on Unsaturated Samples," in Subsurface Characterization and Geohydrologic Site Evaluation, West Chestnut Ridge Site, ORNL/Sub/83-64764/1 Woodward-Clyde Consultants, Wayne, N.J.
- Dunne, T. and L. B. Leopold. 1978. Water in Environmental Planning, W. H. Freeman and Co., San Francisco.
- Elmore, J. L., D. D. Huff, and J. R. Jones. 1984. West Chestnut Ridge Hydrologic Studies, ORNL/TM-9392, Oak Ridge National Laboratory, Oak Ridge, Tenn.
- Embleton, C. and J. B. Thornes. 1979. Process in Geomorphology, Edward Arnold, London.
- Geotek Engineering Company. 1981. Subsurface Investigations for M-47846 Landfill Studies, Contractors Report.
- Geotek Engineering Company. 1983. Piezometer Installation, West Chestnut Ridge, X-10 Plant, Oak Ridge, Tenn., Contractors Report.
- Gooding. 1890. In Process in Geomorphology, C. Embleton and J. B. Thornes, 1979, Edward Arnold, London, 102.

- Heller, J. L. 1959. "The Geology of the Black Oak Ridge Area, Anderson County, Tennessee," Masters Thesis, University of Tennessee.
- Hollyday, E. F., and P. L. Goddard. 1979. Groundwater Availability in Carbonate Rocks of the Dandridge Area, Jefferson County, Tennessee, U.S. Geological Survey, Water Resources Investigations Open-File Report 79-1263. U.S. Government Printing Office 1980 - 647-757, 56 pp.
- Huff, D. D., J. L. Elmore, and D. C. Farmer. 1984. Hydrologic Study and Evaluation of Ish Creek Watershed (West Chestnut Ridge proposed disposal site), ORNL/TM-8960, Oak Ridge National Laboratory, Oak Ridge, Tenn., 29 pp.
- Huff, D. D., and B. J. Frederick. 1984 (in prep.). Hydrologic Investigations in the Vicinity of the Proposed Central Waste Disposal Facility, Oak Ridge National Laboratory, Tennessee, ORNL/TM-9354, Oak Ridge National Laboratory, Oak Ridge, Tenn.
- Jennings, J. N. 1983. "Karst Landforms," Am. Sci., Vol. 71, No. 6, Nov-Dec. 1983.
- Lee, D. W., R. H. Ketelle, and L. H. Stinton, 1983. Use of DOE Site Selection Criteria for Screening Low-Level Waste Disposal Sites on the Oak Ridge Reservation, ORNL/TM-8717, Oak Ridge National Laboratory, Oak Ridge, Tenn.
- Lee, S. Y., O. C. Kopp, and D. A. Lietzke. 1984. Mineralogical Characterization of West Chestnut Ridge Soils, ORNL/NFW-84/25. Oak Ridge National Laboratory, Oak Ridge, Tenn.
- Newton, J. G. 1976. Early Detection and Correction of Sinkhole Problems in Alabama, With a Preliminary Evaluation of Remote Sensing Applications, HPR Report No. 76, State of Alabama Highway Department, Bureau of Materials and Tests, Montgomery, Ala. 36130.
- Parizek, R. R. 1976. "On the Nature and Significance of Fracture Traces and Lineaments in Carbonate and Other Terranes," pp. 47-108, in Karst Hydrology and Water Resources, Vol. I, Karst Hydrology, U.S.,: Yugoslavian Symposium on Karst Hydrology and Water Resources, Dubrovnik, Yugoslavia June 2-7, 1975, published by Water Resources Publications, Alexandria, Va.
- Pin, F. G., and R. H. Ketelle. 1983. Conductivity Mapping of Underground Flow Channels and Moisture Anomalies in Carbonate Terrain Using Electromagnetic Methods, ORNL/TM-8866, Oak Ridge National Laboratory, Oak Ridge, Tenn.
- Rodgers, J. 1953. Geologic Map of East Tennessee with Exploratory Text. Bulletin 58, Part II, Tennessee Division of Geology, Nashville, Tenn.

- Schmidt, V. A. 1982. Magnetostratigraphy of Sediments in Mammoth Cave, Kentucky, *Science*, vol. 217, August 27, 1982, pp. 827-829.
- Sellers, W. D. 1965. *Physical Climatology*, University of Chicago Press, Chicago.
- Smith, R. E., and N. J. Gilbert. 1983. Stability Analyses of Waste Disposal Facilities, Y-12 Plant, Oak Ridge, Tenn. Contractors Report.
- Staub, W. P., and R. A. Hopkins. 1984. Thickness of Knox Group Overburden on West Chestnut Ridge, Oak Ridge Reservation, by Detailed Seismic Refraction Profiling, ORNL/TM-9393, Oak Ridge National Laboratory, Oak Ridge, Tenn.
- Soil Survey of Anderson County, Tennessee. 1981. U.S. Department of Agriculture, Soil Conservation Service.
- Sweeting. 1960. *Process in Geomorphology*, C. Embleton and J. B. Thornes, 1979, Edward Arnold, London, p. 102.
- Swingle, G. D. 1964. "Geologic Map of the Clinton Quadrangle, Tennessee," State of Tennessee, Department of Conservation, Division of Geology.
- West, D. C., and L. K. Mann. 1982. Whole-Tree Harvesting: Third Year Progress Report for 1981 - Nutrient Depletion Estimates and Post Harvest Impacts on Nutrient Dynamics, ORNL/TM-8335, Oak Ridge National Laboratory, Oak Ridge, Tenn. p. 87.
- Woodward-Clyde Consultants. 1984. Subsurface Characterization and Geohydrologic Site Evaluation, West Chestnut Ridge Site, ORNL/Sub/83- 647641/IVI2, prepared by Woodward-Clyde Consultants, Wayne, N.J. for Oak Ridge National Laboratory, Oak Ridge, Tenn.



APPENDIX A  
WELL HYDROGRAPHS



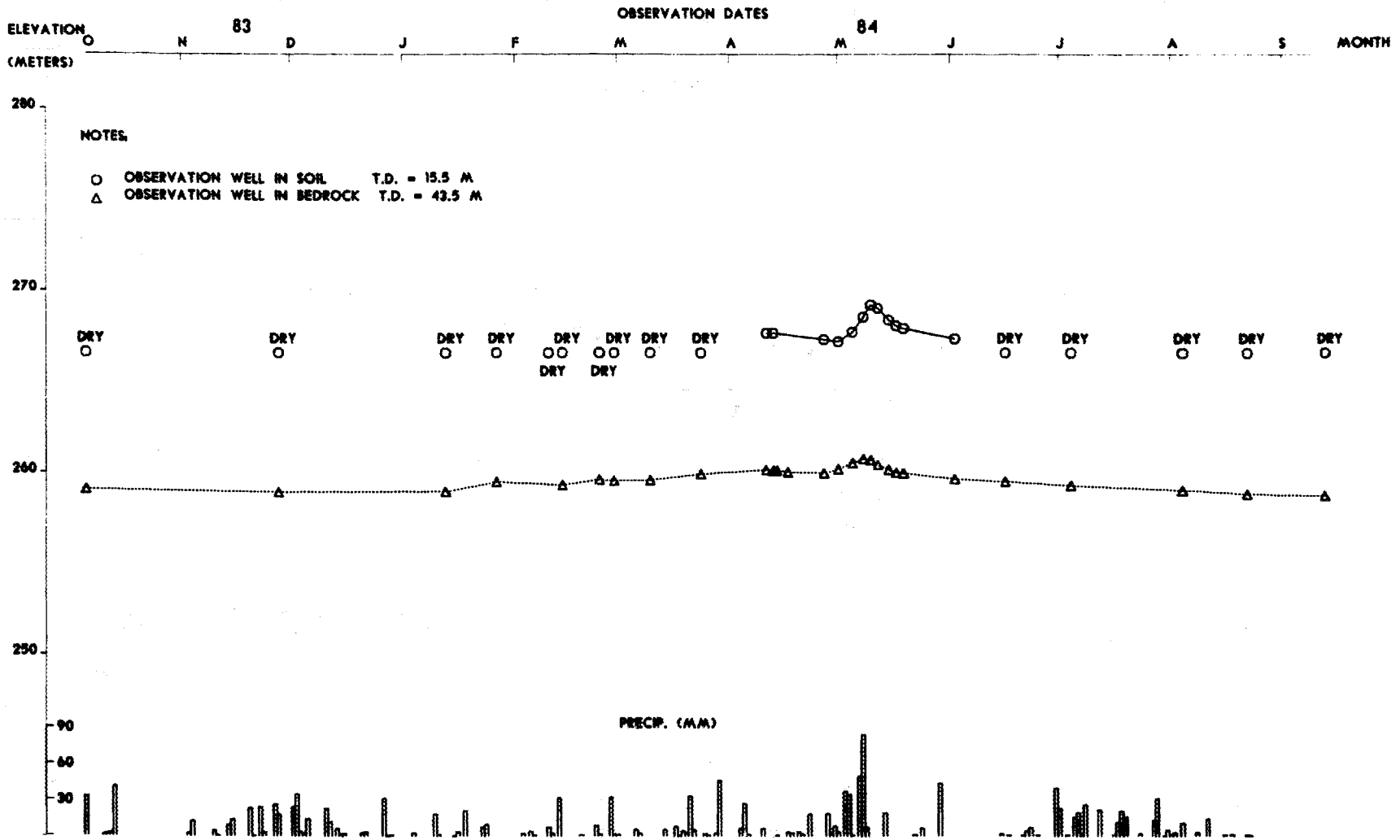




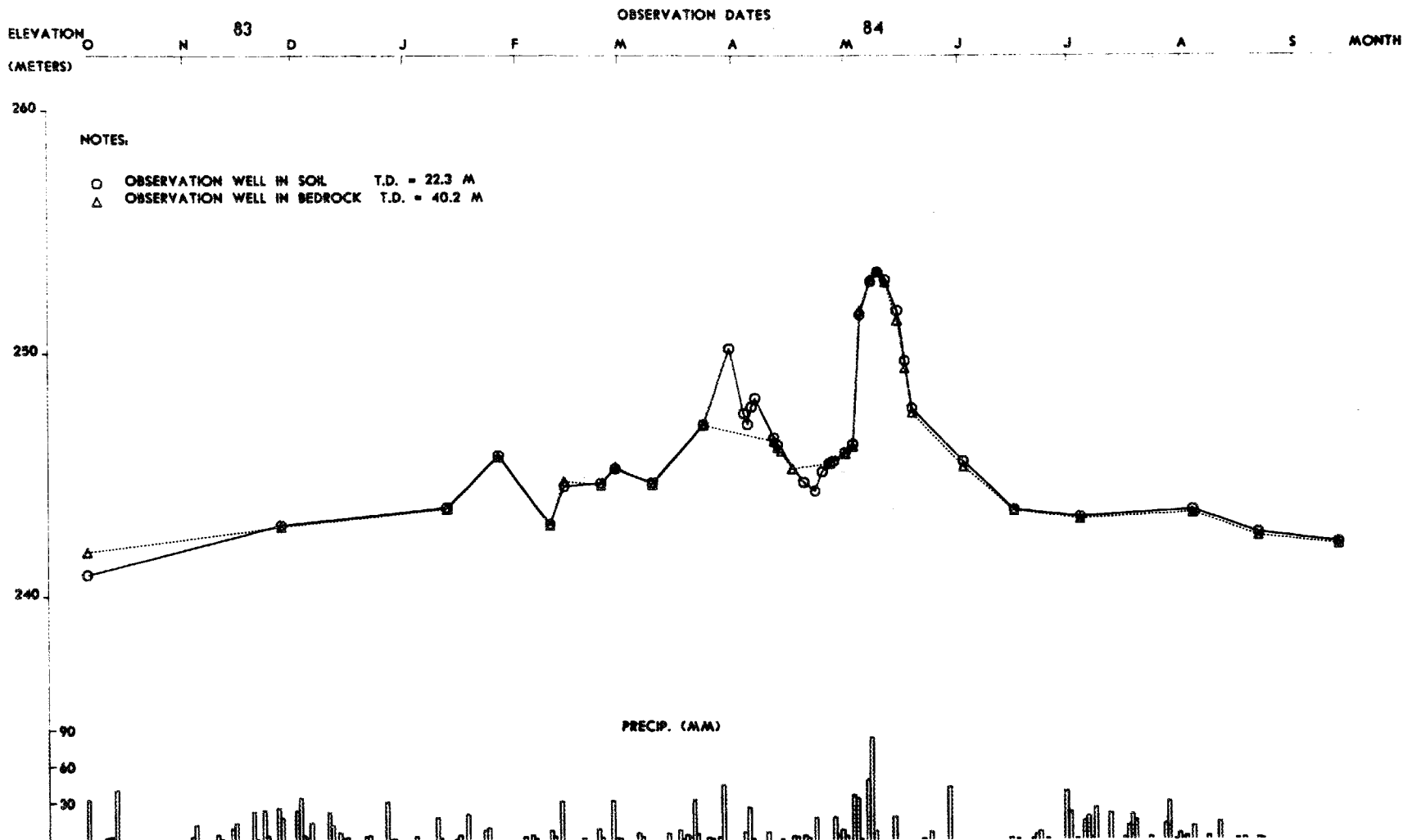




# WELL HYDROGRAPHS FOR WELL PAIR 5



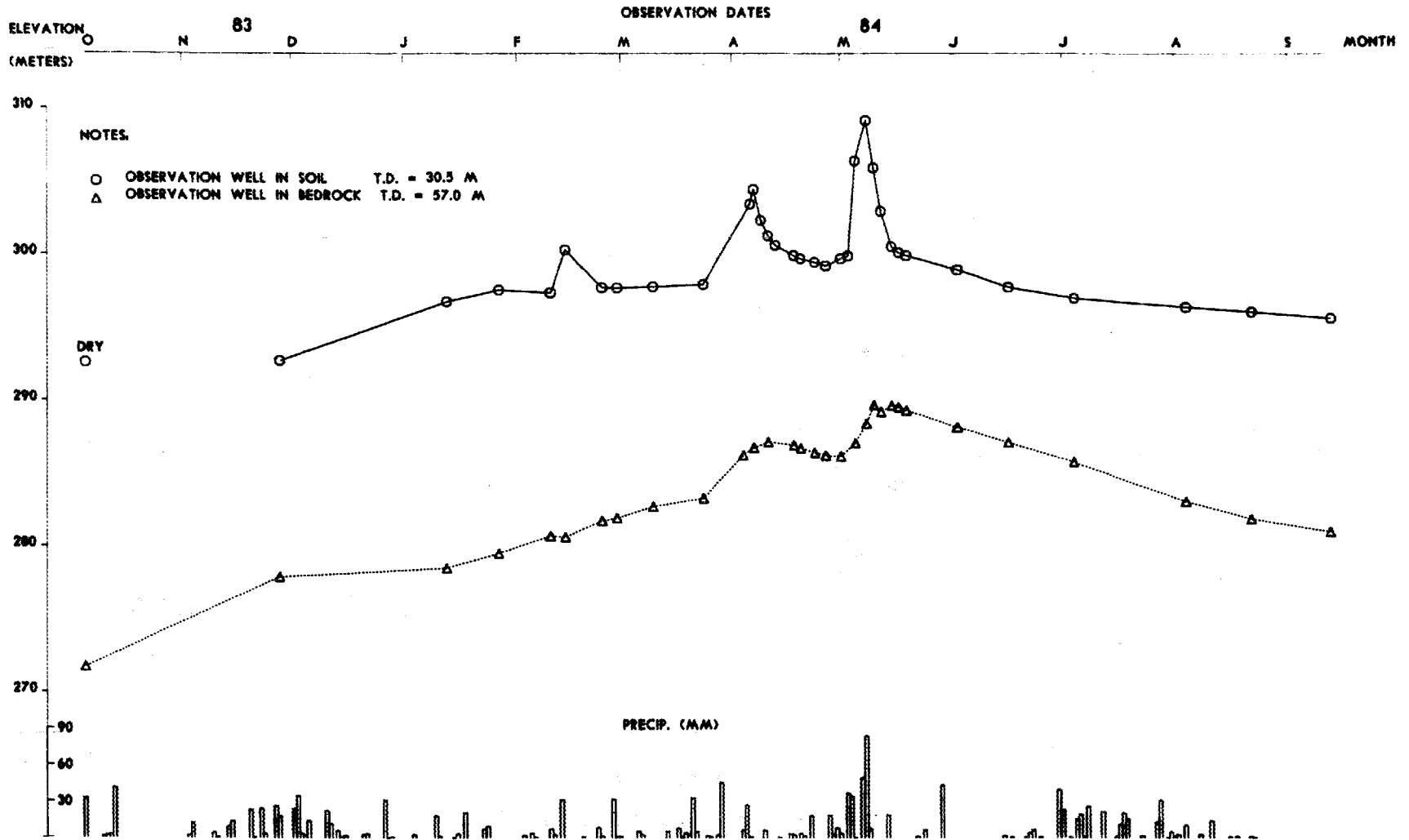
# WELL HYDROGRAPHS FOR WELL PAIR 6



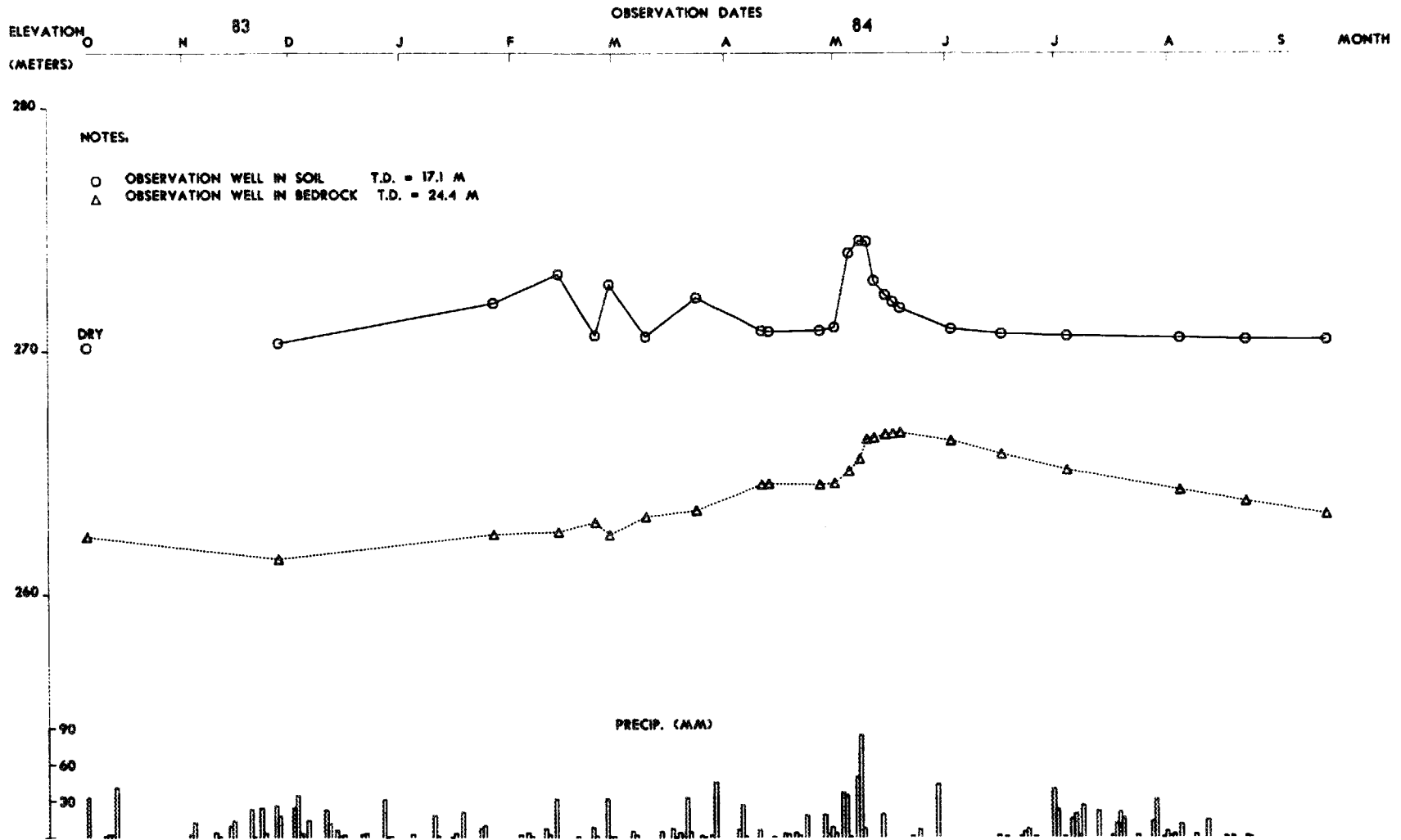




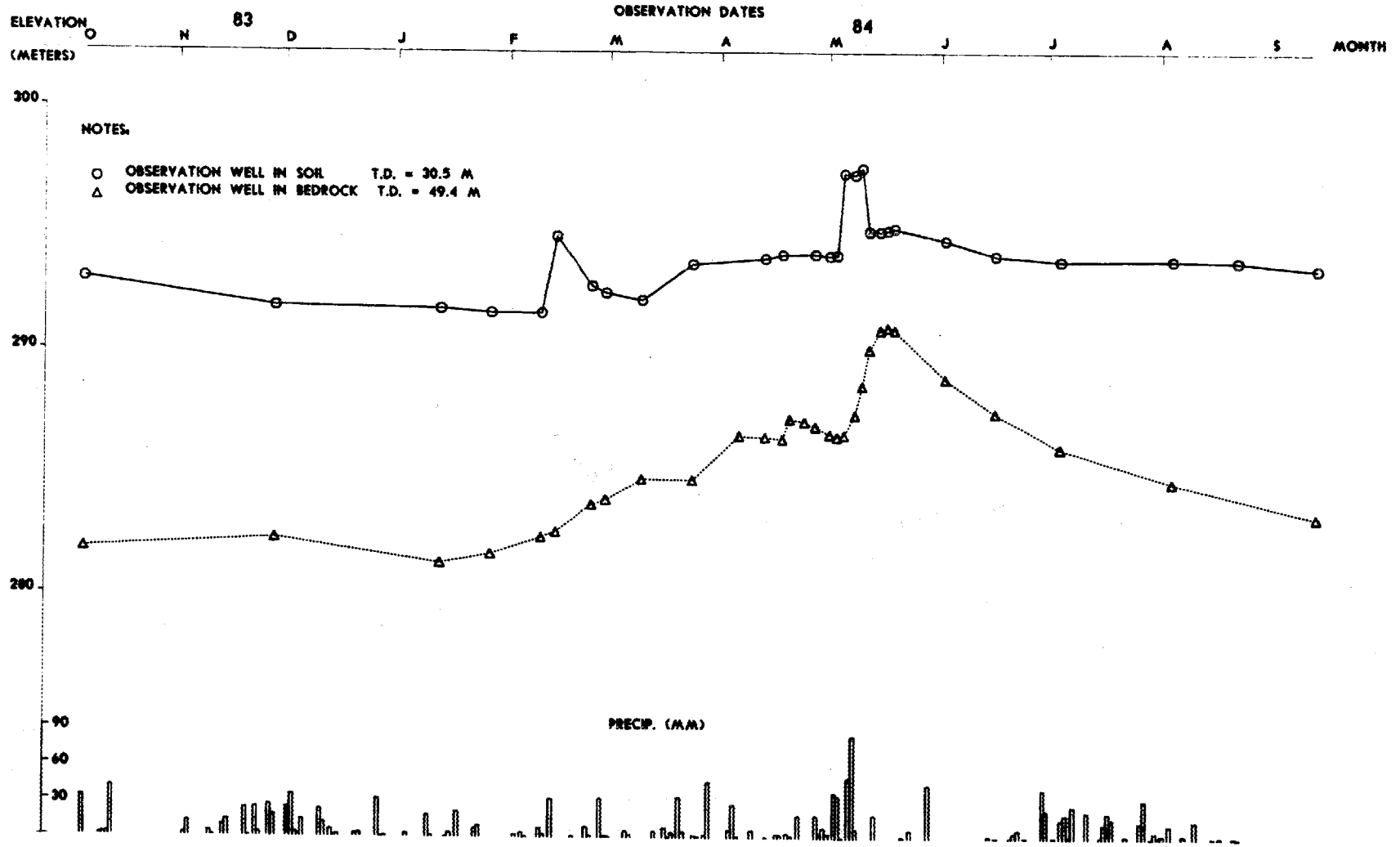
# WELL HYDROGRAPHS FOR WELL PAIR 9



# WELL HYDROGRAPHS FOR WELL PAIR 10



# WELL HYDROGRAPHS FOR WELL PAIR II



# WELL HYDROGRAPH FOR WELL 12

ELEVATION (METERS)      OBSERVATION DATES      MONTH

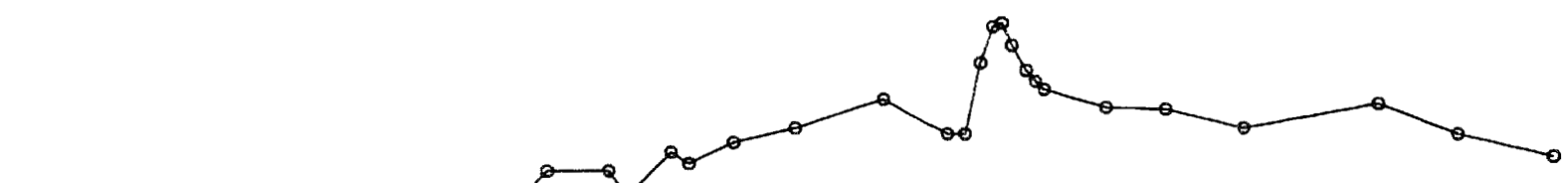
83      84

N      D      J      F      M      A      M      J      J      A      S

290  
280  
270

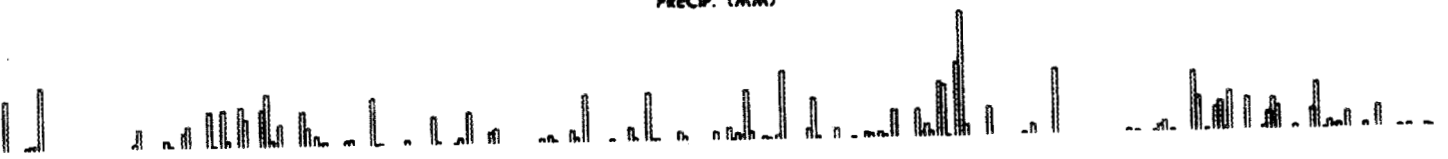
### NOTES:

○ OBSERVATION WELL IN SOIL      T.D. = 30.5 M



### PRECP. (MM)

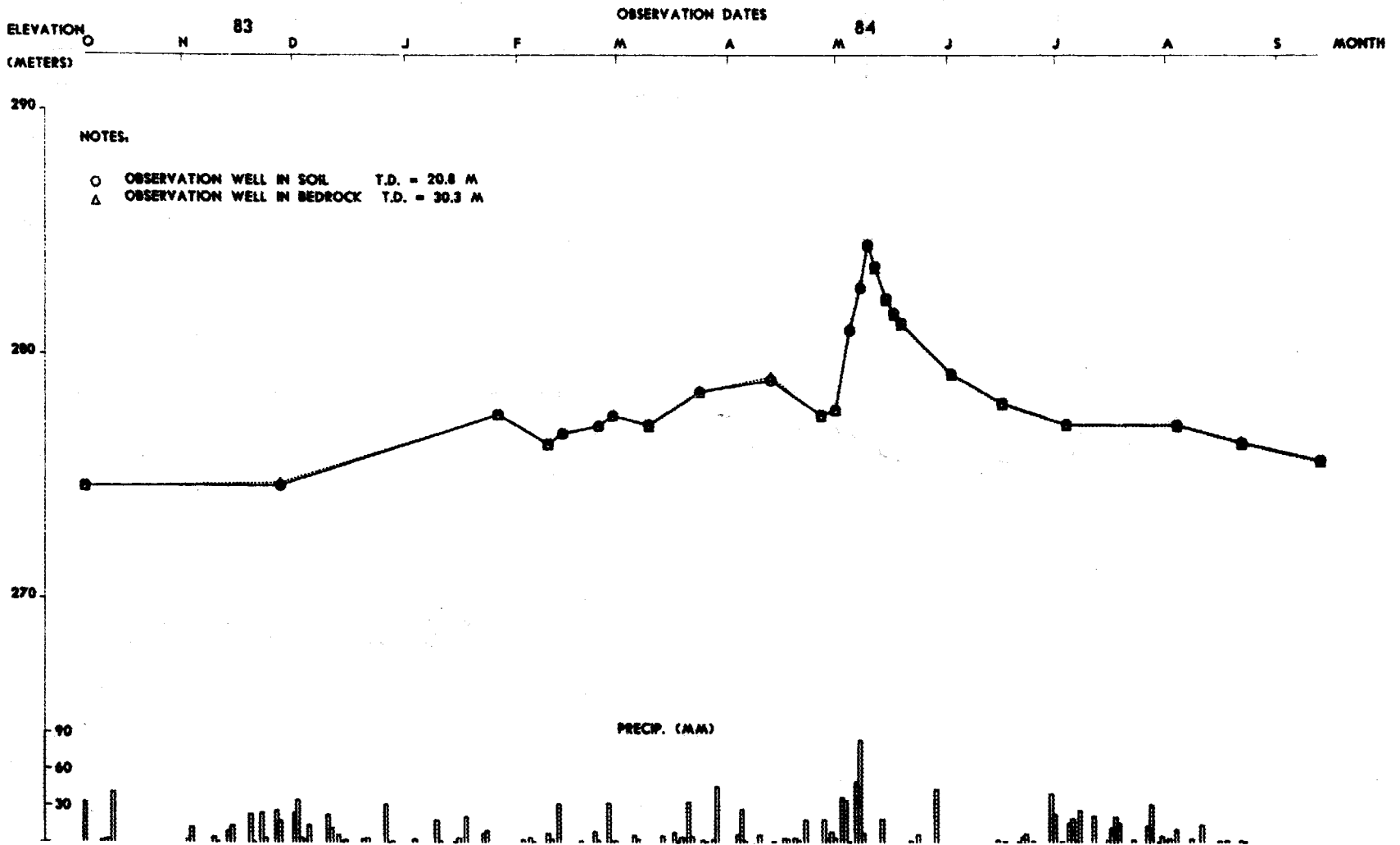
90  
60  
30





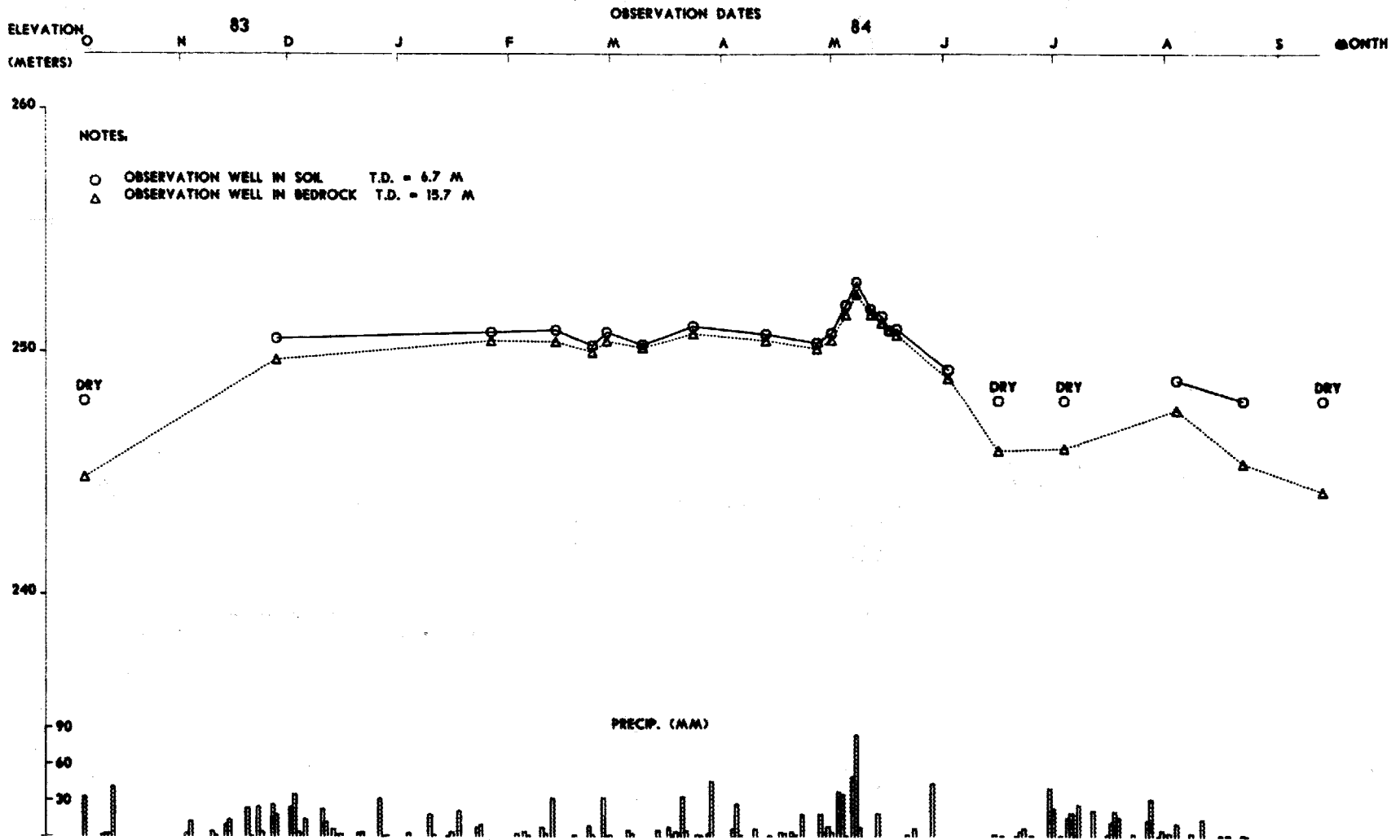


# WELL HYDROGRAPHS FOR WELL PAIR 15

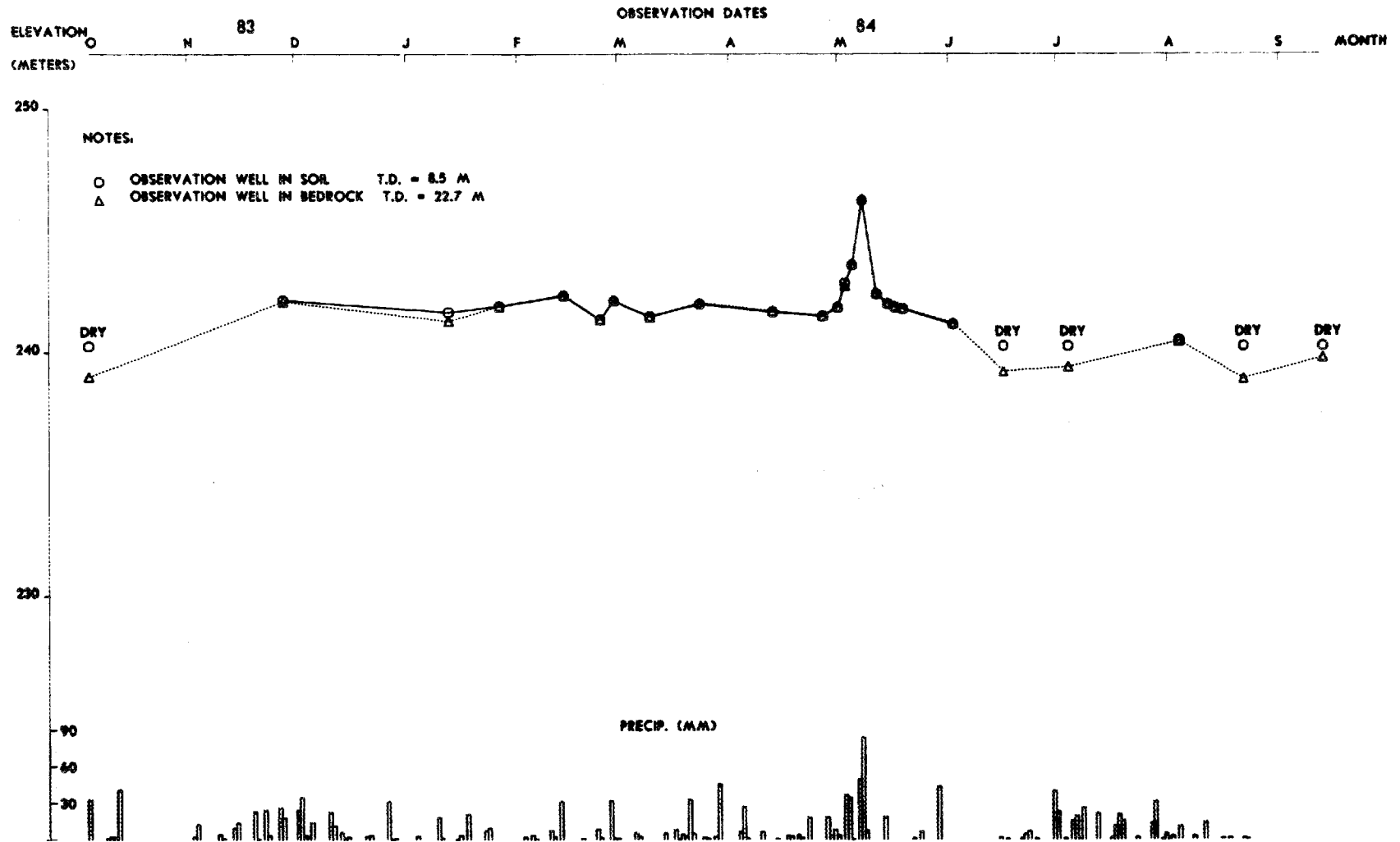




# WELL HYDROGRAPHS FOR WELL PAIR 17

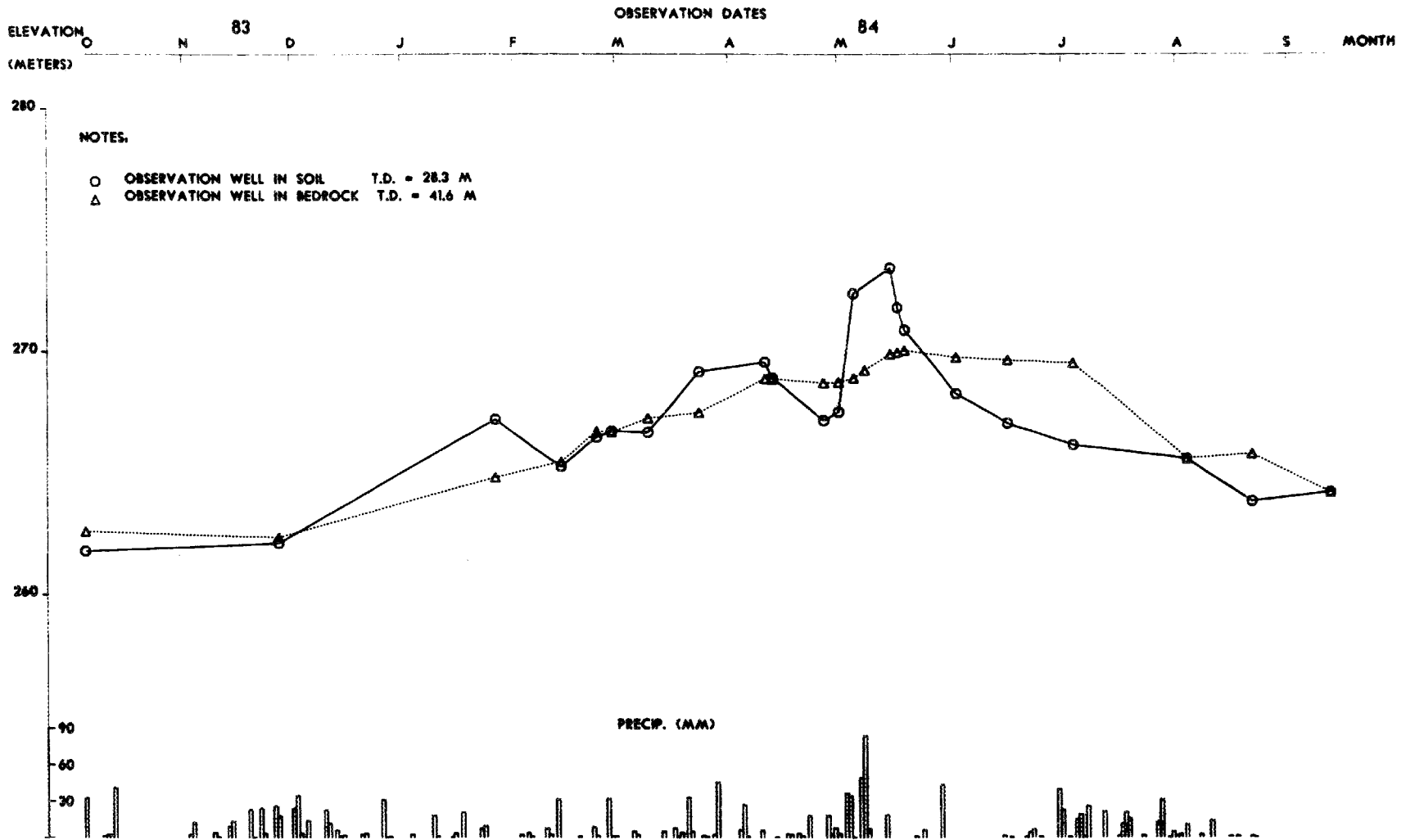


### WELL HYDROGRAPHS FOR WELL PAIR 18





# WELL HYDROGRAPHS FOR WELL PAIR 20



APPENDIX B  
GROUNDWATER TRACER TEST



## APPENDIX B GROUNDWATER TRACER TESTS

### Rationale and Objectives

In karst areas, where flow pathways can be unpredictable, it is important to identify the pathways and any points where subsurface flow returns to the surface water system. A tracer experiment can identify emergence points as well as indicate general flow directions, thus allowing the design of monitoring installations that are known to sample migration pathways from disposal areas. Further, some information on travel time and dilution can be obtained from results. All of these factors are valuable in demonstrating a knowledge of groundwater system behavior.

The presence of a swallow-hole that captures the flow of the unnamed tributary south of New Zion Cemetery just below monitoring station 8 (Fig. B.1) was considered good cause to attempt to determine the subsurface flow pathway of the stream flow to its point of reemergence. A dye tracer test was designed to detect the emergence point and provide approximate time-of-travel information. In addition, qualitative information on the extent of dilution was also considered a possible result of tracer tests. The study area selected for the testing included an area within a radius of about 2 km of the swallow-hole, but only a few sites east of the point of injection were monitored. The reason was that the water table generally slopes from east to west, and groundwater movement was not expected in an easterly direction.

### Methods

Two major injections of fluorescein dye were made. The first one involved 0.5 kg of dye and was initiated on January 18, 1984. Monitoring for the presence of dye over an eight week period did not show any positive results at any of the six surface water sites or the six wells used in the first test. Because a second, more successful test was conducted, details of the first test (which was very similar to the second test) are not discussed here.

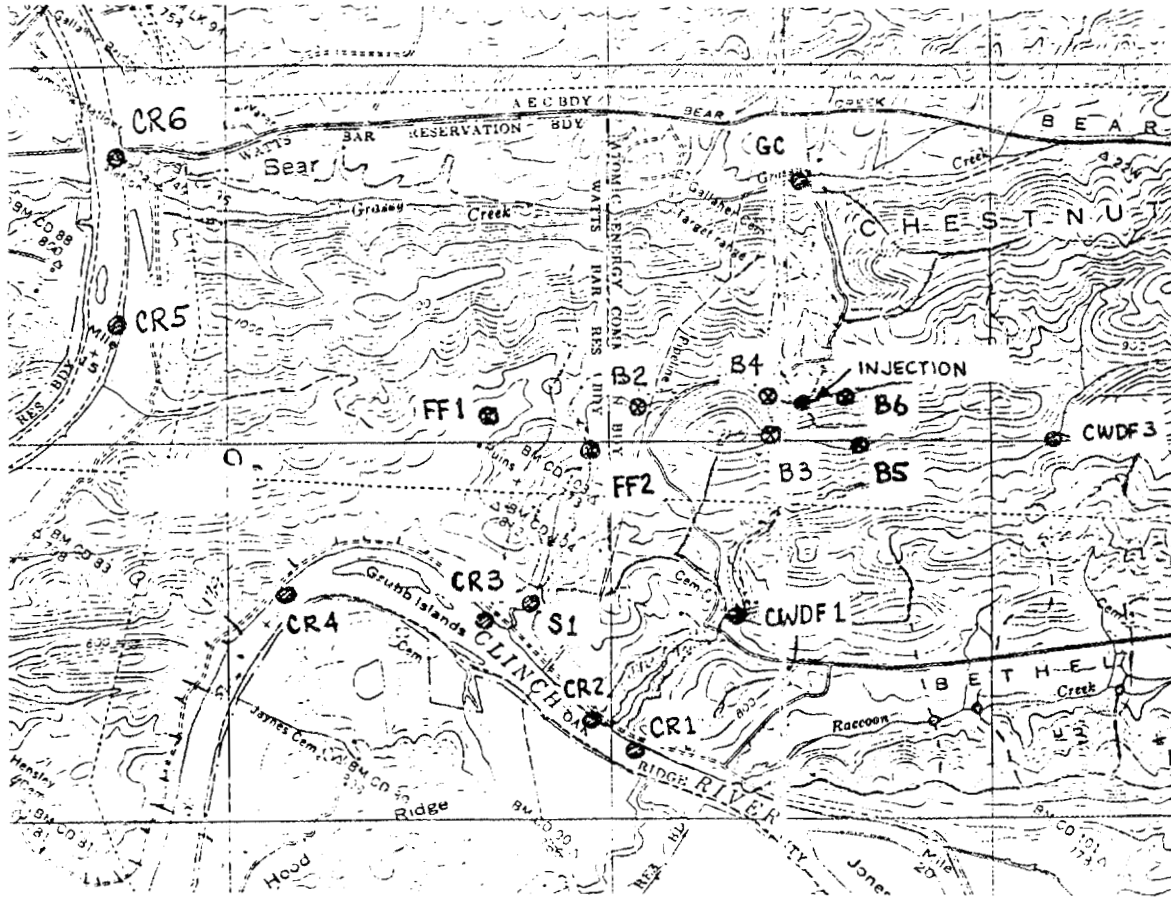


Fig. B.1. Monitoring locations used in dye tracer test.

The second tracer test involved 5.0 kg of fluorescein dye, which was injected on April 11, 1984 between 1130 and 1150 hours. Powdered fluorescein was dissolved in stream water, then poured directly into the stream just upstream from the swallow-hole. The discharge rate was 4.3 L/s at the time of injection. Packets of activated charcoal enclosed in a coarse mesh screen had been emplaced at several locations prior to dye injection to capture evidence of passage of the dye. Figure B.1 shows the location map for the sampling sites employed. At each of the surface water sites, two charcoal packets were in place. One was changed 1 to 7 d intervals and the other was changed at intervals of up to 13 d. At surface water sites the charcoal packet was suspended in the flow from a small cork float that was held in place by a weight and line. In the wells, packets were suspended by a line tied to the well casing at the surface.

In the interval between 5 and 8 d following injection, a positive test for the presence of fluorescein dye was found at site S-1. For testing, the charcoal was removed from the screen packet and leached with a 70% isopropyl alcohol - 5% potassium hydroxide solution, which was added to a container holding the charcoal. Positive results were indicated by the presence of clearly visible dye when a light beam was passed through the solution. Additional confirmation of the presence of dye came when the charcoal packet at site S-1 that represented the 8 to 12 d interval also showed a positive result. In addition, the charcoal that had been in place at site S-1 between 2 d prior to and 12 d following injection also showed a positive test for dye. No other charcoal packets, including those collected at site S-1 after 12 d post-injection, gave a positive test for dye.

### Results

The appearance of dye at site S-1 in the 5 to 8 d interval following injection allows an estimation of velocity for water moving in the subsurface system draining the northwestern portion of the proposed Central Waste Disposal Facility site. Since the travel distance was about 1500 to 1800 m, the velocity ranges between 200 and 360 m/d. The

concentration of dye immediately following injection was about 1000 ppm, which was similar to the first test. It was not possible to quantify the dilution that occurred between the injection point and detection point because the dye was not visually present. However, since the dye is visually detected at concentrations of about 0.1 ppm, it appears that greater than a 10,000-fold dilution occurred.

Since the dye was detected in the drainageway where it was injected, it is reasonable to infer that it followed the general path described by the dry surface channel. Near-field evidence presented by Pin and Ketelle (1983) using electromagnetic methods supports the hypothesis that the subsurface drainage from the swallow-hole travels along the drainageway to the point of emergence above site S-1 and the Clinch River. The key point of the detection of dye at S-1 is that it offers positive proof that one important pathway for subsurface flow migration from the northwest area of the proposed CWDF site emerges at or above site S-1. This suggests that site S-1 should be instrumented and established as a flow and water quality monitoring site for the proposed CWDF area.

Examination of the log of dye tracing leach tests also reveals that the possible presence of dye at sites CR4 and CR5 occurred near the end of April. While these results are questionable, the dye appearance at these sites is consistent with the hypothesis that some of the dye may move along geologic strike from the point of injection to the Clinch River. This possibility reinforces the fact that the lack of positive detection of dye at sites other than S-1 does not prove it wasn't present. It is possible that dye was present at other sites in concentrations that are below detection limits. The fact that dye was not found in the limited sampling of wells near the injection point and along the suspected flow path may warrant further consideration. It is possible that the rather limited duration of the pumping and sampling was inadequate. However, it may also suggest a localized channel or conduit for the flow that was not sampled by the wells. If so, this would argue for increased emphasis on surface water monitoring to detect any contaminant migration from the area.

Measurements of flow at site S-1 were made manually at several points in time when charcoal packets were changed. Table B.1 presents those data, together with corresponding mean daily flow rates at other CWDF flow monitoring stations. Values are presented both as flow rate (L/s) and flow rate per unit area (L/s/km<sup>2</sup>). The latter terms should be fairly comparable among sites. The interesting thing about these data is that on February 10 and April 23, 1984, unit area flow values are much lower at site S-1 than at other locations. This suggests the possibility of a flow-rate dependent threshold for movement of water along the route to site S-1. If true, it could explain why dye was not detected at site S-1 during the first test. Given the possible appearance of dye at sites CR4 and CR5 near the end of April, one might speculate that some flow always moves along strike to the Clinch River, but excess discharge spills over and follows the old stream channel at higher flows.

Table B.1. Comparison of flow rates at CWDF sites during the tracer experiment

DATE	Site 1 ( $2.440^2 \text{ km}^2$ ) <sub>2</sub>		Site 3 ( $1.448^2 \text{ km}^2$ ) <sub>2</sub>		Site 4 ( $0.544^2 \text{ km}^2$ ) <sub>2</sub>		Site 7 ( $0.140^2 \text{ km}^2$ ) <sub>2</sub>		Site 8 ( $0.315^2 \text{ km}^2$ ) <sub>2</sub>		Site S1 ( $1.220^2 \text{ km}^2$ ) <sub>2</sub>	
	L/S	L/S/km <sup>2</sup>	L/S	L/S/km <sup>2</sup>								
2-10-84	9.55	3.9	6.65	4.6	2.32	4.3	1.32	9.4	1.27	4.0	0.99	0.8
4-9-84	48.55	19.9	**		7.32	13.4	3.85	27.5	8.76	27.8	17.35	14.2
4-11-84	31.95	13.1	27.46	15.5	6.52	12.0	2.40	17.1	5.16	16.4	13.99	11.5
4-12-84	28.78	11.8	17.39	12.0	6.01	11.0	2.47	17.6	4.27	13.6	11.45	9.4
4-13-84	25.02	10.2	15.98	11.0	5.56	10.2	2.37	16.9	3.95	12.5	9.97	8.2
4-16-84	18.29	7.5	13.13	9.1	4.37	8.0	2.18	15.6	3.26	10.3	8.14	6.7
4-19-84	14.00	5.7	9.60	6.6	2.56	4.7	1.53	10.9	2.12	6.7	6.66	5.4
4-23-84	48.64	19.9	30.92	21.4	6.72	12.4	2.84	20.3	5.62	17.8	4.79	3.9

## INTERNAL DISTRIBUTION

- |        |                |     |                            |
|--------|----------------|-----|----------------------------|
| 1.     | J. S. Baldwin  | 49. | F. R. Mynatt               |
| 2-11.  | L. D. Bates    | 50. | T. W. Oakes                |
| 12.    | T. R. Butz     | 51. | D. C. Parzyck              |
| 13.    | J. B. Cannon   | 52. | F. G. Pin                  |
| 14.    | J. H. Coobs    | 53. | C. R. Richmond             |
| 15.    | N. H. Cutshall | 54. | M. W. Rosenthal            |
| 16.    | E. C. Davis    | 55. | T. H. Row                  |
| 17.    | L. R. Dose     | 56. | B. P. Spalding             |
| 18.    | D. E. Ferguson | 57. | W. P. Staub                |
| 19.    | T. Grizzard    | 58. | S. H. Stow                 |
| 20.    | C. S. Haase    | 59. | L. E. Stratton             |
| 21.    | F. J. Homan    | 60. | J. Switek                  |
| 22-27. | D. D. Huff     | 61. | E. Takamura                |
| 28-40. | R. H. Ketelle  | 62. | T. Tamura                  |
| 41.    | E. M. King     | 63. | W. T. Thompson             |
| 42.    | D. W. Lee      | 64. | S. D. Van Hoesen           |
| 43.    | S. Y. Lee      | 65. | A. J. Witten               |
| 44.    | T. F. Lomenick | 66. | H. E. Zittel               |
| 45.    | L. W. Long     | 67. | Central Research Library   |
| 46.    | W. E. Manrod   | 68. | ESD Library                |
| 47.    | L. J. Mezga    | 69. | Lab Records                |
| 48.    | M. S. Moran    | 70. | Lab Records - RC           |
|        |                | 71. | Document Reference Section |

## EXTERNAL DISTRIBUTION

71. Office of Assistant Manager, Energy Research and Development, DOE-ORO, P. O. Box E, Oak Ridge, TN 37831.
72. D. R. Brown, DOE-ORO, P. O. Box E, Oak Ridge, TN 37831.
73. C. Lunar, Argonne National Laboratory, 9700 South Cass Ave., Argonne, IL 60439.
74. Dr. O. C. Kopp, Department of Geological Sciences, University of Tennessee, Knoxville, TN 37996-1410.
75. E. F. Hollyday, U.S.G.S. Water Resources Division, A413 Federal Building, U.S. Courthouse, Nashville, TN 37203.
76. P. E. LaMoreaux, P. O. Box 2310, Tuscaloosa, AL 35403.
77. S. M. Gillis, Professor, Economics and Public Policy, Department of Economics, Duke University, Durham, NC 27706.
78. F. R. Kalhammer, Vice President, Electric Power Research Institute, P. O. Box 10412, Palo Alto, CA 94303.
79. T. R. LaPorte, Professor, Political Science, Institute of Government Studies, University of California, 109 Moses Hall, Berkeley, CA 94720.
80. Martin Lessen, Consulting Engineer, 12 Country Club Drive, Rochester, NY 14618.
81. W. H. Williams, Division Manager, AT&T Information Systems, Building 83, Room 1B23, 100 Southgate Parkway, Morristown, NJ 07960.
- 82-108. Technical Information Center, Department of Energy, P.O. Box 62, Oak Ridge, TN 37831